Sirindhorn International Institute of Technology
Thammasat University

Thesis CE-MS-2010-01

EXPANSION BEHAVIORS AND PREDICTION OF NET EXPANSION OF CONCRETE WITH HYPER EXPANSIVE ADDITIVE

Dung Tien Nguyen

EXPANSION BEHAVIORS AND PREDICTION OF NET EXPANSION OF CONCRETE WITH HYPER EXPANSIVE ADDITIVE

A Thesis Presented

by

Dung Tien Nguyen

Master of Science
Civil Engineering Program
Sirindhorn International Institute of Technology
Thammasat University
August 2010

EXPANSION BEHAVIORS AND PREDICTION OF NET EXPANSION OF CONCRETE WITH HYPER EXPANSIVE ADDITIVE

A Thesis Presented

By

Dung Tien Nguyen

Submitted to

Sirindhorn International Institute of Technology

Thammasat University

In partial fulfillment of the requirement for the degree of

MASTER OF SCIENCE IN ENGINEERING

Approved as to style and content by:

Advisor	_____
	Asst. Prof. Pisanu Toochinda, Ph.D.
Co-Advisor	_____
	Prof. Somnuk Tangtermsirikul, D.Eng.
Committee Member and	_____
Chairperson of Examination Committee	Assoc. Prof. Winyu Rattanapitikon, D.Eng.
Committee Member	_____
	Dr. Raktipong Sahamitmongkol, Ph.D.
External Examiner:	Assoc. Prof. Burachat Chatveera, D.Eng

August 2010

Acknowledgment

I would like to express my appreciation and gratitude to my advisor, Professor Pisanu Toochinda, for his never-ending encouragement and useful suggestions during my research. His crucial comments directly contributed to this study.

I would like to express the deepest acknowledgements to my co-advisor, Prof. Dr. Somnuk Tangtermsirikul, for his continuing encouragement and kind support throughout the duration of my research work. Above all and the most needed, he provided me valuable advices and enthusiastic guidances in various ways. Without his guidances and persistent helps, this thesis would not have been possible.

I gratefully thank Professor Winyu Rattanapitikon, chairman of thesis committee, for his constructive comments and willing advices as the valuable contribution related to my academic works with excellent cooperation and guidance.

I deeply acknowledge to Dr. Raktipong Sahamitmongkol, committee member, who provided an insightful view of my work. His useful advices, kindly encouragement and hard work in many aspects of my research areas as well as extraordinary experiences have enriched my intellectual maturity throughout the work. I am thankful to his cooperation and assistance in this research.

A special thank is conveyed to Professor Burachat Chatveera for serving as an external examiner. His comments significantly improved my thesis.

My sincere thanks go to many students in the School of Civil Engineering and Technology, SIIT, who kindly helped me during my academic works.

I am deeply indebted to the Asian Development Bank (ADB) for providing me scholarship that enabled me to complete master program at SIIT. Besides, my special thanks go to the SIIT faculty and staffs who have assisted me throughout my course.

I sincerely thank Dr. Nguyen Nhu Quy, Department of Building Materials, University of Civil Engineering, Vietnam for his foresight paved the way for my academic career.

Finally, I am forever grateful to my parents and brother for their unconditional supports and invaluable encouragements.

Abstract

The aim of this research is to investigate expansion and shrinkage mechanisms of expansive concrete, which is used to prevent cracking of concrete structures due to shrinkage. The effects of amount of hyper expansive additive (HEA), fly ash content on properties of expansive concrete such as compressive strength in free and restrained condition, tensile strength and cracking strain were also studied. The results indicated that the expansion in both free and restrained conditions increased, while tensile and compressive strength under free and restrained conditions decreased with increase of the amount of expansive additive or fly ash. On the other hand, the amount of fly ash and expansive additive just slightly affected cracking strain.

This research also investigated the effects of normal expansive additive (EA) on compensation of shrinkage of ultra high strength fiber reinforced mortar (UHSFRM). The results show that 10% EA was able to produce net expansion for UHSFRM and maintain at that level after 14 days.

In addition, based on experimental data, this study proposed the method for prediction of net expansion under restraint which could be used to compute the compensating strain to prevent shrinkage cracking.

Furthermore, in this research, net expansion under 2D and 3D restraint were also tested. The results showed that the net expansion along main direction was not affected by restraint in other directions. This allows the application of the model obtained from the results of 1D restraint for prediction of the net expansion of 2D and 3D restraint such as in case of 2-way reinforced slabs and beams with stirrup, respectively.

Moreover, this research proposes a cracking age prediction method for restrained shrinkage cracking which is useful for obtaining mix proportion to prevent cracking. Parameters including restrained expansion, free shrinkage, tensile creep and cracking strain were taken into account in the calculation. The model was verified by test results of expansive concrete mixtures (with normal expansive additive (EA) and hyper expansive additive (HEA) as well as concrete mixtures with and without fly ash, with 3 levels of 1D restraint (22.04%, 31.35% and 52.15% restraining steel ratio). The results indicated that the model is qualitatively satisfactorily for both conventional concrete and expansive concrete. However, the predicted cracking ages were slightly shorter than the actual ages because of the ignorance of tensile creep in the calculation. Furthermore, despite the enhancement of early age net expansion of expansive concrete with fly ash, fly ash also increased subsequent shrinkage. Under testing conditions, it was noticed that expansive concrete with higher fly ash replacement cracked earlier.

Table of contents

Chapter Title **Page**

Signature page i

Acknowledgment ii

Abstract iii

Table of contents iv

List of figures vii

List of tables ix

1. Introduction 1

1.1 General 1

1.2 Statement of problems 2

1.3 Objectives of study 2

1.4 Scope of the study 2

2. Literature Review 4

2.1 Expansive cement and expansive additive 4

2.2 Properties of expansive concrete 4

2.3 Shrinkage and cracking of concrete 6

2.4 Prediction of cracking age 8

2.5 Tensile creep 9

3. Experimental Program and Methodology 12

3.1 Experimental outline 12

3.2 Materials 13

3.2.1 Cement 13

3.2.2 Fly ash 13

3.2.3 Expansive additives 13

3.2.4 Aggregates 13

3.3 Mix proportions 14

3.3.1 Mix proportions of concrete 14

3.3.2 Mix proportion of ultra high strength fiber reinforced mortar (UHSFRM) *15*
3.4 Experiment on performance of expan sive concrete 15
3.4.1 Free expansion/shrinkage measurement *15*
3.4.2 Compressive strength *16*
3.4.3 Cracking strain and tensile strength *16*
3.5 Experiment for net expansion/shrinkage of UHSFRM under restrained condition 17
3.6 Experiment for net expansion of expansive concrete under restraint 17
3.6.1 Net expansion under 1D internal restraint condition *17*
3.6.2 Net expansion under 1D external restraint condition *18*
3.6.3 Net expansion under 1D combined internal and external restraint condition *18*
3.6.4 Net expansion under multi-dimensional restraint condition *19*

4. Results and Discussion 21
4.1 Performance of expansive concrete 21
4.1.1 Free expansion of concrete with HEA *21*
4.1.2 Compressive strength *23*
4.1.3 Tensile strength & cracking strain *26*
4.2 Net expansion/shrinkage of UHSFRM 28
4.3 Expansion of expansive concrete under restraint 29
4.3.1 Net expansion under 1D internal restraint *29*
4.3.2 Net expansion under 1D external restraint *33*
4.3.3 Net expansion under 1D combined external and internal restraint *36*
4.3.4 Net expansion under multi-directional restraint *36*
4.3.5 Prediction of net expansion *38*

5. Prediction of Shrinkage Cracking Age 41
5.1 Shrinkage cracking analysis 41
5.1.1 Shrinkage cracking of expansive concrete *41*
5.1.2 Shrinkage cracking of conventional concrete *43*
5.1.3 Cracking age analysis and verification *44*
5.2 Measurement of parameters for prediction of cracking age 44

5.2.1 Free expansion/shrinkage measurement *44*
5.2.2 Measurement of cracking strain *47*
5.2.3 Measurement of modulus of elasticity *48*
5.3 Prediction of cracking age without tensile creep strain 49
5.3.1 Prediction of cracking age of conventional concrete (non-expansive concrete) *49*
5.3.2 Prediction of cracking age of expansive concrete under 1D external restraint *51*
5.3.3 Prediction of cracking age of expansive concrete under combined external and internal restraint *55*
5.4 Creep at actual cracking age 56

6. Conclusion and Recommendations 61
6.1 Conclusion 61
6.2 Recommendations 61

References 63
Appendix 65

List of figures

Figure 3-1 Outline of research 12
Figure 3-2 Free expansion/shrinkage measurement 15
Figure 3-3 The equipment for casting of samples for restrained compressive strength measurement 16
Figure 3-4 Compressive strength samples under restraint before and after removing restraining steels 16
Figure 3-5 Specimen before and after testing for cracking strain and tensile strength 17
Figure 3-6 Arrangement of test for cracking strain and tensile strength 17
Figure 3-7 Specimens used for testing net expansion under 1D internal restraint condition 18
Figure 3-8 Externally restrained specimen (unit: mm) 19
Figure 3-9 Frame used for testing net expansion under 1D combined internal and external restraint condition 19
Figure 3-10 Model of specimen used for testing net expansion under 2D restraint 20
Figure 3-11 Model of specimen used for testing net expansion under 3D restraint 20
Figure 4-1 Free expansion of expansive concrete with 20 % FA 21
Figure 4-2 Free expansion of expansive concrete with 30 % FA 21
Figure 4-3 Cracks appear on the specimens using much HEA 22
Figure 4-4 Free expansion of expansive concrete without FA 22
Figure 4-5 Comparing free expansion of HEA and EA expansive concrete at 3 days of age 23
Figure 4-6 Compressive strength development of expansive concrete in free condition 24
Figure 4-7 Compressive strength of EA and HEA expansive concrete at 28 days in free condition 24
Figure 4-8 Compressive strength development of expansive concrete under restraint 25
Figure 4-9 Compressive strength of EA and HEA expansive concrete at 28 days in restrained condition 25
Figure 4-10 Tensile strength of expansive concrete 27
Figure 4-11 Cracking strain of expansive concrete 28
Figure 4-12 Net expansion/shrinkage of UHSFRM using 1% 6 mm steel fiber 29
Figure 4-13 Net expansion/shrinkage of UHSFRM using 1% 13 mm steel fiber 29
Figure 4-14 Net expansion of expansive concrete using 20% fly ash under 1D internal restraint during curing period 30

Figure 4-15 Net expansion of expansive concrete using 30% fly ash under 1D internal restraint during curing period. 31
Figure 4-16 Relationship between dosage of HEA and internal net expansion 32
Figure 4-17 Comparing net expansion of FA30HEA20 and FA30EA30 33
Figure 4-18 Net expansion under 22.04% 1D external restraint during curing period.....33
Figure 4-19 Net expansion under 31.35% 1D external restraint during curing period.....34
Figure 4-20 Net expansion under 51.25% 1D external restraint during curing period.....34
Figure 4-21 The relationship between net expansion under internal and external restraint and restraining ratio at 7 days 35
Figure 4-22 1D net expansion under combined external and internal restraint condition 36
Figure 4-23 Net expansions of single and multi-directional restraint of mix FA30HEA20 ..37
Figure 4-24 Prediction of net expansion at 7 days of curing.....38
Figure 4-25 Comparison between prediction and actual net expansion 39
Figure 5-1 Conceptual illustration of expansion mechanism of expansive concrete under restraint.....41
Figure 5-2 Shrinkage mechanisms of expansive concrete under restraint.....43
Figure 5-3 Free expansion/shrinkage of concrete without fly ash.....45
Figure 5-4 Free shrinkage of fly ash concrete 45
Figure 5-5 Free expansion and shrinkage of expansive concrete using fly ash 46
Figure 5-6 Cracking analysis of cement-only concretes.....50
Figure 5-7 Cracking analysis of non-expansive fly ash concretes 51
Figure 5-8 Cracking age analysis of expansive concrete with EA 52
Figure 5-9 Cracking age analysis of expansive concrete with HEA and without fly ash.....52
Figure 5-10 Cracking age analysis of expansive concrete with HEA and 30% fly ash.....53
Figure 5-11 Cracking age analysis of expansive concrete with HEA and 20% fly ash.....53
Figure 5-12 Rate of free shrinkage of conventional and expansive concrete 54
Figure 5-13 Cracking age analysis of HEA expansive concrete at 52.15% restraining ratio 55
Figure 5-14 Cracking age analysis of expansive concrete with HEA under 31.35% external and 2.79% internal restraining ratio.....56
Figure 5-15 Cracking age analysis of expansive concrete with HEA under 52.15% external and 2.79% internal restraining ratio.....56
Figure 5-16 Relationship between tensile creep coefficient and ratio water to binder.....59
Figure 5-17 Effect of fly ash replacement and amount of expansive additive on tensile creep coefficient.....60

List of tables

Table 3-1 Chemical compositions and physical properties of binders 13
Table 3-2 Physical properties of aggregates 14
Table 3-3 Mix proportions of concrete 14
Table 3-4 Mix proportions of UHSFRM 15
Table 5-1 Cracking strain 47
Table 5-2 Compressive strength and modulus of elasticity 48
Table 5-3 Calculated tensile creep coefficient at actual cracking ages 58

Table A 1 Free shrinkage of non-expansive concrete [21], [29] 67
Table A 2 Length change of specimens for measurement of free expansion/shrinkage of EA expansive concrete [21] 67
Table A 3 Length changes of specimens for measurement of free expansion/shrinkage of HEA expansive concrete without fly ash 68
Table A 4 Length change of specimens for measurement of free expansion/shrinkage of HEA expansive concrete using 20% fly ash 69
Table A 5 Length change of specimens for measurement of free expansion/shrinkage of HEA expansive concrete using 30% fly ash 70
Table A 6 Net expansion of HEA expansive concrete using 20% fly ash 71
Table A 7.a Net expansion of HEA expansive concrete using 30% fly ash 71

Table B 1 Compressive strength of HEA expansive concrete using 20% fly ash, under free expansion 74
Table B 2 Compressive strength of HEA expansive concrete using 30% fly ash, under free expansion 74
Table B 3 Compressive strength of HEA expansive concrete without fly ash, under restraint 74
Table B 4 Compressive strength of HEA expansive concrete using 20% fly ash, under restraint 74
Table B 5 Compressive strength of HEA expansive concrete using 30% fly ash, under restraint 75

Table C 1 Tensile strength of HEA expansive concrete without fly ash 77

Table C 2 Tensile strength of HEA expansive concrete using 20% fly ash.....77
Table C 3 Tensile strength of HEA expansive concrete using 30% fly ash.....77
Table C 4 Cracking strain of HEA expansive concrete without fly ash 77
Table C 5 Cracking strain of HEA expansive concrete using 20% fly ash.....77
Table C 6 Cracking strain of HEA expansive concrete using 30% fly ash.....78

Table D 1 Net expansion/shrinkage of UHSFRM with 6 mm long steel fiber 80
Table D 2 Net expansion/shrinkage of UHSFRM with 13 mm long steel fiber 80

Chapter 1 Introduction

1.1 General

Shrinkage is an unfavourable property of concrete. Under restrained condition, shrinkage can create tension in concrete. In addition, concrete is generally weak in tension. The tensile stress caused by restrained shrinkage often exceeds the tensile strength of concrete. Therefore, conventional concrete often cracks. These cracks are mentioned as one of the largest adversities of concrete structures because they can induce lower durability and structural stability. In order to prevent this cracking problem, many methods can be applied such as controlling shrinkage, increasing cracking capacity of concrete, reducing restraint or applying expansive concrete which is one of the common methods used to compensate shrinkage of concrete.

During its early age, expansive concrete expands so that its expansion compensates long term shrinkage of the concrete. Hence, expansive concrete can prevent cracking due to shrinkage. Expansive concrete can be manufactured by using expansive cement or adding expansive additive in concrete at the time of mixing.

In the expansive cement, the volume changes attributed to the volume augmentation are significantly higher than the reduction of volume resulting from shrinkage. The difference gives results in expansion [1]. Depending on the relation between these two volume changes one can distinguish the following materials: shrinkage-less cement, low-expansive cement, expansive cement (medium expansion) and expansive cement—self-prestressing (high expansion) [2]. According to the ASTM C 845-96 [3], the classification of expansive cements covers the three following groups: K, M and S. Expansive cement K is produced from anhydrous calcium sulfoaluminate ($4CaO\text{-}3Al_2O_3\text{-}SO_3$), calcium sulfate, and uncombined calcium oxide. Expansive cement M is produced from calcium aluminate cement and calcium sulfate. Expansive cement S is produced from tricalcium aluminate (C_3A) and calcium sulfate.

The application of expansive additives subsequently mixed with portland cement is another type of production. With controlled amount of additive the expansive cements with required expansion or low shrinkage can be produced. This method can be used in the production of low shrinkage or expansive concrete directly in the construction-site. The expansive additives with calcium sulfoaluminate (C_4A_3S), anhydrite ($CaSO_4$) and calcium oxide (CaO) are produced in Japan [1]. The expansion of concrete is mainly based on the transformation of a mixture of calcium sulfo aluminates (C_4A_3S), lime (CaO) and anhydrite ($CaSO_4$) into ettringite (Equation 1) while the CaO type causes concrete to expand mainly by the transformation of lime into calcium hydroxide (Equation 2).

$$C_4A_3S + 8CaSO_4 + 6CaO + 96H_2O \rightarrow 3C_3A.3CaSO_4.32H_2O \quad (1)$$

$$CaO + H_2O \rightarrow Ca(OH)_2 \quad (2)$$

The application of the expansive concrete has mainly been the shrinkage compensating concrete. It has been proven that this kind of concrete can efficiently reduce shrinkage cracking. Although the expansive concrete does not prevent concrete from shrinkage, it can beforehand create a designed incremental volume after setting to balance subsequent

shrinkage. In addition, expansive concrete can also be applied to pre-stress normal reinforced concrete member. This is a so-called chemically pre-stressing concrete.

1.2 Statement of problems

Nowadays, expansive concrete becomes more and more popular; however, there are some problems that still limit the usage of expansive concrete or expansive additive such as:

1. Expansive additive is a high-cost material. Hence, cost-performance analysis is necessary.
2. In fact, expansive additive is only needed for elements of structure which are under restraining conditions (internal or external restraints or combination of both). In those conditions, it is still difficult to predict the effective expansion of expansive concrete. In addition, the net expansion in the case of 2D and 3D has not been predicted.
3. No design method for a mix proportion of expansive concrete for preventing cracking.
4. There is still a doubt on how to efficiently apply expansive concrete when encountering restrained shrinkage cracking problems.

Therefore, it is necessary to consider and analyze processes of expansion and shrinkage of concrete when expansive concrete is applied.

1.3 Objectives of study

Based on the above discussions, this research is focused on the following main points:

- To investigate the performance of expansive concrete using Hyper expansive additive (HEA) (C-S-A type) and Thai fly ash.
- To formulate a method that can be used to predict the value of net expansion in the expansive concrete under uni-axial and multi-directional restraints.
- To formulate a method that can be used to analyze cracking in the expansive concrete and predict cracking age.
- To study whether expansive additive can be applied to curb high shrinkage in the ultra high strength fiber reinforced concrete or not.

1.4 Scope of the study

With the above objectives, the scope of this research is concentrated on the following experiments:

a. Hyper expansive concrete
- Amount of Hyper expansive additive: 5, 10, 15 and 20 kg/m^3
- Water to binder ratio: 0.5
- Binder content: 350 kg/m^3
- Fly ash content: 0, 20 and 30% by wt. of total binder
- Type of cement: Ordinary Portland cement type 1 (C1)
- Type of expansive agent: C-S-A type (low free calcium oxide)
- Restraining conditions: internal and external restraints, single and multi-directional restraints

This study is aimed to be applied for thin members (wall, slab, pavement, beam etc.) in which stress distribution over cross section is uniform.

b. Ultra high strength fiber reinforced mortar

- Amount of Normal expansive additive: 103 and 154 kg/m^3 (10% and 15% of total binder)
- Water to binder ratio: 0.21
- Binder content: 1028 kg/m^3
- Silica fume content: 7.2 % by wt. of total binder
- Type of cement: Ordinary Portland cement type 1 (C1)
- Type of expansive agent: CaO type (high free calcium oxide)
- Types of fiber: 6-mm and 13-mm long corresponding to 37.50 and 81.25 aspect ratio, respectively.

Chapter 2 Literature Review

2.1 Expansive cement and expansive additive

Konik et al [1] researched on production of expansive additive and Portland cement. The expansive additive was produced from sulfate–calcium component and aluminate clinker, containing 60% Al_2O_3. The sulfate–calcium component is prepared by flue gas desulphurization gypsum and calcareous raw material mixture burning. The ground sulfate component, mixed with ground aluminate clinker transforms into the effective expansive additive for cement. The following main phases were present in this expansive material: anhydrite, calcium oxide and monocalcium aluminate. The expansive substance was added to CEM I 42.5 cement as 7 and 12% addition. The cement with 7% (by weight) expansive additive is a shrinkage-less material, while the mixture with 12% (by weight) expansive additive is an expansive binder.

Fu et al [4] studied on developing a new composite expansive additive for use in producing shrinkage-compensating cement by addition to Portland cement. Setting time, workability loss, free expansion, restrained expansion and compressive strength results were obtained for cement pastes and mortars containing different amounts of expansive additive. The effect of superplasticizer on the properties of fresh and hardened expansive cement mortar was also investigated. Results indicated that expansive cement with an appropriate amount of pre-hydrated high alumina cement based expansive additive passed all the requirements of relevant ASTM standards and was the potentially partical.

Yan et al [5] studied the hydration of shrinkage-compensating binders with different compositions and water to binder ratios (w/b). The authors concluded that, composition and w/b affected significantly the hydration rate and degree of shrinkage-compensation, as well as their expansive and mechanical properties. Hydration is limited at low w/b. The lower is the w/b, the lower are the total heat of hydration and their final hydration degree. The rate of heat release and total heat of hydration of ternary binders consisting of Portland cement, expansive agent and mineral admixtures are lower than that of binary binder consisting of Portland cement and expansive agent for the highest w/b. Their water demand correspondingly reduces the hydration of the other components and their hydration time is prolonged comparing to the binary binder. At low w/b the total heat of hydration of ternary binders increases continuously and surpasses that of binary binder for higher hydration times

Cohen [6] surveyed the theories of expansion in sulfoaluminate - type expansive cements. There are two major theories: the Crystal Growth Theory and the Swelling Theory. According to the first theory, expansion is caused by the growth of ettringite crystals from the surfaces of the expansive particles or from the solution resulting in a crystallization pressure and, hence, expansive force. According to the second theory, expansion is caused by water-adsorption and swelling characteristics of ettringite gel which forms by a through-solution mechanism. Observations supporting and contradicting both theories are briefly reviewed.

2.2 Properties of expansive concrete

Sun et al [7] researched on the effect of hybrid fibers and expansive agent on the shrinkage and permeability of high-performance concrete (HPC). HPC incorporated with expansive agent and hybrid fibers, i.e., steel fibers, polyvinyl alcohol fiber (PVA fiber), and

polypropylene fiber (PP fiber), was produced. The properties measured included shrinkage and water permeation of the concrete. The effect of hybrid fibers and/or expansive agent on the shrinkage and water permeation properties was investigated. Test results indicated that the hybrid fibers of different types and sizes could reduce the size and amount of crack at different scales. Hybrid fibers combined with expansive agent provided better enhancement for shrinkage resistance and impermeability of HPC than monoincorporation of hybrid fibers or expansive agent. The improvement of the shrinkage resistance and the impermeability of the concrete resulted from the combined use of expansive agent and hybrid fibers, which was dependent on the amount of expansive agent, types and sizes of hybrid fibers, total volume fraction of fibers, proportions of hybrid fibers, and so on. The relevant mechanisms were also discussed based on the analysis of the test results of pore structure of the concrete.

Lam et al [8] presented a study on free expansion and compressive strength of concrete with expansive additive. In this research, the effect of amount of expansive additive (EA), type of binder, water to binder ratio and curing condition on free expansion and compressive strength of expansive concrete were studied. Concrete made from ordinary Portland cement (OPC1), high early strength cement (OPC3), limestone powder (LP) and fly ash (FA) under moist curing, water curing and air curing were investigated. The results showed that, expansive additive was more effective to produce free expansion of fly ash concrete than other concrete. Free expansion of expansive concrete developed within 3 days, after that the free expansion of concrete was constant or reduced slightly due to autogenous shrinkage. When free expansion strain exceeded 800 micron, the compressive strength of expansive concrete dropped more than 20% of the non expansive additive concrete.

Tazawa et al [9] studied the behaviors of expansive concretes cured in pressurized water at high temperature (TPC curing). The studied behaviors were such as variations in strain, weight and strength. These behaviors were compared with those cured by autoclave curing (AC curing) at the same pressure and temperature. The authors indicated that both of these curing methods were effective in reducing autogenous shrinkage and drying shrinkage at longer age after the curing. When TPC curing was adopted, the required expansion of concrete could be attained at smaller dosage of expansive agents. After the curing, length changes due to hygrometric or hygroscopic conditions were almost eliminated for later age.

Shuguang and Yue [10] conducted a research on the hydration, hardening mechanism, and microstructure of high performance expansive concrete. The study was performed on high performance expansive fly ash concrete (HPEC) and high performance concrete. Different mechanical properties of HPEC and high performance concrete were investigated under free- and confined-curing conditions. By means of XRD and SEM methods, the hydration progress and microstructure of HPEC were also investigated. The authors concluded that, an expansive agent consisting of alunite and gypsum can obviously increase the amount of AFt, which can make concrete expand and compensate for shrinkage. Under the free-curing condition, the inner microstructure of expansive cement paste and concrete is loose, with many cracks in the paste and paste-aggregate interface. Confined-curing condition could improve the microstructure of expansive concrete, especially by intensifying and densifying the paste-aggregate interface.

Lam et al [11] presented a study on durability properties of concrete using an expansive additive. In his research, the effect of expansive additive (EA) content, fly ash (FA) content and water to binder ratio (W/B) on durability such as carbonation resistance of concrete, sulfate resistance of mortar, chloride penetration and chloride binding capacity of paste were studied. The results indicated that, when EA content was not greater than 30 kg/m^3, carbonation resistance of both expansive concrete with and without fly ash were better than that of concrete without expansive additive. But when amount of EA was higher than 30 kg/m^3, carbonation resistance of fly ash expansive concrete became worse. Expansive additive had a negative effect on sulfate resistance and chloride binding capacity of concrete but tended to reduce chloride permeability.

2.3 Shrinkage and cracking of concrete

Almusallam et al [12] researched on how different mix proportions affected plastic shrinkage cracking of concrete in hot environments. The effect of mix proportions, i.e. cement content and water–cement ratio, on plastic shrinkage cracking of concrete in hot and arid environments was investigated. The cumulative effect of these parameters on plastic shrinkage of concrete was assessed by measuring the rate of bleeding, water evaporation, and time and intensity of cracks. The results indicated that cement content and water–cement ratio significantly affect the parameters controlling plastic shrinkage of concrete. Lean-stiff concrete mixes cracked earlier than the rich-plastic concrete mixes. The intensity of cracks in the former was, however, less than that in the latter. Plastic shrinkage cracking occurred when the rate of evaporation was in the range of 0.2–0.7 kg m^{-2} h^{-1}, as against a value of 1 kg m^{-2} h^{-1} suggested by ACI 305. The rate of evaporation and bleeding was the least in a lean-stiff concrete mix made with a cement content of 300 kg m^{-3} and a water–cement ratio of 0.40, indicating that this mix composition can be beneficially utilized in hot environments to minimize plastic shrinkage cracking.

Benboudjema et al [13] surveyed about interaction between drying, shrinkage, creep and cracking phenomena in concrete. A hydro-mechanical model, accounting for the full coupling of drying, shrinkage, creep and cracking was presented. In the model, a new basic creep constitutive law, based on microscopic considerations of the role of water, was elaborated. Further, the existing model for drying creep of Bažant and Chern Bazant and Chern [14] was improved by the introduction of a second material parameter which accounts for the interaction between the solid skeleton and liquid water layers in a drying and creeping material. The model was subsequently used for investigating the effect of cracking on the delayed behavior of concrete and displaying the frontier between the intrinsic behavior of the material and the structural effects.

Slowik et al [15] simulated capillary shrinkage cracking in cement-like materials. In drying suspensions, water loss leads to a capillary pressure build-up in the liquid phase. This effect may also be observed in fresh cement-based materials subjected to evaporation at an open surface. If under decreasing water content the near-surface solid particles are no longer covered by a plane water film, menisci develop along with an associated build-up of negative capillary pressure, resulting in shrinkage and possibly in cracking. A 2D model for simulating the described physical process was presented. For arranging the particles in the 2D specimen a stochastic–heuristic algorithm was used. Subsequently, the course of the water front between the particles was calculated by assuming a constant curvature of the water surface. Particle mobility was taken into account by adopting interparticle forces and performing equilibrium iterations. The model allowed one to study the influences of the

particle size distribution as well as of the properties of the liquid phase on the capillary pressure build-up and on the cracking risk.

Barr et al [16] conducted a research on shrinkage of concrete stored in natural environments. The research reported the influence of the natural environment on the drying shrinkage of a range of concretes, with and without steel fibre reinforcement. A combination of increasing cement content, the addition of silica fume (SF) and reduced water/binder ratio was used to obtain a wide range (C30–C70) of concrete strengths. Both prism and cylinder test specimens were used in the study and a fibre concentration of 2% (by weight) was used in the fibre reinforced concrete (FRC) mixes. The experimental results were compared with predicted shrinkage strains obtained from the ACI 209 model. The results showed that the effect of varying relative humidity and temperature in the natural environment had only a limited effect on the drying/autogenous shrinkage. The addition of 2% fibre to the various mixes had a negligible effect on shrinkage for the lowest strength (C30) but the restraint on the development of shrinkage was enhanced as the strength of the concrete was increased. Comparison between experimental results and predicted shrinkage strains was not good for the high-strength concretes, although good correlation was observed for the lower strengths (C30–C45).

Gesoglu et al [17] studied shrinkage cracking of lightweight concrete (LWC) made with cold-bonded fly ash aggregates. In this research, shrinkage cracking performance of lightweight concrete (LWC) was investigated experimentally on ring-type specimens. LWC with and without silica fume were produced at water to cementitious material ratios (w/cm) of 0.32 to 0.55 with cold-bonded fly ash coarse aggregates and natural sand. Coarse aggregate volume ratios were 30%, 45%, and 60% of the total aggregate volume in the mixtures. A total of 12 lightweight aggregate concrete mixtures were tested for compressive strength, static elastic modulus, split-tensile strength, free shrinkage, weight loss, creep, and restrained shrinkage. The authors found that the crack opening on ring specimens was wider than 2 mm for all concretes. Free shrinkage, weight loss, and maximum crack width increased, while compressive and split-tensile strengths, static elastic modulus, and specific creep decreased with increasing coarse aggregate content. The use of silica fume improved the mechanical properties but negatively affected the shrinkage performance of LWC. Shrinkage cracking performance of LWC was significantly poorer than normal weight concrete.

Holt and Leivo [18] studied on cracking risks associated with early age shrinkage. When assessing the cracking potential of concrete it is critical to refer to the total shrinkage: both early age and long-term deformation, in both drying and autogenous conditions. A Finnish test arrangement had been used to measure linear and volumetric deformations of concrete immediately after mixing. The slabs were tested in both drying and autogenous conditions. Long-term shrinkage could be measured on the same slabs to give an accurate representation of the total free shrinkage. From these measurements it was possible to assess the likelihood of cracking due to early age shrinkage. Results showed that both drying and autogenous shrinkage can be significant in certain early age scenarios. Environmental factors greatly affected drying shrinkage, while material properties affected autogenous shrinkage. This paper provides insight regarding how to interpret early age deformations, how environmental and material factors play a role, and how to minimize shrinkage and thus cracking potential in the early ages.

2.4 Prediction of cracking age

Passuello et al [19] used shrinkage reducing admixtures and fibers to reduce the cracking potential of the concrete. The reduction of the risk of cracking was evaluated by the reduction of drying shrinkage due to the addition of shrinkage reducing admixtures (SRA) and by the increase of the crack opening resistance due to the addition of fibers. Both technologies were considered individually and used in combination. It was noted that the addition of SRA delayed the time of cracking and the addition of fiber reduces the crack opening. However, the addition of the shrinkage reducing admixture (SRA) to the fiber-reinforced concrete led the concrete to a better cracking behavior even when the fiber dosage was reduced. Finally, the cracking time was predicted by applying two different theoretical approaches.

Yuan and Wan [20] formulated a numerical simulation procedure based on a micromechanical model and empirical formulas on the property development of young concrete to predict potential early-age cracking after concrete placing. The numerical model could account for the effects of hydration, moisture transport and creep. Environmental influences, such as removal of formworks, curing conditions and variations of surrounding temperature and relative humidity, were investigated. In calculating stress field with age caused by these synthetic physical–mechanical processes, three-dimensional finite element and finite difference (3D-FE-FD) methods were combined together.

Lam [21] proposed a formula to predict cracking age of expansive concrete as follows:

$$\varepsilon_f(t) = \varepsilon_{t,res}(t) - \varepsilon_{cr,t}(t) - \varepsilon_{c,res}(t) + \varepsilon_{cr,c}(t) \quad (2\text{-}1)$$

Where
ε_f : restrained strain in concrete.
$\varepsilon_{t,res}$: tensile strain caused by restrained shrinkage of concrete.
$\varepsilon_{c,res}$: compressive strain caused by restrained expansion of concrete .
$\varepsilon_{cr,t}$ and $\varepsilon_{cr,c}$: tensile creep and compressive creep of concrete, respectively.
All of the above parameters are time dependent properties.
Predicting cracking is based on a criterion of cracking strain of concrete:

$$\varepsilon_f(t) > \varepsilon_{crackingstrain}(t) \quad (2\text{-}2)$$

If the condition in 2-2 is satisfied, the concrete cracks.
To compute the value of restrained strain ε_f(t), the author divided the cracking process of expansive concrete into two parts; i.e expansion part and shrinkage part.

Expansion part:
The author applied force equilibrium of expansion progress to achieve:

$$\varepsilon_{c,res} = \frac{E_s A_s}{E_s A_s + E_{ca} A_c} . \varepsilon_{ef.free} \quad (2\text{-}3)$$

A_s and A_c : cross-sectional area of restraining object and that of concrete, respectively.
E_s and E_{ca}: modulus of elasticity of steel and average modulus of elasticity of concrete.
$\varepsilon_{ef,free}$: effective expansion of expansive concrete.

The values of cross-section and modulus of concrete, steel can be measured by experiment. The author assumed that relationship between effective expansion and net expansion is linear. He conducted four ratios to measure net expansion and got the value of effective expansion $\varepsilon_{ef,free}$ with his assumption.
Substitute the values of cross-section, elasticity of modulus and effective expansion to Equation (2-3) to achieve $\varepsilon_{c,res}$.

Shrinkage part:
The author applied force equilibrium of shrinkage progress to obtain:

$$\varepsilon_{t,res} = \frac{E_s A_s}{E_s A_s + E_c A_c} . \varepsilon_{sh.free} \tag{2-4}$$

Where
$\varepsilon_{sh,free}$: free shrinkage measured from experiment
Substitute free shrinkage and cross-section, modulus of concrete and that of steel into 2-4 to obtain restrained tensile strain inside concrete $\varepsilon_{t,res}$
Substitute compressive strain $\varepsilon_{c,res}$ and tensile strain $\varepsilon_{t,res}$ into Equation (2-1). Besides that, the author assumed that $\varepsilon_{cr,t}$(t) is very small and ignored it. Therefore, restrained tensile strain of the concrete can be computed and compared with cracking strain as in Equation (2-2) to identify cracking.

The limitations of this method are:
- According to analysis of restrained strain, role of net expansion, which is able to reduce restrained tensile strain, had not been taken into account. As the results, restrained tensile strain becomes larger and the results of prediction are much shorter.
- The prediction requires both prediction of tensile creep and compressive creep.
- Ignoring compressive creep and tensile creep limits accuracy of the prediction of cracking age.
- Determination of effective expansion $\varepsilon_{ef,free}$ based on assumption might be inaccurate. The relationship between effective expansions with restraining steel ratio is assumed to be linear. In addition, just four ratios with a large interval restraining ratio (0.79%, 1.57%, 3.14% and 31.15%) were conducted to predict effective expansion. Hence, the results of the predicted effective expansion calculation were still far from the actual ones.

2.5 Tensile creep

Vandewalle [22] conducted an experimental study on creep and shrinkage of concrete both at variable and constant ambient conditions. The considered variable ambient conditions correspond to the natural climatic variations present in Belgium. The parameters were period (season) when the concrete was cast and loaded, cement type and concrete composition. Both sealed and unsealed cylindrical specimens were used. The experimental results show that both the ‘season’ in which the concrete was cast and the ‘humidity cycles’ influence the shrinkage deformation. The creep coefficient mostly depended on the ‘season’.
Kim and Lee [23] developed an analysis method in order to predict the differential drying shrinkage in which the creep of concrete was also considered. In this research, differential drying shrinkage strain was measured at various positions in concrete by using embedded strain gauges. The internal drying shrinkage strain differs significantly according to the

depth from exposed surface. The validity of analysis method was verified by comparing test results with analytical results. The authors concluded that the internal drying shrinkage strain significantly varies according to the depth from drying surface, and the stresses induced by this differential drying shrinkage may cause surface cracks. Thus the differential drying shrinkage must be considered in the analysis of thick concrete structures. The analysis method of differential drying shrinkage, the creep of concrete needs to be considered, and the analytical results obtained by this method were in good agreement with test results. According to the differential drying shrinkage strain measured at various positions of concrete by using the embedded strain gauges, it seems that the technique using the embedded strain gauges is suitable for measuring the internal drying shrinkage strain distribution.

Garas et al [24] studied short-term tensile creep and shrinkage of ultra-high performance concrete (UHPC). The tensile creep and free shrinkage deformations of UHPC were examined through short-term testing to assess the influences of stress/strength ratio, steel fiber reinforcement, and thermal treatment. The use of fibers and the application of thermal treatment decreased 14-day drying shrinkage by more than 57% and by 82%, respectively. Increasing the stress-to-strength ratio from 40% to 60% increased the tensile creep coefficient by 44% and the specific creep by 11%, at 14 days of loading. Incorporating short steel fibers at 2% by volume decreased the tensile creep coefficient by 10% and the specific creep by 40%, at 14 days. Also, subjecting UHPC to a 48-h thermal treatment at 90 °C, after initial curing, decreased its tensile creep coefficient by 73% and the specific creep by 77% at 7 days, as compared to ordinarily cured companion mixes. Comparison of tensile creep behavior to compressive creep in UHPC reveals that these phenomena differ fundamentally and that further evaluation is necessary to better understand the underlying mechanisms of tensile creep in UHPC. Results from this study also showed that the effects of both thermal treatment and fiber reinforcement were more pronounced in tensile creep behavior than tensile strength of different UHPC mixes. This emphasizes the importance of tensile creep testing to predict long-term tensile performance.

Lee et al [25] evaluated a basic creep model with respect to autogenous shrinkage. This paper shows the results obtained from an experimental study to evaluate a basic creep model. In this study, four different mix proportions were placed, and tests on the specimens for autogenous shrinkage and basic creep were conducted with respect to age and stress level. The primary test variable was the water/cement ratio (w/c). From this research, it was found that for low w/c concrete, as well as at an early age of normal-strength concrete, a significant difference existed between apparent basic creep (including autogenous shrinkage) and real basic creep (excluding autogenous shrinkage). Furthermore, creep strain was not directly proportional to the applied stress level after one day. It was also discovered that when the current basic creep model that includes autogenous shrinkage is used in creep analysis, considerable errors as well as some computational problems may occur. It was therefore recommended to modify the equations of the current basic creep model with respect to autogenous shrinkage.

Tao and Weizu [26] reported an experimental study on the early-age tensile creep behavior of high strength concrete (HSC) comprising of silica fume concrete, fly ash concrete and plain concrete under uni-axial restraining stresses. A series of restraint shrinkage tests were carried out adopting semi-adiabatic and isothermal conditions to determine the effects of temperature history on the tensile creep properties for young concretes. Furthermore, the effects of restraining stress history on creep were also discussed under three different

degrees of restraint. It was found that the initial thermal dilation deformation delayed the development of tensile creep and weakened the creep potential of early age concretes. It was also observed that the young concrete subjected to a lower restraining tensile stress history had a higher potential of visco-elastic response in tension at early ages.

Chapter 3 Experimental Program and Methodology

3.1 Experimental outline

An experimental program was designed to investigate effect of Hyper expansive additive (HEA) on performance of expansive concrete such as free expansion, compressive strength (including free and restrained conditions), tensile strength as well as cracking strain. These properties were tested with varied amount of HEA and fly ash. In addition, normal expansive additive (EA) was also applied for compensating high shrinkage of Ultra High Strength Fiber Mortar (UHSFM) which was tested by using 2 types of fiber which are 6-mm and 13-mm long. Especially, expansion under restrained condition was focused in this research. Mixes of HEA expansive concrete were experimented by varying amounts of HEA as well as restraining steel ratio (ρ) in both internally and externally restrained condition. Specimens under 2D and 3D restraint were also tested to find out the mechanism of net expansion in multi-directional restraint. Moreover, in order to verify the model for shrinkage cracking age prediction, the specimens (including conventional concrete, fly ash concrete and expansive concrete) under high restraining ratios were tested in this study. The experimental program is summarized as shown in Figure 3-1.

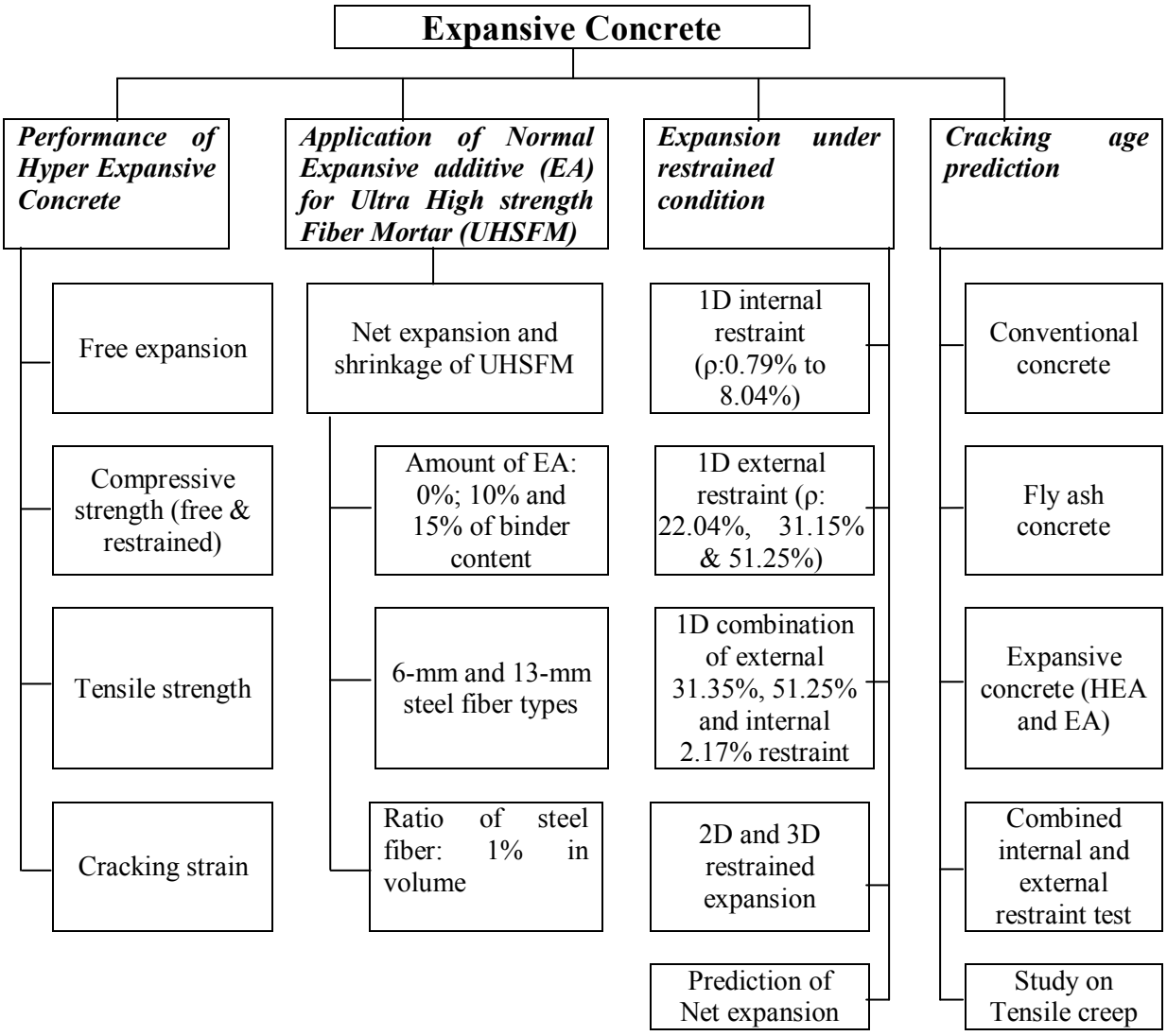

Figure 3-1 Outline of research

3.2 Materials

In this research, an ordinary Portland cement type 1 (C1) was used. Expansive additive was C-S-A type Hyper expansive additive (HEA). Beside that, Thai fly ash was also used in this research. River sand and crushed limestone was used as aggregates. The maximum size of coarse aggregate was 19 mm.

3.2.1 Cement

Ordinary Portland cement type 1 (C1) was used for all mixtures. The test results of chemical compositions and physical properties of the cement are given in Table 3-1.

3.2.2 Fly ash

Fly ash obtained from Mae-Moh power plant in Thailand was used in all fly ash mixtures. This fly ash is a product of lignite coal after being burned as fuel in the plant. It is considered as class B fly ash (high calcium) according to TIS 2135 and EIT 1014-46. Chemical compositions and physical properties of the fly ash are given in Table 3-1.

3.2.3 Expansive additives

Expansive additives that were used in this project were EA (normal expansive agent) and HEA (Hyper expansive agent) in Table 3-1. They are identified as CaO type for EA (high free CaO content) [21], [27] and C-S-A type (low free CaO content) for HEA [27]. The chemical composition and physical properties of the expansive additives are also given in Table 3-1.

3.2.4 Aggregates

Natural river sand and crushed limestone were used as fine aggregate and coarse aggregate, respectively. The properties and gradation of fine and coarse aggregates comply with ASTM C33-97 [28] Physical properties of the aggregates are shown in Table 3-2.

Table 3-1 Chemical compositions and physical properties of binders

Material	SiO_2 (%)	Al_2O_3 (%)	Fe_2O_3 (%)	CaO (%)	MgO (%)	SO_3 (%)	Na_2O (%)	K_2O (%)	Free CaO (%)	LOI (%)	Fineness* (cm^2/g)	Specific gravity
OPC1	20.20	4.70	3.73	63.40	1.37	1.22	-	0.28	-	2.72	3430	3.15
FA	36.10	19.40	15.10	17.40	2.97	0.77	0.55	2.17	-	2.81	2460	2.27
EA	9.60	2.50	1.30	67.30	0.40	18.00	-	-	26.84	0.40	5130	3.04
HEA	4.35	0.96	1.14	78.84	0.93	10.95	<0.01	0.05	<0.01	2.64	5260	3.14

**Using Blaine's method.*

Table 3-2 Physical properties of aggregates

Physical properties	Sand	Coarse Aggregate
Specific gravity	2.60	2.68
Absorption, %	0.89	0.46
Fineness modulus	2.13	-
Maximum size, mm	4.75	19
Unit weight, g/cm^3	1.63	1.62
Void ratio, %	37.31	39.55

3.3 Mix proportions

3.3.1 Mix proportions of concrete

Expansive concrete containing different fly ash contents (0, 20 and 30%) and amounts of HEA (5, 10, 15 and 20 kg/m^3) with W/B of 0.5 were used in this research, the ratio of paste volume to void volume of aggregate phase (γ) was controlled at 1.3. The details of mix proportions of the tested concrete are given in Table 3-3. In order to compare the performance of EA and HEA expansive concrete, the mixtures No. 7 and No. 8 were obtained from a previous research [21] for normal expansive concrete (EA expansive concrete). In order to verify prediction of cracking age model, this research consulted the results of non-expansive concrete mixes in [21], [29].

Table 3-3 Mix proportions of concrete

No	Mix	W/B	C, kg/m^3	FA, kg/m^3	EA, kg/m^3	HEA, kg/m^3	S, kg/m^3	G, kg/m^3	gamma, γ
1	w35	0.35	470.00	0.00	0.00	0.00	773.80	1021.20	1.40
2	w50	0.50	350.00	0.00	0.00	0.00	824.00	1038.00	1.30
3	w55	0.55	361.52	0.00	0.00	0.00	773.80	1021.20	1.40
4	w55FA30	0.55	245.23	105.10	0.00	0.00	773.80	1021.20	1.40
5	w55FA50	0.55	171.62	171.62	0.00	0.00	773.80	1021.20	1.40
6	w50FA30	0.50	245.00	105.00	0.00	0.00	808.00	1018.00	1.30
7	FA0EA30	0.50	320.00	0.00	30.00	0.00	823.00	1037.00	1.30
8	FA30EA30	0.50	224.00	96.00	30.00	0.00	809.00	1020.00	1.30
9	FA0HEA15	0.50	335.00	0.00	0.00	15.00	824.00	1037.00	1.30
10	FA0HEA20	0.50	330.00	0.00	0.00	20.00	824.00	1037.00	1.30
11	FA20HEA5	0.50	276.00	69.00	0.00	5.00	814.00	1025.00	1.30
12	FA20HEA10	0.50	272.00	68.00	0.00	10.00	814.00	1026.00	1.30
13	FA20HEA15	0.50	268.00	67.00	0.00	15.00	814.00	1026.00	1.30
14	FA20HEA20	0.50	264.00	66.00	0.00	20.00	814.00	1026.00	1.30
15	FA30HEA5	0.50	241.5	103.50	0.00	5.00	810.00	1020.00	1.30
16	FA30HEA10	0.50	238.00	102.00	0.00	10.00	810.00	1021.00	1.30
17	FA30HEA15	0.50	234.50	100.50	0.00	15.00	811.00	1021.00	1.30
18	FA30HEA20	0.50	231.00	99.00	0.00	20.00	811.00	1021.00	1.30

3.3.2 Mix proportion of ultra high strength fiber reinforced mortar (UHSFRM)

Table 3-4 Mix proportions of UHSFRM

No	Mix	SF length (mm)	W/B	Paste (vol.%)	Silica fume (%)	EA(%)	SP, %	SF, vol. %
1	SF(6mm)EA0%	6	0.21	55	7.2	0	2	1
2	SF(6mm)EA10%	6	0.21	55	7.2	10	2	1
3	SF(6mm)EA15%	6	0.21	55	7.2	15	2	1
4	SF(13mm)EA0%	13	0.21	55	7.2	0	2	1
5	SF(13mm)EA10%	13	0.21	55	7.2	10	2	1
6	SF(13mm)EA15%	13	0.21	55	7.2	15	2	1

Note: SF means steel fiber, EA means normal expansive additive, SP means superplasticizer

There were 6 different mixes of UHSFRM. All mixes contained silica fume and steel fiber. This research used two lengths of fiber i.e. 13-mm and 6-mm. The amounts of EA were 0%, 10% and 15% of total binder amount. The details of mix proportions of this mortar are given in Table 3-4.

3.4 Experiment on performance of expansive concrete

3.4.1 Free expansion/shrinkage measurement

The specimens with the size of 75×75×250 mm^3 were used for free expansion/shrinkage tests. These tests conform to ASTM C 157/C 157M-99 [30]. Initial lengths were recorded at 8 hours after mixing and the specimens were sealed for 7 days after mixing and subsequently exposed to drying environment (28^{o}C and 75% humidity). Afterwards, the specimens were periodically measured for free shrinkage test. Figure 3-2 shows the specimens and measurement of free expansion/shrinkage. Two specimens were used for each mixture and result is the average of their measured values.

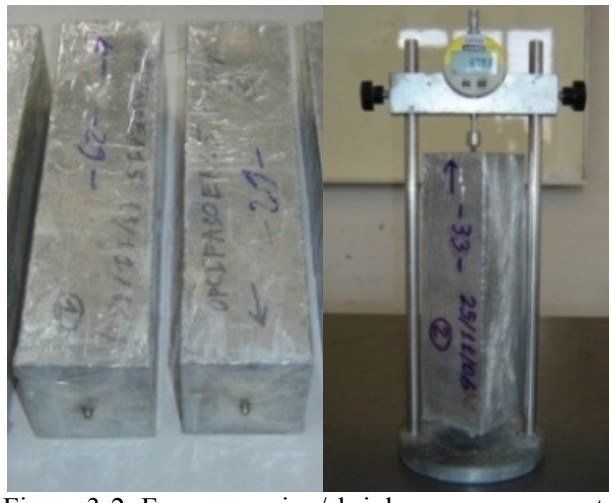

Figure 3-2 Free expansion/shrinkage measurement

3.4.2 Compressive strength

Compressive strength under free condition was tested by using cylinder specimens with the size ϕ100x200 mm. The specimens were sealed for 7 days after mixing and subsequently exposed to drying environment (28^{o}C and 75% humidity). This test conforms to ASTM C 39/C 39M-99 [31].

In the case of testing for restrained compressive strength, the 100x100x100 mm cube specimens and equipments were specially designed (Figure 3-4). Restraining steel ratio of the samples was 1.57%. The restraining steel bars were removed before testing (Figure 3-4). Two specimens were used for each mixture and the compressive strength result was the average of their measured values.

3.4.3 Cracking strain and tensile strength

Bending tests on 100x100x350 mm [32] prism specimens (see Figure 3-6) were conducted to measure flexural cracking strength as well as cracking strain of concrete at 3 days, 7 days, 28 days and 56 days. The specimens were sealed for 7 days after mixing and subsequently exposed to drying environment (28^{o}C and 75% humidity). The flexural cracking strains were measured by strain gages. Two specimens were used for each mixture and the result is the average of their measured values.

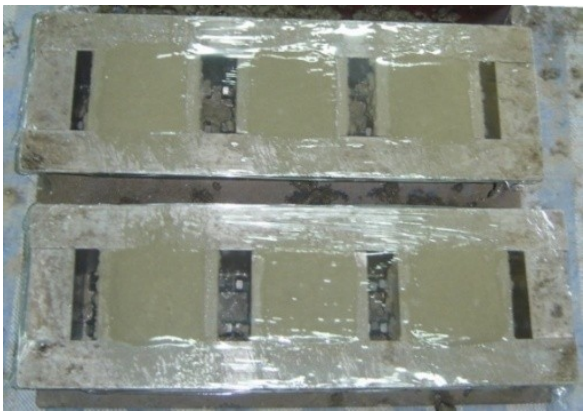

Figure 3-3 The equipment for casting of samples for restrained compressive strength measurement

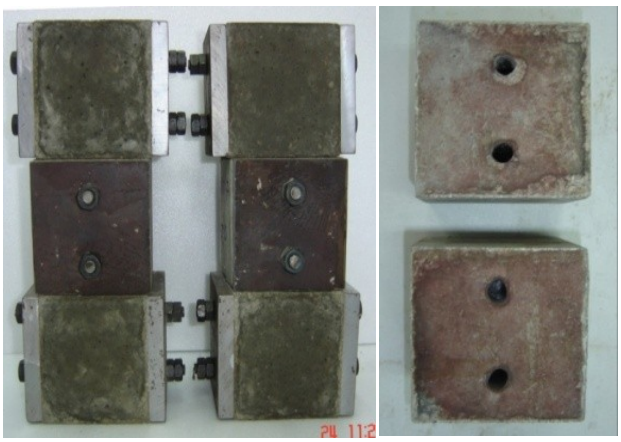

Figure 3-4 Compressive strength samples under restraint before and after removing restraining steels

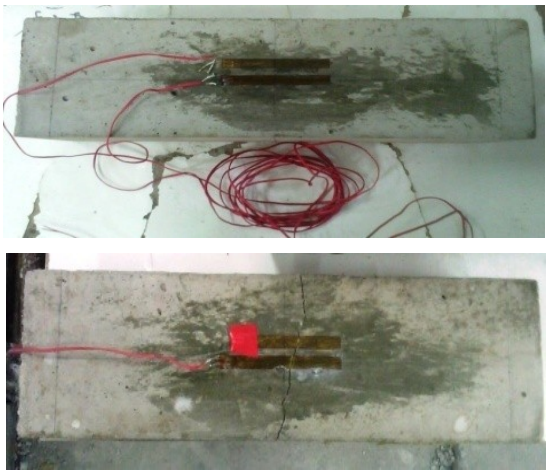

Figure 3-5 Specimen before and after testing for cracking strain and tensile strength

Figure 3-6 Arrangement of test for cracking strain and tensile strength

3.5 Experiment for net expansion/shrinkage of UHSFRM under restrained condition

The specimen as shown in Figure 3-2 was also used to test net expansion/shrinkage of UHSFRM. The mix proportions of mortar were shown in Table 3-4. The specimen's size is 75×75×250 mm. Initial lengths were recorded at 3 hours after mixing and the specimens were sealed for 7 days after mixing and subsequently exposed to drying environment (28^{o}C and 75% humidity). Two specimens were used for each mixture and result is the average of their measured values.

3.6 Experiment for net expansion of expansive concrete under restraint

3.6.1 Net expansion under 1D internal restraint condition

This study tested the net expansion under internal restraint with varied restraining steel ratios; i.e, 0.79%, 1.57%, 3.14% and 8.04% of the specimen cross-sectional area, respectively. The specimens with the size of 100x100x350 mm were used for testing net expansion under 1D internal restraint condition. The specimens were restrained by steel bars and two ends were fixed by steel plates (Figure 3-7). The specimens were seal-cured in curing room with the temperature controlled at 28^{o}C. The strain of specimens was measured by strain gages which are attached to the reinforcing steel bars before casting concrete. Data logger was used to record expansion strain of the specimens.

The measurement of strain was initiated after casting. Two specimens were used for each mixture and 2 strain gages were used for each specimen except for specimens with only one steel bar. The result were the average of the measurement of four strain gages on two specimens

3.6.2 Net expansion under 1D external restraint condition

Concrete specimen with geometry shown in Figure 3-8 was used for testing net expansion under 1D external restraint condition. The restraining ratio was 31.35% for all specimens except for the specimens FA30HEA10, FA30HEA5, FA20HEA10 and FA20HEA10 of which restraining ratio was 22.04%. In addition, some mixes using 15 and 20 kg/m^3 of HEA were also test at 52.15% restraining ratio. The net expansion of the specimens was measured by strain gages attached to the restraining steel frame. The specimens were sealed for 7 days after mixing and subsequently exposed to drying environment (28^{o}C and 75% humidity).

The measurement of strain was initiated immediately after casting and continued until the end of curing. Afterwards, the specimens were observed to measure cracking age which was the age of concrete when cracking took place. Two specimens were used for each mixture and 2 strain gages were applied to each specimen. The results of externally restrained expansion were the average of the measurement of four strain gages on two specimens (two strain gages on each specimen) and the measured cracking age was the average of two specimens.

3.6.3 Net expansion under 1D combined internal and external restraint condition

Expansion under combination between internal restraint and external restraint was tested. The mould as shown in Figure 3-9 was used with external restraint ratios of 31.35%, 52.15% and internal restraint ratio of 2.79%.

Expansion of the specimens was measured by strain gages attached to the restraining steel frame as in the external restraint expansion case. The measurement of strain was conducted immediately after casting and lasted for 7 days after curing. Two specimens were used for each mixture and 2 strain gages were applied to each specimen. The results of expansion under combined restraint were the average of the measurement of four strain gages on two specimens (two strain gages on each specimen). The specimens were sealed for 7 days after mixing and subsequently exposed to drying environment (28^{o}C and 75% humidity).

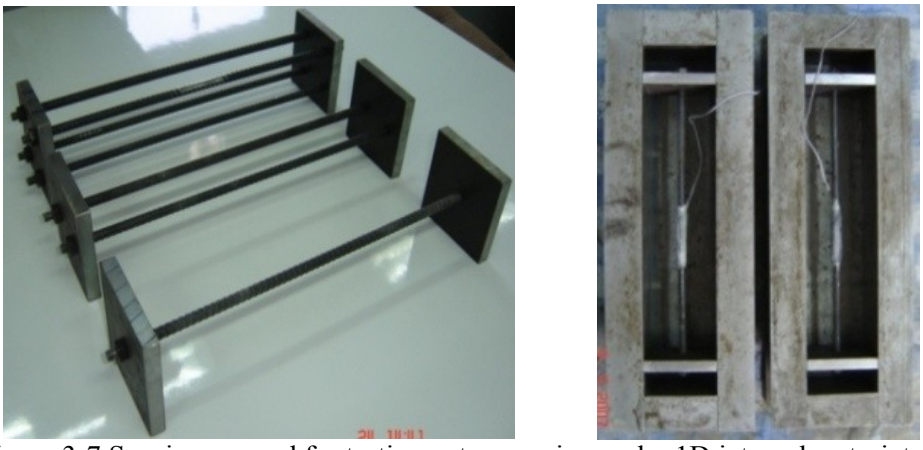

Figure 3-7 Specimens used for testing net expansion under 1D internal restraint condition

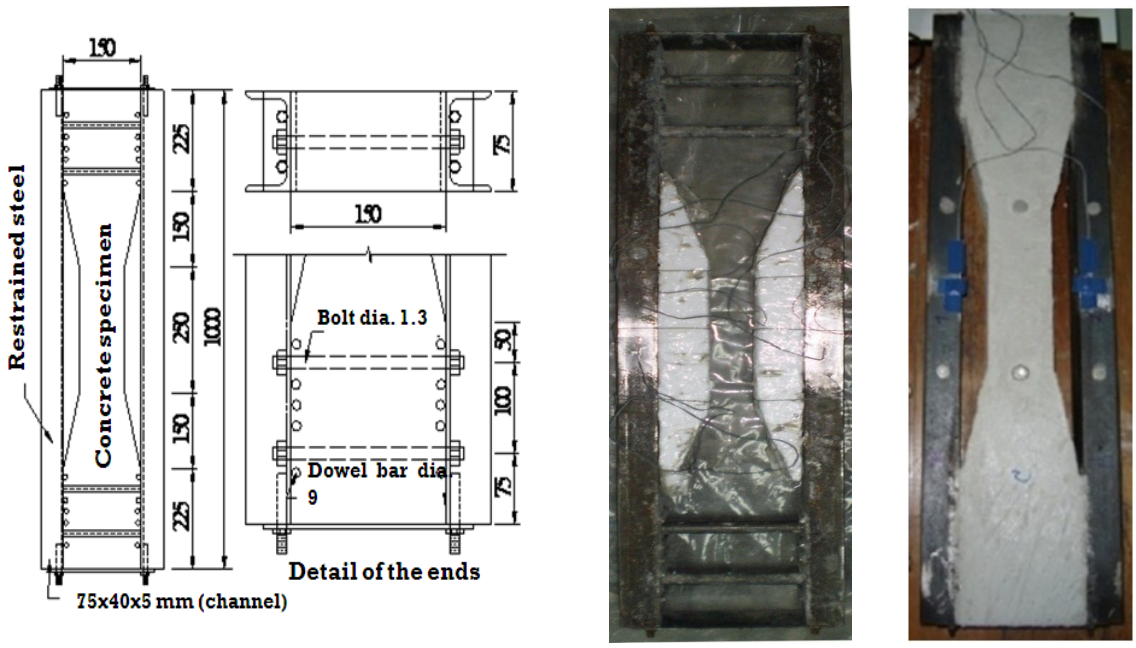

Figure 3-8 Externally restrained specimen (unit: mm)

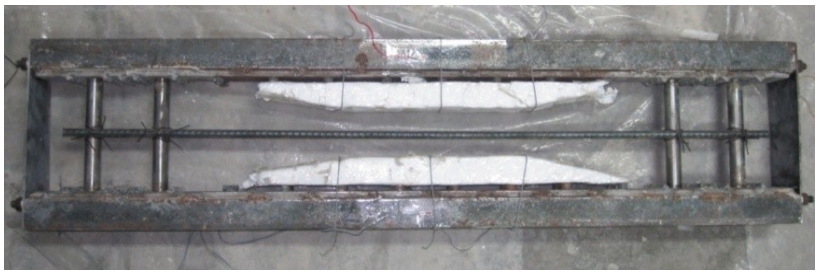

Figure 3-9 Frame used for testing net expansion under 1D combined internal and external restraint condition

3.6.4 Net expansion under multi-dimensional restraint condition

3.6.4.1 Net expansion under 2D restraint

Figure 3-10 demonstrates mould used for testing net expansion under 2D restraint. Expansion of concrete was restrained by a steel frame with 14.55% restraining steel ratio. At the same time, it was also restrained by steel bars (another direction) with 3.14% restraining ratio. Strain gages were well-positioned to 2 appointed bars and also attached to the steel frame along both sides. Two specimens were used for each mixture. The specimens were seal-cured in curing room with the temperature controlled at 28^{o}C and 75% humidity. The result of net expansion of each direction was the average of the measurement of strain gages in that direction.

3.6.4.2 Net expansion under 3D restraint

Figure 3-11 illustrates the model of mould used for testing 3D restraint condition. One main restraint direction was set with fixed restraining ratio of 4.52%. In order to study net expansion under 3D restraining condition, stirrup steel was varied with restraining ratios of 0.00%, 0.48%, 0.81% and 1.13% in transverse direction (other directions). Strain gages are well-positioned and attached on 2 bars. Two specimens were used for each mixture and 2 strain gages were used for each specimen. The specimens were seal-cured in curing room with the temperature controlled at 28^{o}C and 75% humidity. Data logger was used to record

expansion strain of specimens. The measurement of strain was initiated after casting. The result is the average of their measured values.

Figure 3-10 Model of specimen used for testing net expansion under 2D restraint

Figure 3-11 Model of specimen used for testing net expansion under 3D restraint

Chapter 4 Results and Discussion

4.1 Performance of expansive concrete

4.1.1 Free expansion of concrete with HEA

Figure 4-1 and Figure 4-2 indicate the free expansion of expansive concrete with different mix proportions. The tendency is apparent that the higher amount of expansive additives, the higher free expansion the expansive concrete produces. Especially, in the case that expansive additive is larger than 20 kg/m^3, free expansion increases so sharply that the specimen demonstrates some cracks on the surface of the specimens as can be seen in Figure 4-3. Beside that, free expansion remarkably increases when the amount of HEA rises from 10 kg/m^3 to 15 kg/m^3 in both cases of 20% and 30% fly ash replacement. It increases about 350μ when HEA is increased from 10 kg/m^3 to 15 kg/m^3 in both cases of fly ash replacement. But, the increase of free expansion was just 74μ and 193μ for fly ash replacement of 20% and 30%, respectively, when increasing HEA form 15 kg/m^3 to 20 kg/m^3.

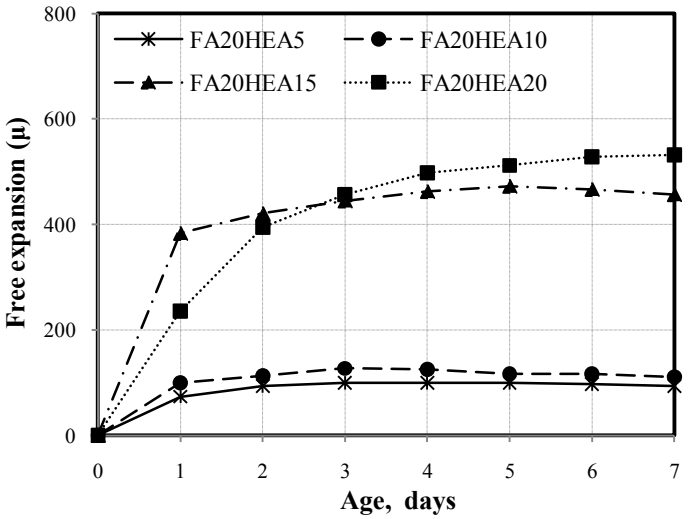

Figure 4-1 Free expansion of expansive concrete with 20 % FA

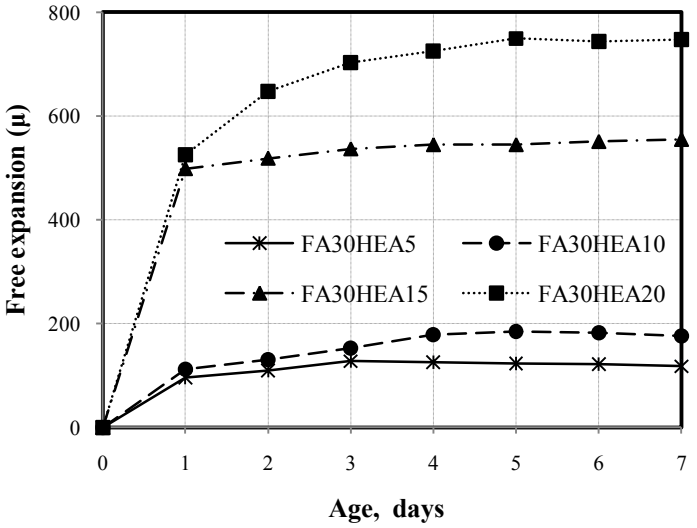

Figure 4-2 Free expansion of expansive concrete with 30 % FA

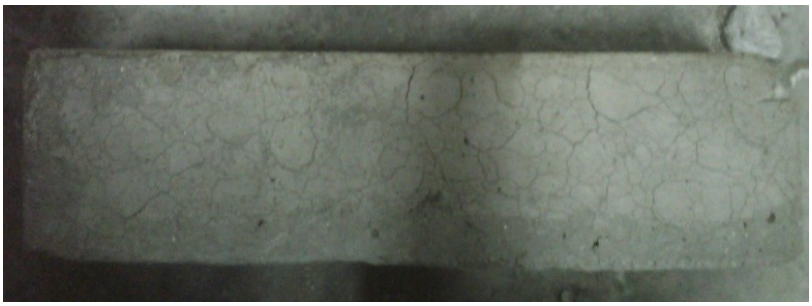

Figure 4-3 Cracks appear on the specimens using much HEA

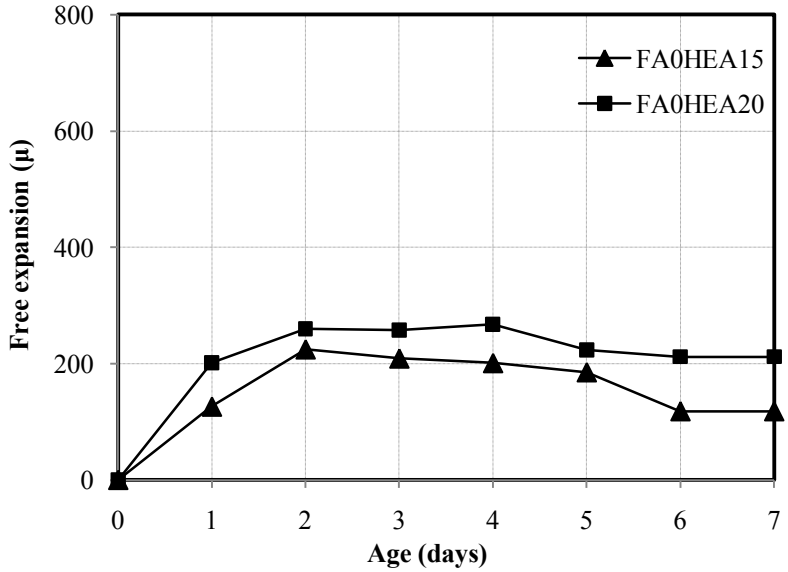

Figure 4-4 Free expansion of expansive concrete without FA

Fly ash is very effective for free expansion, especially when high amount expansive additive is used. The results showed that when the dosage of fly ash was increased from 20% to 30%, the free expansion of mixtures using 5 kg/m^3, 10 kg/m^3, 15 kg/m^3 and 20 kg/m^3 of HEA increased by 24μ, 71μ, 97μ and 216μ, respectively. Besides, it can be seen that free expansion of expansive concrete using 30% fly ash with 15 kg/m^3 and 20 kg/m^3 HEA is nearly 2 and 3 times, respectively larger than those of expansive concrete without fly ash (Figure 4-1, Figure 4-2 and Figure 4-4). This trend can be understood that fly ash leaves higher free water which is useful for the reaction between expansive agent and cement products. Thus, higher fly ash amount produces greater free expansion.

According to the measurements, free expansion period almost completely takes place in the first 3 days and it slowly increases after 3 days of curing. However, it seems not to increase when low dosage of HEA as 5kg/m^3 was used.

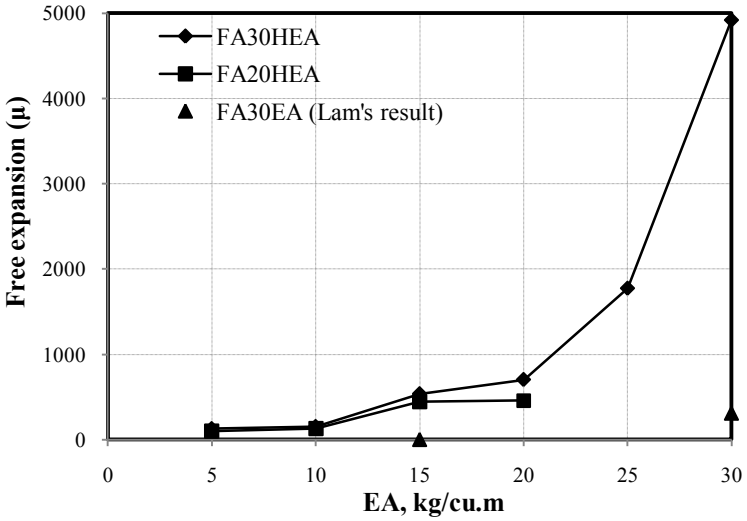

Figure 4-5 Comparing free expansion of HEA and EA expansive concrete at 3 days of age

Figure 4-5 showed the difference between free expansions of EA expansive concrete [21] and HEA expansive concrete. The results demonstrate that free expansions of HEA concrete are much higher than those of EA expansive concrete..

4.1.2 Compressive strength

4.1.2.1 Compressive strength in free condition

Tendency of compressive strength under free condition of expansive concrete is similar to compressive strength of normal concrete. Fly ash reduces compressive strength as can be seen in Figure 4-6. In the case of expansive concrete with 30% fly ash, the compressive strength is approximately 5 MPa lower than that of concrete with 20% fly ash at 28 days. This difference is larger at early ages. This phenomenon occurs because reaction of fly ash is slower than hydration of cement and its compressive strength strongly develops at long term. Therefore, at 7 days, compressive strength of expansive concrete mixtures, which use 30% fly ash, are much lower than those of expansive concrete using 20% fly ash. This difference becomes smaller after 28 days.

Dosage of HEA affects compressive strength under free condition as shown in Figure 4-6. The tendency shows that compressive strength in free condition is lower when amount of HEA is higher. It can be understood that the product of HEA is ettringite which causes lower strength. In addition, the expansion also leaves many microscopic voids inside concrete. Thus, HEA leads to the reduction of free compressive strength. The amount of HEA remarkably affects compressive strength under free condition when the amount of HEA is larger than 10 kg/m^3, especially in the case of 30% fly ash replacement.

Figure 4-7 shows the comparison of compressive strength under free condition of EA and HEA expansive concrete at 28 days. It is apparent that compressive strength under free condition of EA concrete is approximately 10 MPa greater than that of HEA concrete with same amount of expansive additive and fly ash. Even in the case of 20% fly ash replacement, compressive strength under free condition of HEA expansive concrete is lower than that of EA expansive concrete using 30% fly ash.

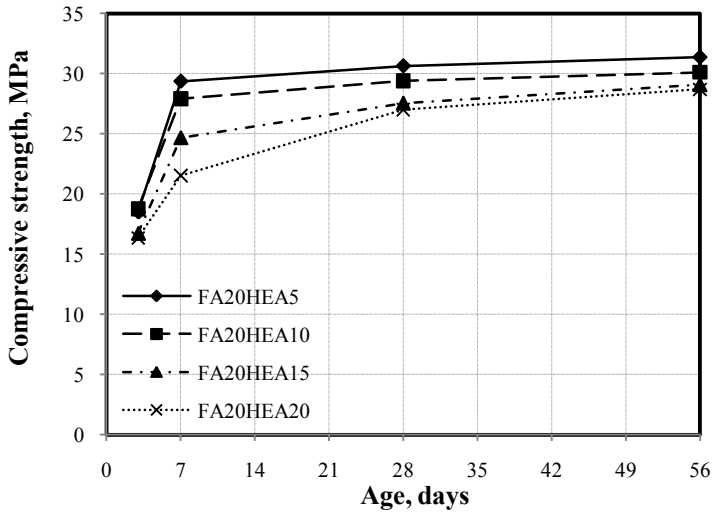

a) Expansive concrete with 20% FA

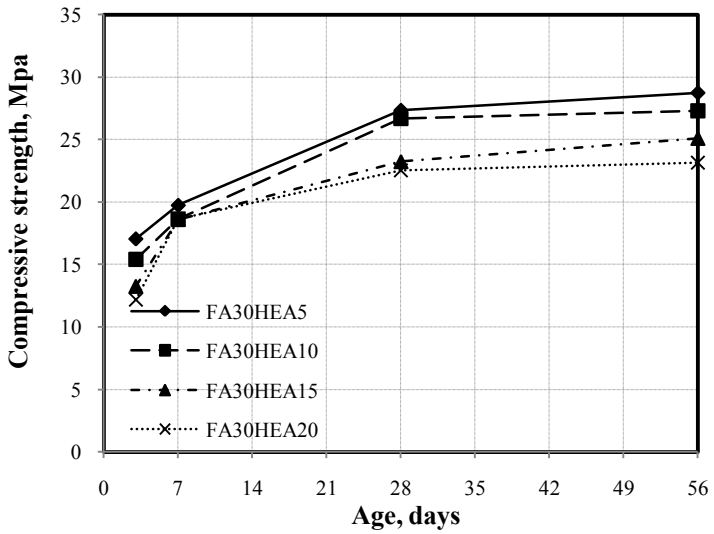

b) Expansive concrete with 30% FA

Figure 4-6 Compressive strength development of expansive concrete in free condition

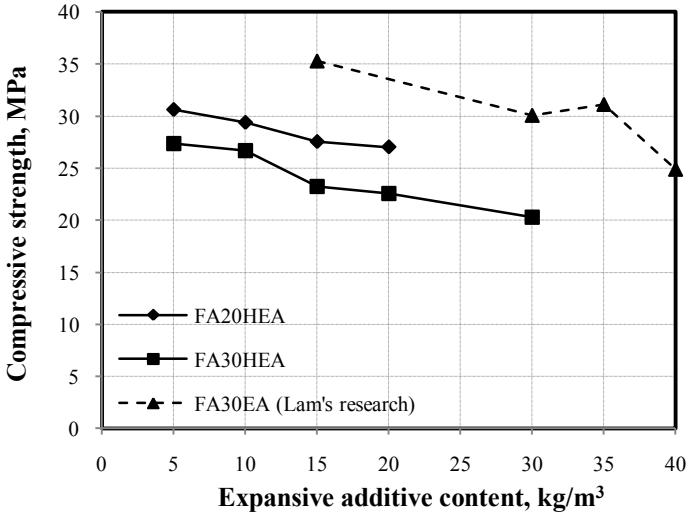

Figure 4-7 Compressive strength of EA and HEA expansive concrete at 28 days in free condition

4.1.2.2 Compressive strength in restrained condition

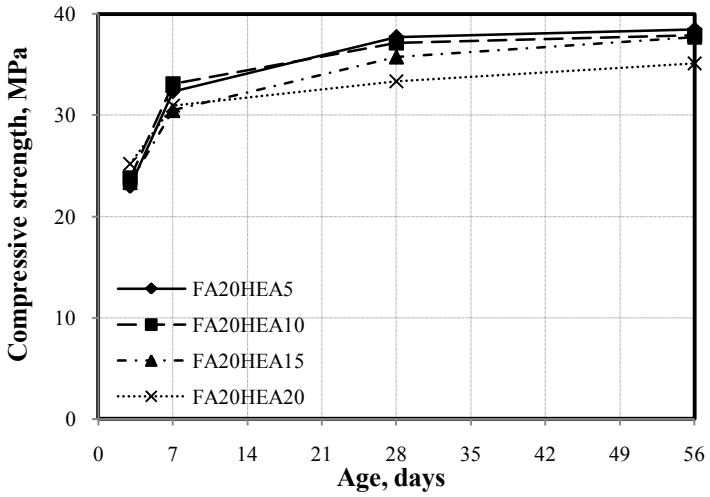

a) Expansive concrete with 20% FA

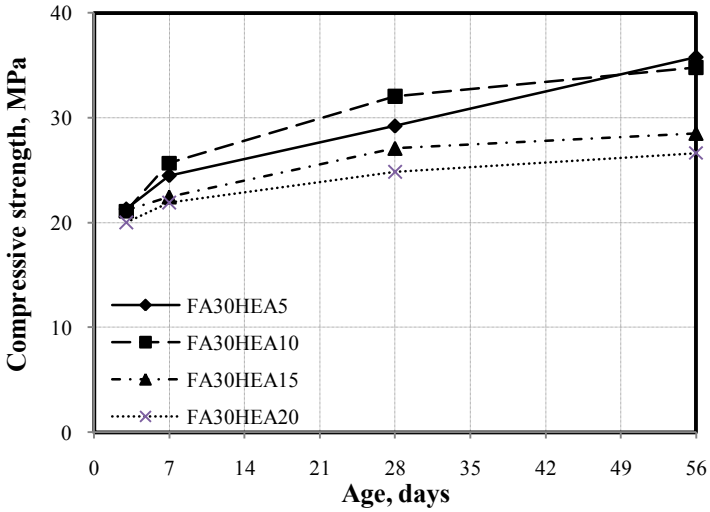

b) Expansive concrete with 30% FA

Figure 4-8 Compressive strength development of expansive concrete under restraint

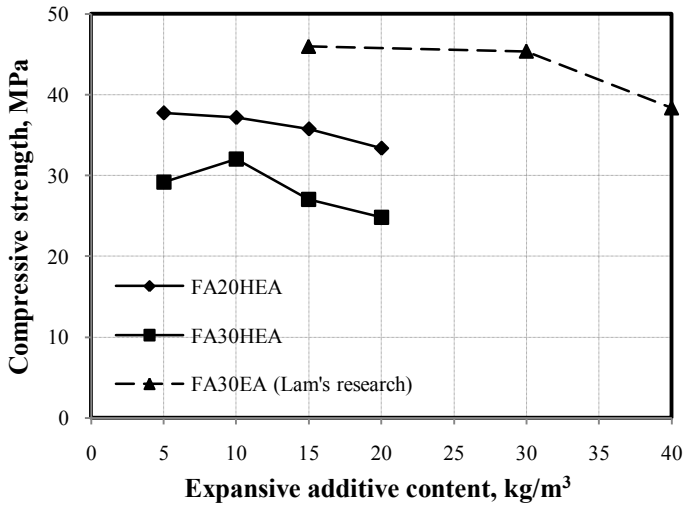

Figure 4-9 Compressive strength of EA and HEA expansive concrete at 28 days in restrained condition

Figure 4-8 illustrates the results of compressive strength in restrained condition. The results demonstrate that under restraint, compressive strengths are much higher than those in the case of free expansion. Especially, in the case of 20% fly ash replacement, compressive strength under restraint condition is about 7MPa higher than that of the free condition.

Under restraint, the amount of HEA still affects compressive strength. Higher HEA dosage results in lower compressive strength. However, in some cases such as 5 kg/m^3 and 10 kg/m^3 HEA, compressive strength is not much different at both 20% and 30% fly ash replacement. In both cases of fly ash, compressive strength of mixes which using 5kg/m^3 HEA just higher than the mixes using 10kg/m^3 HEA at long ages (28 and 56 days) beforehand compressive strength of mixes 5kg/m^3 HEA is not larger than that of 10kg/m^3 HEA .

Figure 4-9 illustrates the comparison of compressive strength under restraint condition of EA and HEA expansive concrete at 28 days. It can be seen that even EA concrete contains larger amount of fly ash and expansive additive, their restrained compressive strength are higher than those of HEA concrete.

4.1.3 Tensile strength & cracking strain

4.1.3.1 Tensile strength

The results of tensile strength are shown in Figure 4-10. In both cases of fly ash replacement, tensile strength is negatively affected by the amount of HEA. The tensile strengths of expansive concrete using 20% fly ash are approximately 0.23 MPa, 0.43 MPa and 0.19 MPa smaller when the amount of HEA increases from 5 kg/m^3 to 10 kg/m^3, 15 kg/m^3 and 20 kg/m^3, respectively at any time. However, in the case of 30% fly ash replacement, the difference depends on the age of expansive concrete.

The results illustrate that the tensile strength becomes much lower when the amount of expansive additive is larger than 10 kg/m^3. This phenomenon has close relationship with the results of free expansion. Free expansion is much larger when HEA is increased from 10 kg/m^3 to 15 kg/m^3. Tensile strength also shows great reduction when HEA is increased from 10 kg/m^3 to 15 kg/m^3.

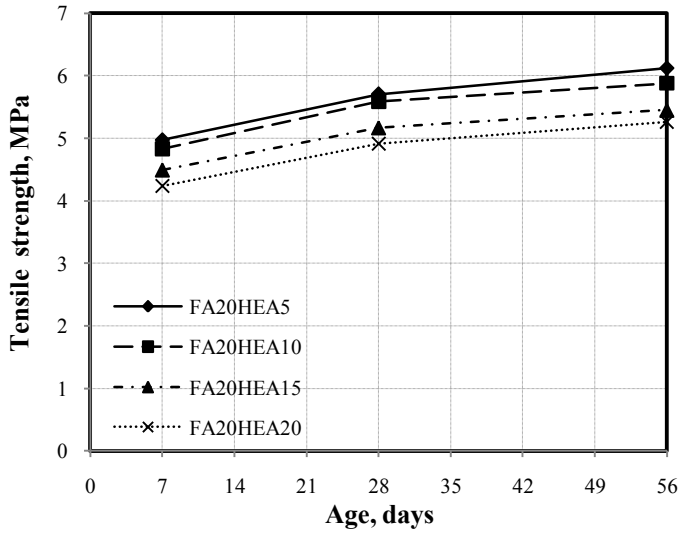

a) Expansive concrete with 20% fly ash

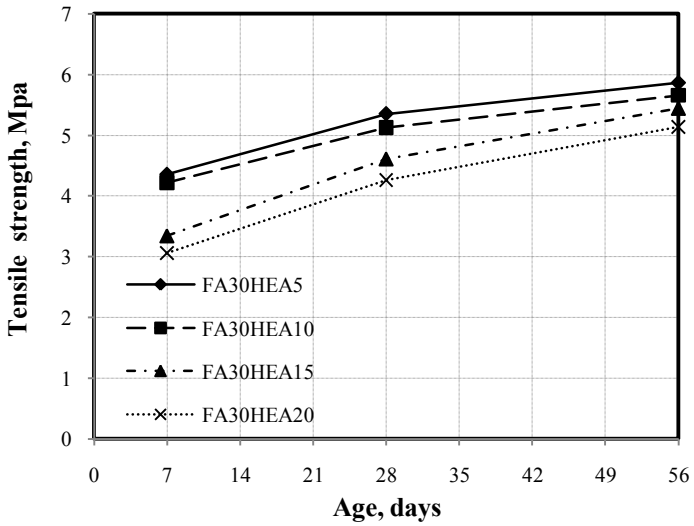

b) Expansive concrete with 30% fly ash

Figure 4-10 Tensile strength of expansive concrete

4.1.3.2 Cracking strain

Figure 4-11 shows the results of cracking strain of expansive concrete using HEA at 7 days to 56 days. The results indicate that the amount of HEA causes the reduction of cracking strain. Cracking strain of the mixes using 5kg/m^3 is larger than those of the others. Especially, in the case of 30% fly ash replacement, cracking strain is approximately 30μ smaller when increasing the amount of expansive additive from 5kg/m^3 to 10kg/m^3 at every ages of testing. While, in the case of 20% fly ash replacement, this difference is just around 15μ at 28 days and 56 days.

In the case of 20% fly ash, the amount of HEA in the range of 10kg/m^3 to 20kg/m^3 just slightly influences cracking strain. In the case of 30% fly ash replacement, cracking strain of the mix using 10kg/m^3 and 15kg/m^3 of HEA is slightly different. But, it drops about 30μ when expansive additive rises to 20kg/m^3.

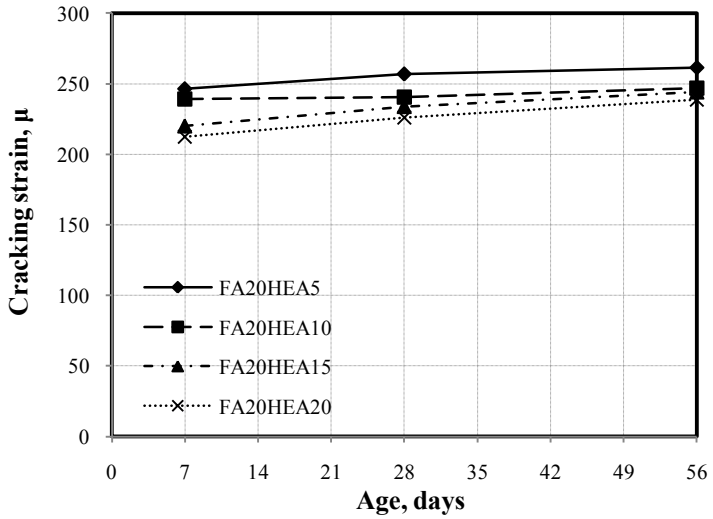

a) Cracking strain of expansive concrete with 20% fly ash

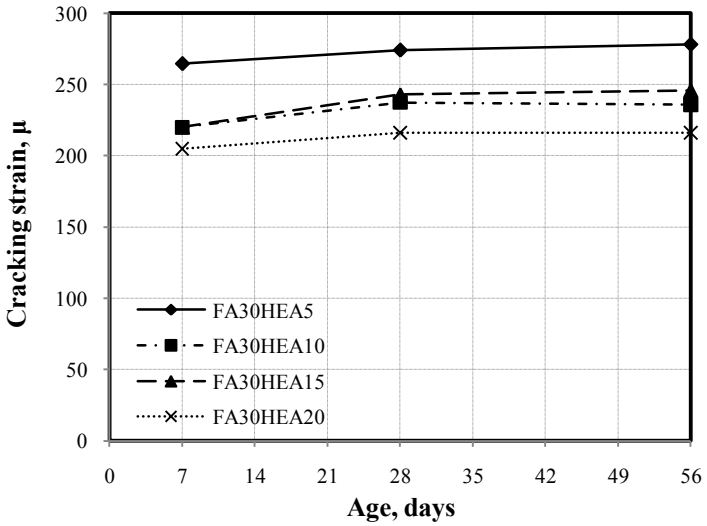

b) Cracking strain of expansive concrete with 30% fly ash

Figure 4-11 Cracking strain of expansive concrete

Fly ash slightly impacts the development of cracking strain. For mixes using 20% fly ash, cracking strain still increases slightly at 56 days. While, in the case of 30% fly ash replacement, cracking strain seems to stay constant at long term (after 28 days). On the other hand, cracking strains of expansive concrete with 20% fly ash is slightly higher than those of expansive concrete with 30% fly ash.

4.2 Net expansion/shrinkage of UHSFRM

The results of net expansion/shrinkage of UHSFRM are shown in Figure 4-12 and Figure 4-13. The results illustrate that 10% EA could induce net expansion in specimens. Especially, in the case of 15% EA, the specimen highly expanded. It went up to approximately 630μ and 1070μ at 1 day for specimens with 1% 13mm steel fiber and 1% 6mm steel fiber.

According to the results, 13-mm fiber might produce more restraining effect than that of 6-mm fiber. In the case of without EA, the restrained shrinkage of 6mm steel fiber is around 730μ at 14 days, while that of 13mm steel fiber is approximately 380μ. Besides that, the net expansion for SF(13mm)EA10% and SF(13mm)EA15% are around 290μ and 630μ, respectively. Whereas, those of SF(6mm)EA10% and SF(6mm)EA15% are approximately 390μ and 1070μ, respectively. This phenomenon might be because, when volume of fiber steel is equal, the shorter fiber steel is distributed widely and leave much gap among fibers due to discontinuity. In contrast, longer fiber steel produce continuous restraint as well as the gap among fibers is less. Therefore, in the case of 6-mm fiber, UHSFRM shrinks or expands easier than the case of 13-mm fiber.

Regardless of dosage of EA, net expansion of UHSFRM seems to be maximum at 1 day. Low w/b causes the limited reaction of EA and water. However, under curing, at the age 14 days, UHSFRM stayed constant in expansion both in the cases of using 10% and 15% EA.

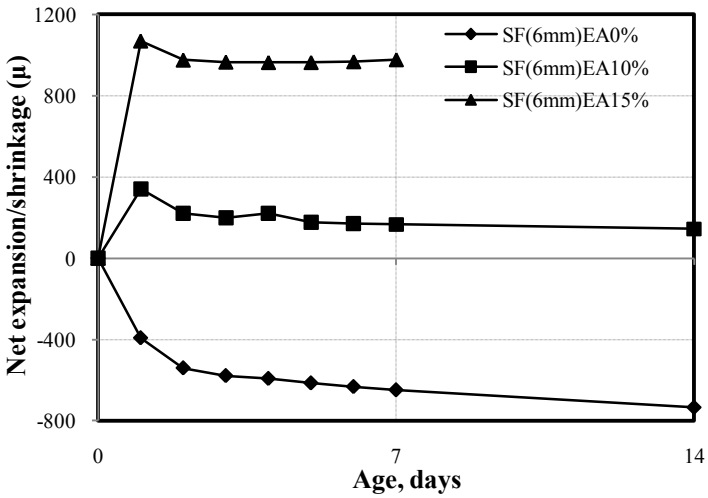

Figure 4-12 Net expansion/shrinkage of UHSFRM using 1% 6 mm steel fiber

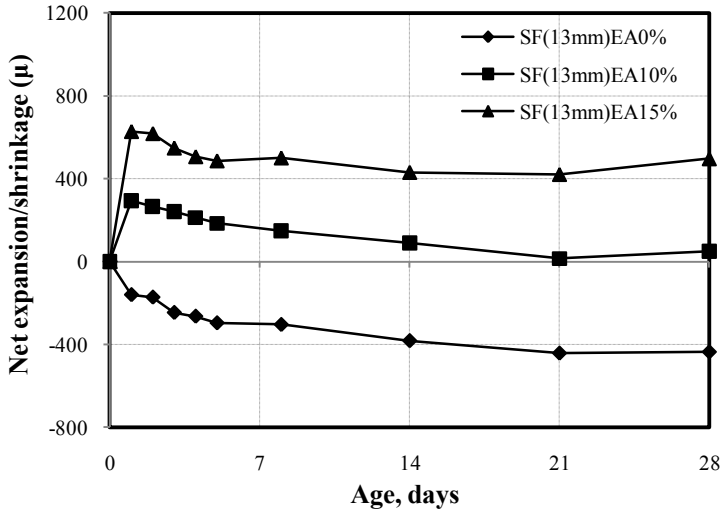

Figure 4-13 Net expansion/shrinkage of UHSFRM using 1% 13 mm steel fiber

4.3 Expansion of expansive concrete under restraint

4.3.1 Net expansion under 1D internal restraint

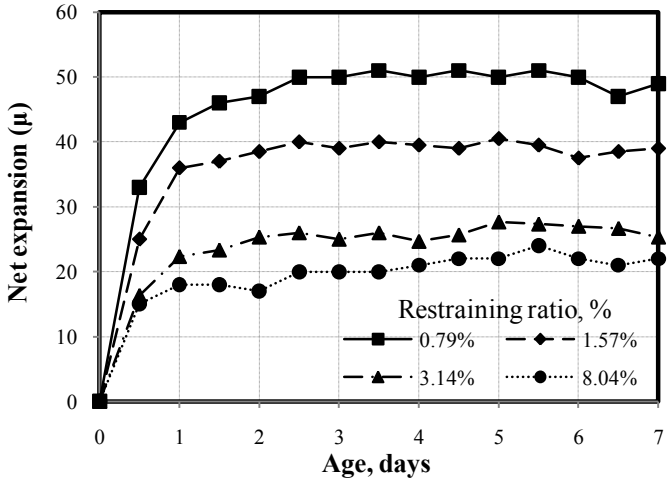

a) Net expansion of FA20HEA5

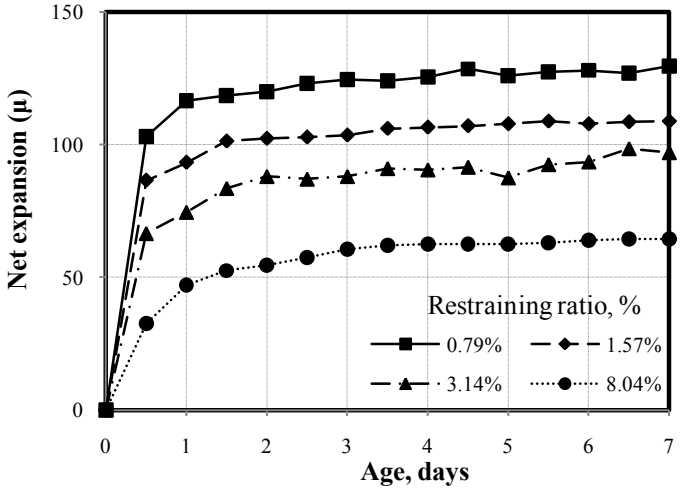

b) Net expansion of FA20HEA15

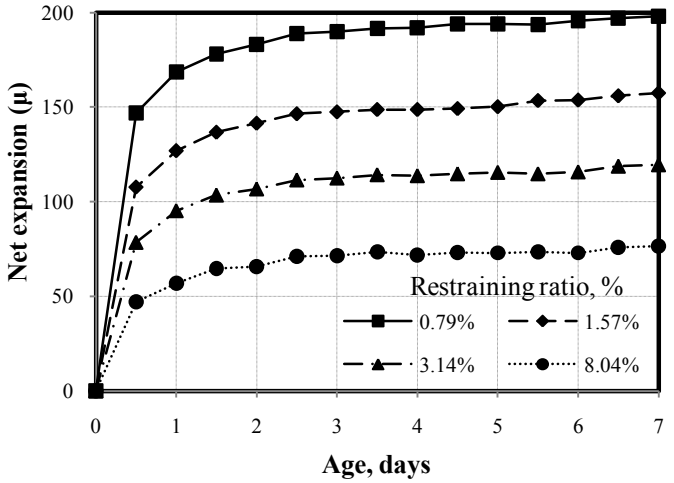

c) Net expansion of FA20HEA20

Figure 4-14 Net expansion of expansive concrete using 20% fly ash under 1D internal restraint during curing period

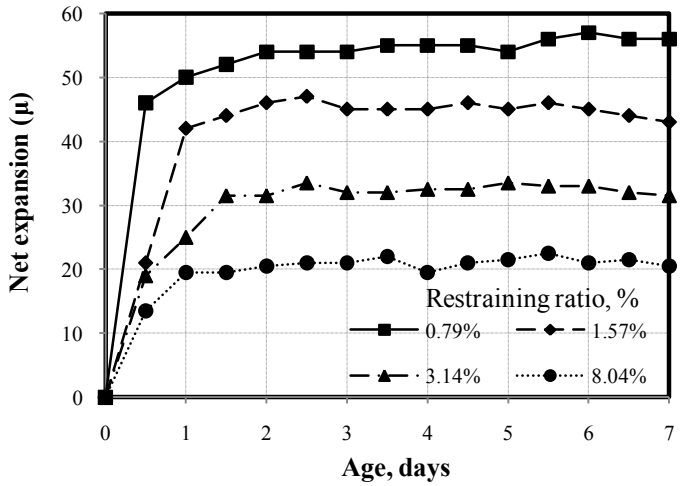

a) Net expansion of FA30HEA5

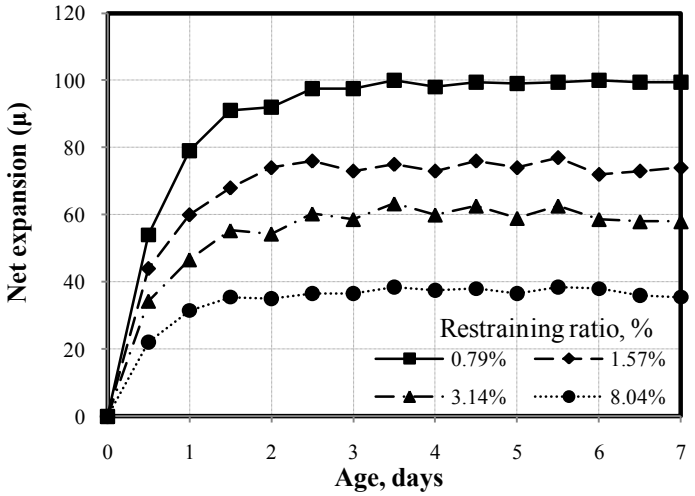

b) Net expansion of FA30HEA10

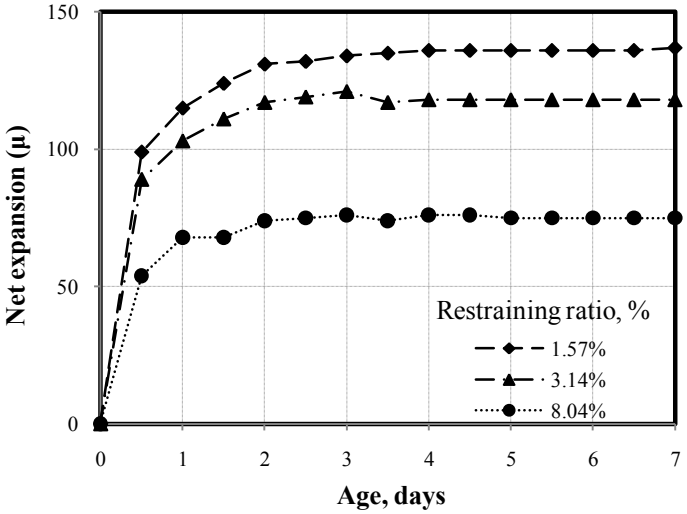

c) Net expansion of FA30HEA15

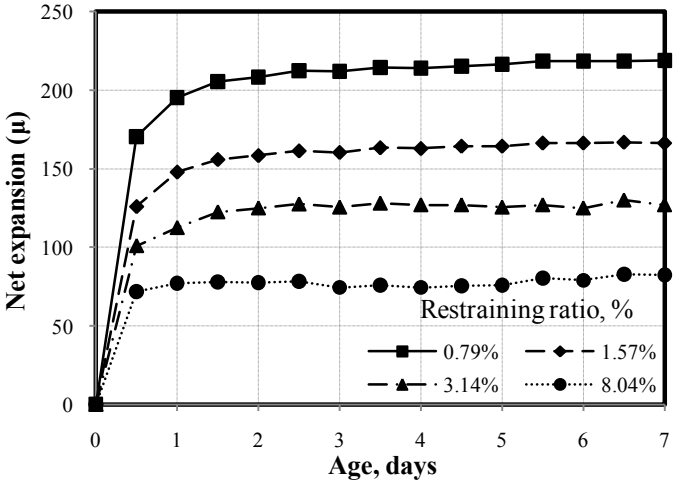

d) Net expansion of FA30HEA20

Figure 4-15 Net expansion of expansive concrete using 30% fly ash under 1D internal restraint during curing period.

The net expansions during curing period are shown in Figure 4-14 and Figure 4-15. The net expansion mostly takes place at early ages (2 days) and is almost stable afterwards (in curing condition).

According to Figure 4-16, the net expansion of expansive concrete increased remarkably when the amount of HEA expansive additive was in the range of 10 kg/m^3 to 15 kg/m^3 HEA at all restraining ratios. These phenomena are similar to the case of free expansion but the magnitude is much less than those of the free condition. The results also showed that the higher expansive additive produces the higher net expansion. Furthermore, net expansion much depends on restraining ratio. The results indicate that higher restraining ratio produces lower net expansion. This phenomenon is obvious in the case of high dosage of HEA.

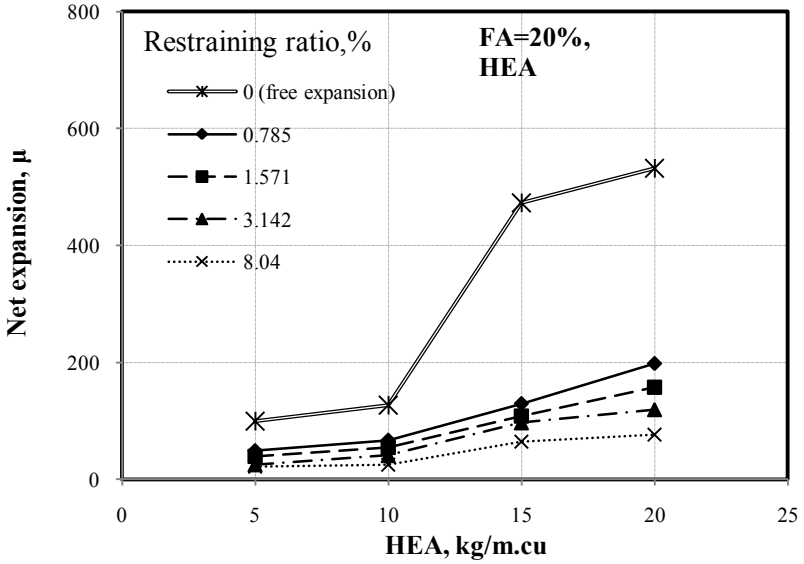

a) Net expansion of concrete with 20% fly ash and HEA

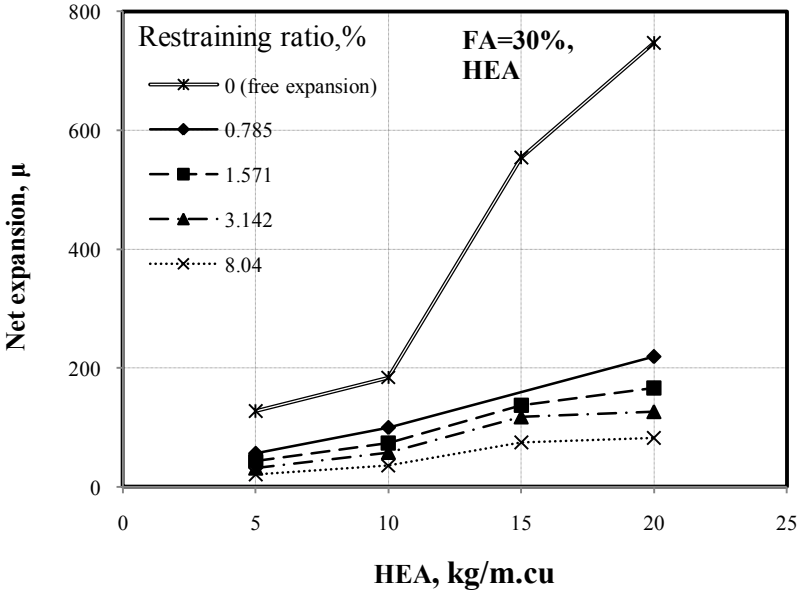

b) Net expansion of concrete with 30% fly ash and HEA

Figure 4-16 Relationship between dosage of HEA and internal net expansion

Figure 4-16 indicates that fly ash slightly increases net expansion. Comparing the cases of similar dosage of HEA, concrete with 30% fly ash replacement gives larger net expansion than those with 20% fly ash replacement.

Experimental data show that the mixtures FA30HEA20 and FA30EA30 demonstrate similar free expansion (755μ [21] and 747μ, respectively). However, the mix with 30 kg EA produces larger net expansion than the mix of 20 kg HEA in all restraining ratios, especially, at restraining ratio lower than 1.57% (see Figure 4-17).

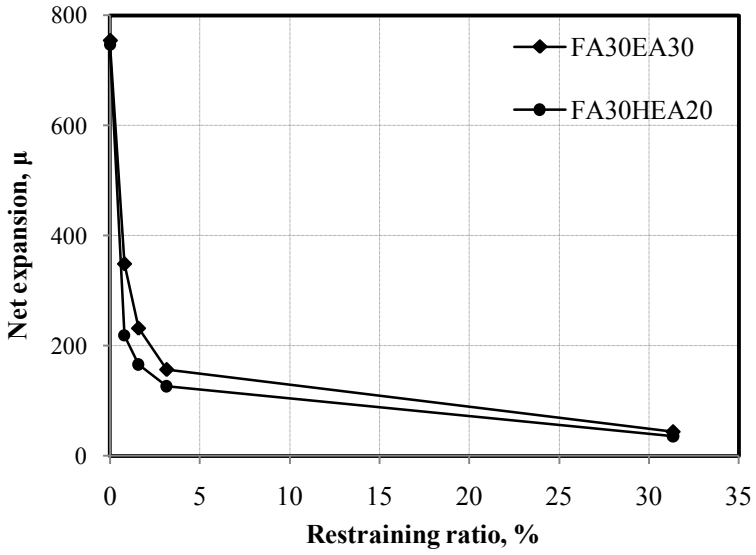

Figure 4-17 Comparing net expansion of FA30HEA20 and FA30EA30

4.3.2 Net expansion under 1D external restraint

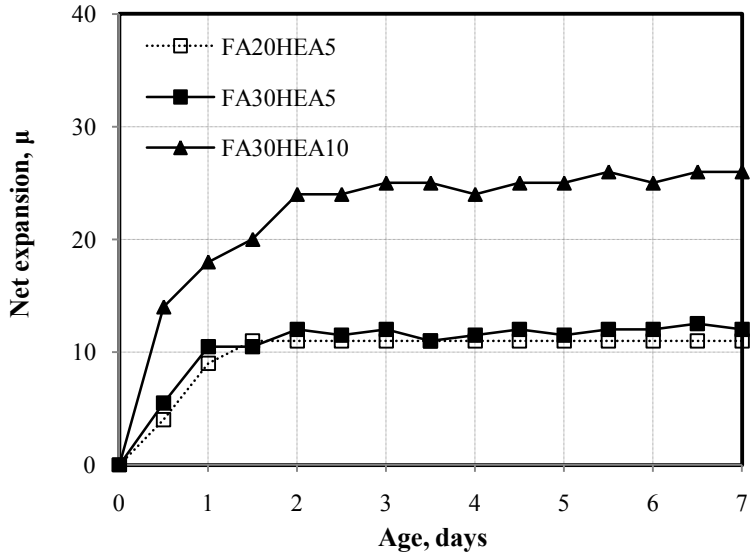

Figure 4-18 Net expansion under 22.04% 1D external restraint during curing period

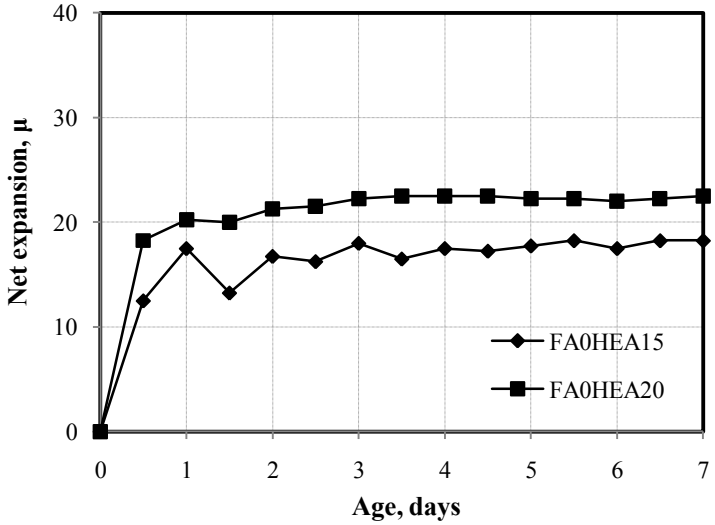

a) HEA concrete without fly ash

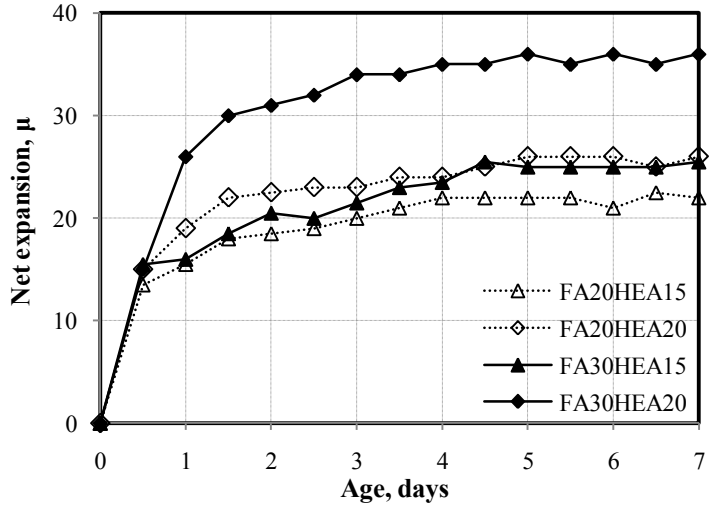

b) HEA concrete with fly ash

Figure 4-19 Net expansion under 31.35% 1D external restraint during curing period

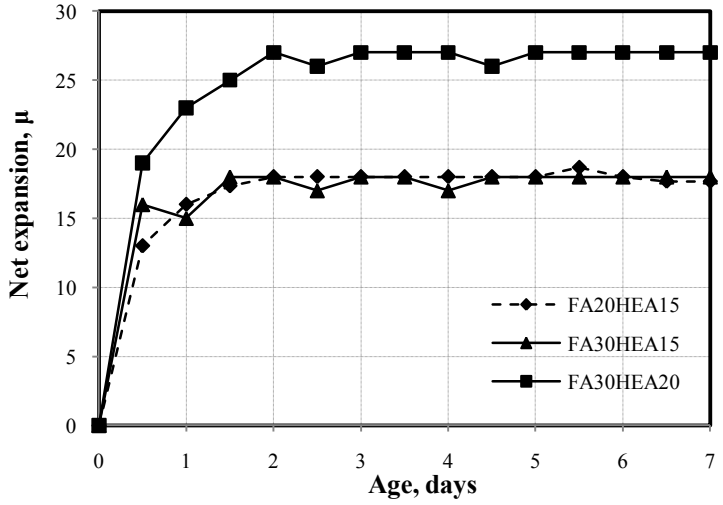

Figure 4-20 Net expansion under 51.25% 1D external restraint during curing period

Net expansions under 1D external restraint are shown in Figure 4-18, Figure 4-19 and Figure 4-20. It can be seen that the tendencies are similar to the case of internal restraint. Higher HEA produces larger net expansion under external restraint. However, fly ash just has a small effect on net expansion under external restraint. In addition, the higher restraint produces lower net expansion under external restraint. In the case of external restraint experiment, the external restraining steel ratio was very high, hence, the effect of the amount of HEA or fly ash and restraining ratio are not as large as those of internal restraint cases. The net expansion under external restraint almost completed within 2 days. Afterwards, it just slightly expanded or became constant when HEA was lower than 20kg/m^3.

Figure 4-21 indicates net expansion under 1D internal restraint and external restraint at 7 days of curing. The results show that at restraining ratio lower than 8.04%, net expansion strongly reduces when restraining ratio is increased. Rate of reduction net expansion with higher restraining ratio is lower when restraining ratio is larger than 8.04%.

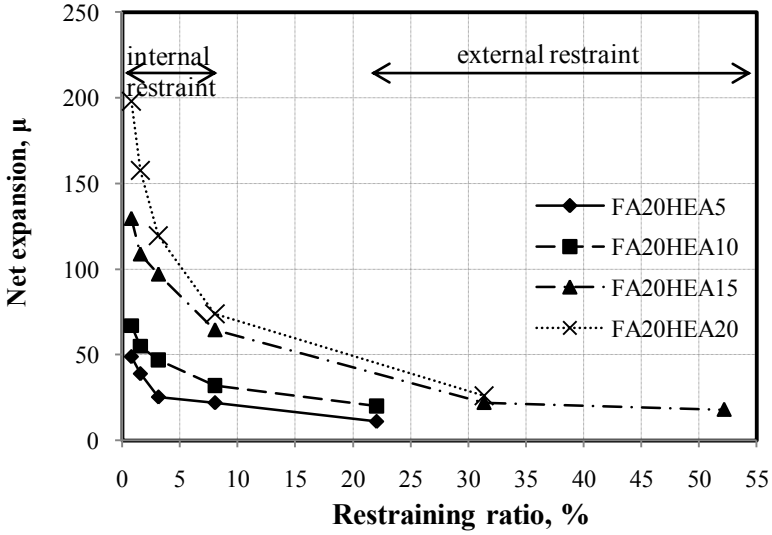

a) HEA concrete using 20% fly ash

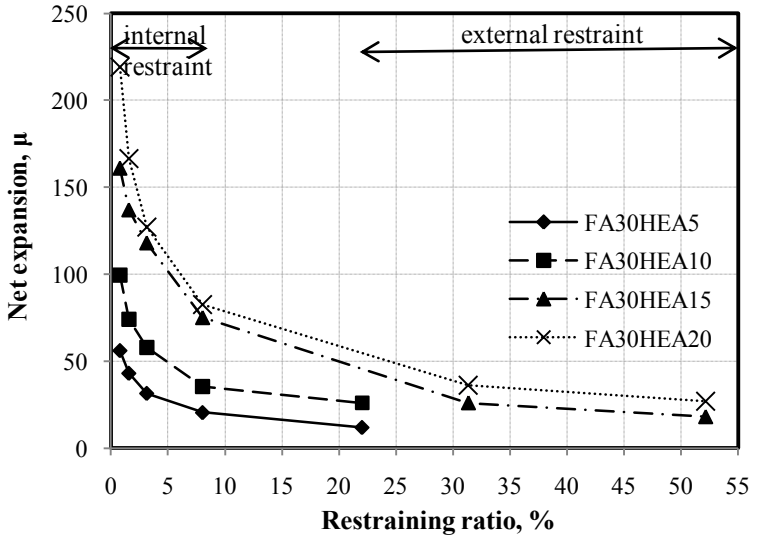

b) HEA concrete using 30% fly ash

Figure 4-21 The relationship between net expansion under internal and external restraint and restraining ratio at 7 days

4.3.3 Net expansion under 1D combined external and internal restraint

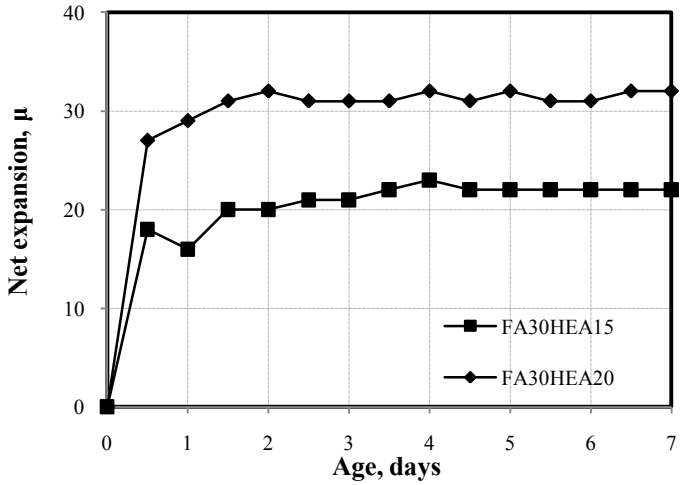

a) Net expansion under 1D 31.35% external and 2.17% internal restraint

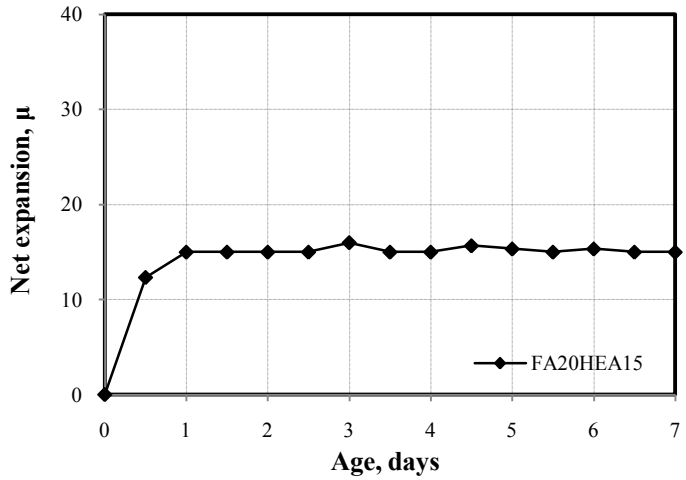

b) Net expansion under 1D 51.25% external and 2.17% internal restraint

Figure 4-22 1D net expansion under combined external and internal restraint condition

1D combined internal and external net expansion results are shown in Figure 4-22. In comparison, the net expansions in Figure 4-22a experiment are smaller than those in Figure 4-19 for the 31.35% external restraining ratio. Besides, the net expansion of mix FA20HEA15 in Figure 4-22b is smaller than that in Figure 4-20b for the 51.25% external restaint. These reductions are caused by the supplement of internal restraint.

The results under combined external and internal restraint of Figure 4-22a are close to the interpolated results of Figure 4-21b. On the other hand, the results in Figure 4-22b are close to the extrapolated results of Figure 4-21a. Thus, the tendency of net expansion in combined restraint condition may be similar tendency of only internal and external restraint. Therefore, the net expansion in combined restraint can be estimated in the same way as the case of external or internal restraint.

4.3.4 Net expansion under multi-directional restraint

Figure 4-23 describes the progress of net expansion of mix FA30HEA20 which is tested under single and multi directional restraints.

In the case of 2D restraining condition (Figure 4-23a), the net expansion at direction of 3.14% restraining ratio produces the similar results with the specimen under 1D restraint which is also restrained at 3.14%. In the other restraining direction, the net expansion is around 66μ with restraining ratio of 14.55%. This value is close to an interpolated value from Figure 4-21b which is for 1D restraint.

In the case of 3D restraining condition (Figure 4-23b), although restraining ratios of stirrup are varied, specimens produce the similar net expansion at main direction where they have the same restraining ratio of 4.52%. In addition, these values are very close to those of 1D restraint with the same restraining ratio.

It seems that the net expansion along direction is not affected by other restraint directions. It allows the prediction of the net expansion for 2D and 3D restraint by just applying the same method with the case of 1D restraint.

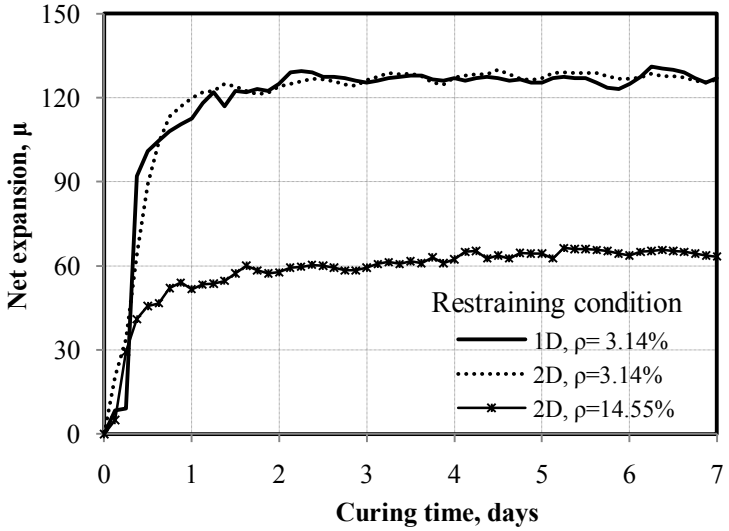

a) Net expansion of 1D and 2D restraint

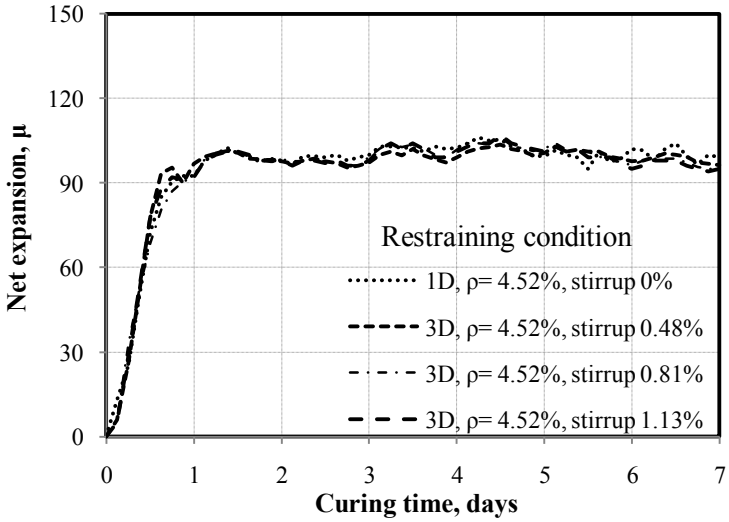

b) Net expansion of 1D and 3D restraint

Figure 4-23 Net expansions of single and multi-directional restraint of mix FA30HEA20

4.3.5 Prediction of net expansion

Based on the experimental data, the relationship between net expansion at 7 days of curing and the amount of Hyper expansive additive, fly ash as well as restraining steel ratio can be estimated by Equation (4-1). The prediction of net expansion was calculated as shown in Figure 4-24. The differences between prediction and actual net expansion are shown in Figure 4-25.

$$\varepsilon_{exp,net}^{t7} = (136\ln(0.023\mathrm{HEA}+1)+1)^{1.11}(0.0004\rho^3+0.025\rho^2+0.2\rho+0.1)^{-0.44}.2^{0.0011FA.HEA} \quad (4\text{-}1)$$

Where

$\varepsilon_{exp,net}^{t7}$: net expansion at 7 days of curing, μ

HEA : amount of Hyper expansive additive, kg/m^3

FA : amount of fly ash, % of total binder

ρ : restraining steel ratio, %

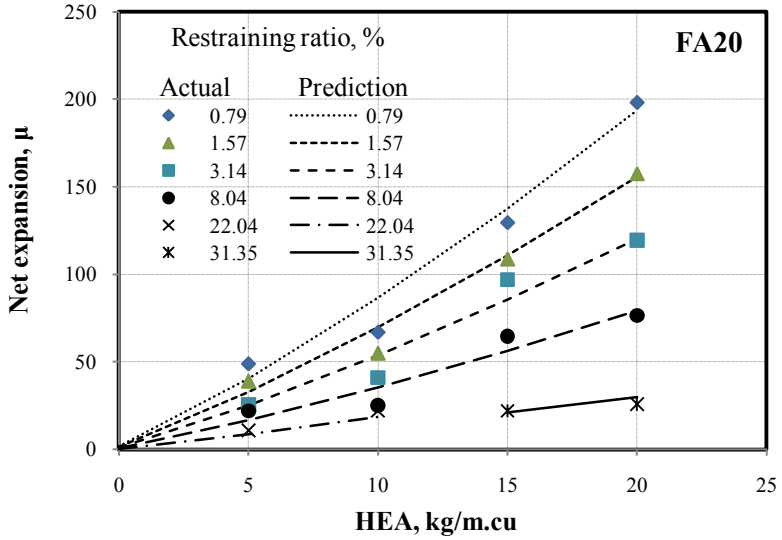

a) Expansive concrete with 20% fly ash

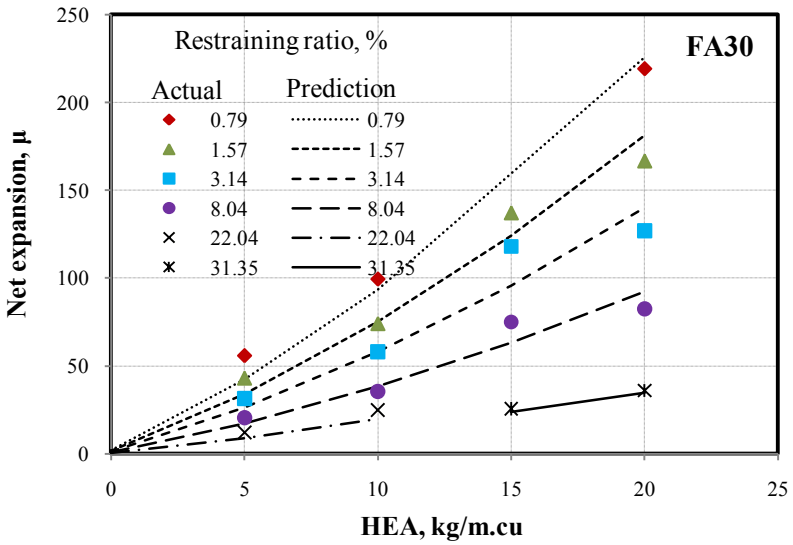

b) Expansive concrete with 30% fly ash

Figure 4-24 Prediction of net expansion at 7 days of curing

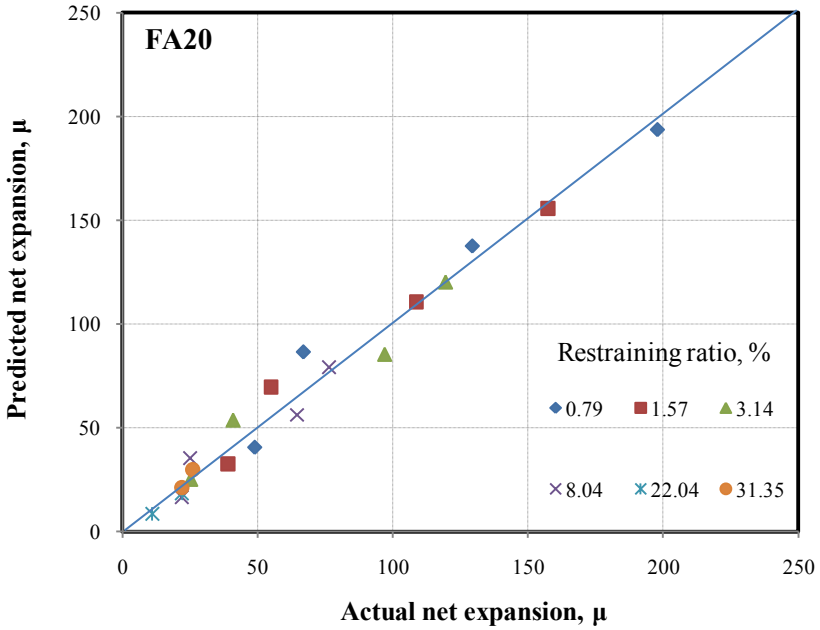

a) HEA concrete with 20% fly ash

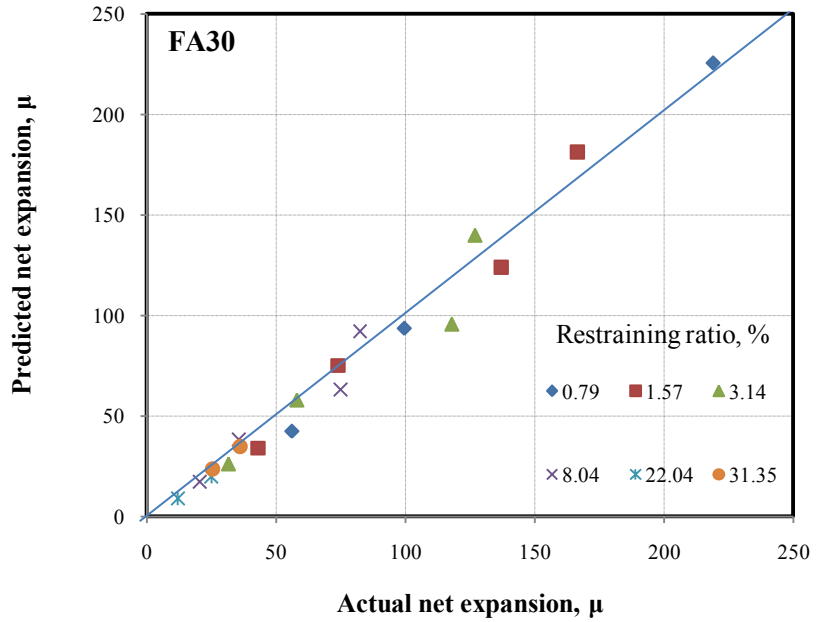

b) HEA concrete with 30% fly ash

Figure 4-25 Comparison between prediction and actual net expansion

This prediction can also be applied to 2D or 3D restraint condition because the experiment indicated that the net expansion was not affected by other directions of restraint.

In reality, the net expansion might be changed due to the differences in paste content, water to binder ratio and curing condition. Thus, the outcome from prediction should be taken into account by those factors. Therefore, the real net expansion should be obtained by Equation 4-2:

$$\varepsilon_{exp,net}^{(real)}(t) = \varepsilon_{Net,exp}^{t7} . K_{\gamma} . K_{W/B} . K_{curing} . K_T . K_t \quad (4\text{-}2)$$

Where

$\varepsilon_{exp,net}^{t7}$: net expansion at 7 days of curing

K_γ : coefficient for paste content

$K_{W/B}$: water to binder coefficient

K_{curing} : curing type coefficient

K_T : temperature coefficient

K_t : curing time coefficient

Gamma coefficient (K_γ) depends on the amount of cement paste. The higher cement paste content is, the higher expansive products can be generated (for the same ratio of expansive additive replacement). Besides, aggregate content, whose volume is not changed, is reduced when the paste content is increased. Hence, the net expansion shall be greater with increasing paste content. The concrete mixtures used in the tests in this study were designed to have γ equal to 1.3. Thus, K_γ is larger than 1 with γ is higher than 1.3 (the same ratio of expansive additive replacement) and vice versa, it less than 1 when γ is lower than 1.3.

Water to binder coefficient ($K_{W/B}$) also affects the expansion capacity of expansive concrete under restraint. According to Lam [21], the higher water to binder ratio leads to the greater free expansion. Hence, $K_{W/B}$ should be higher than 1 when W/B is larger than 0.5; in contrast, it is lower than 1 when W/B is less than 0.5.

Curing type coefficient (K_{curing}) affects the expansion of expansive concrete. Results in [21] indicated that the free expansion was good under seal or water-air curing but was reduced for air curing. Hence, the net expansion will be adjusted for different type of curing. Beside that, temperature is an important factor that should be taken into account for expansion. The results showed that the expansion increased with higher temperature [8]. The tests in this study were conducted at 28°C and seal curing. Temperature coefficient (K_T) thus should be adjusted in the future for different temperature of curing.

Expansive concrete may be cured with different curing duration other than 7 days. According to the experimental results, net expansion seems to stop after 7 days curing, hence, it can be assumed that net expansion in case of curing longer than 7 days is equal to net expansion at 7 days. If concrete is cured less than 7 days, curing time coefficient (K_t) should be taken into account.

In this research, the net expansion of HEA expansive concrete was studied with some constant parameters such as paste content, water to binder ratio, and curing condition. The results will be different if those parameters are changed (see analysis in 4.3.5). Therefore, in order to apply the prediction of net expansion widely, the net expansion should be studied further by varying those parameters.

Chapter 5 Prediction of Shrinkage Cracking Age

5.1 Shrinkage cracking analysis

In this study, shrinkage cracking is defined as a visible crack caused by shrinkage which may allow ingress of deteriorating substance and reduce durability of reinforced concrete.

To analyze cracking age of concrete, experimental studies on concrete specimens under restraining condition were carried out to evaluate cracking resistance in term of cracking age. Results of conventional concrete were obtained from Lam [21] (with mixtures of w50 and w50FA30) and Tongaroonsri [29] (with mixtures of w35, w55, w55FA30 and w55FA50). This research studied shrinkage cracking age of both conventional concrete and expansive concrete. Ten mixes of expansive concrete with HEA were tested as described in 3.3.1 and referred to Lam [21] for 2 mixes of EA expansive concrete (FA0EA30 and FA30EA30).

5.1.1 Shrinkage cracking of expansive concrete

In the case of expansive concrete, the analysis can be divided into two periods; expansion period and shrinkage period. Figure 5-1 shows the mechanisms of expansive concrete during expansion period. With restraint, the net expansion strain ($\varepsilon_{exp,net}$) of the concrete become smaller than the free expansion ($\varepsilon_{exp,free}$) of the same concrete.

5.1.1.1 Expansion period

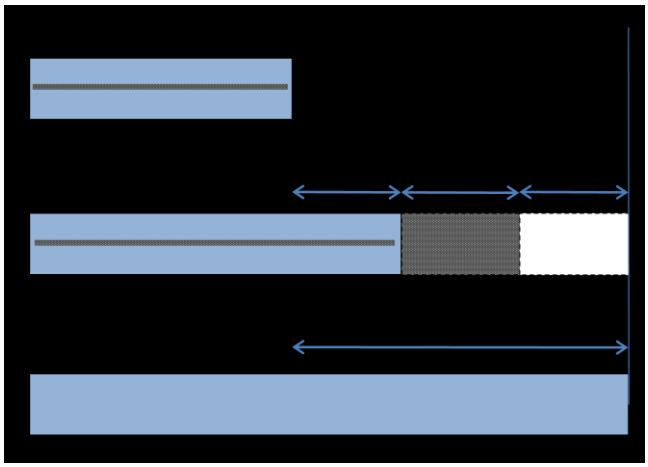

Figure 5-1 Conceptual illustration of expansion mechanism of expansive concrete under restraint

Where

$\varepsilon_{exp,free}$: Free expansion

$\varepsilon_{exp,net}$: Net expansion

$\varepsilon_{c,e}$: Elastic strain in compression

$\varepsilon_{c,p}$: Plastic strain

+ *Stress strain relation (Hook's law) for reinforcing steel:*

$$\sigma_s(t) = E_s . \varepsilon_{exp,net}(t) \quad (5\text{-}1)$$

+ Stress strain relation (Hook's law) for concrete:

$$\sigma_{c,e}(t) = E_c(t) . \varepsilon_{c,e}(t) \quad (5\text{-}2)$$

Where
$\sigma_s(t)$ and $\sigma_{c,e}(t)$: the stresses produced in steel bar and concrete at any time t during curing time, respectively.
E_s : the modulus of elasticity of steel, (MPa)
$E_c(t)$: the modulus of elasticity of concrete at any time t, (MPa)
t: age of concrete, (days)

+ During this expansion period, stress is assumed to be uniform over concrete cross-section. The compression in concrete is balanced by the tension in the reinforcement or restraining objects as described by force equilibrium in Equation (5-3)

$$\sigma_s(t) . A_s = \sigma_{c,e}(t) . A_c \quad (5\text{-}3)$$

Where
A_s and A_c : the cross-sectional area of steel bar and concrete, respectively.

+ Substitute Equation (5-1) and (5-2) into the force equilibrium (5-3), the elastic strain ($\varepsilon_{c,e}$) in concrete during the expansion period can be estimated from Equation (5-4).

$$\varepsilon_{c,e}(t) = \rho . n(t) . \varepsilon_{exp,net}(t) \quad (5\text{-}4)$$

Where

$\rho = \frac{A_S}{A_C}$: the restraining steel ratio and $n(t) = \dfrac{E_s}{E_c(t)}$

5.1.1.2 Shrinkage period

If curing period is sufficiently long (approximately 7 days) and w/b is adequately high, most of expansive additive hydrates before the concrete are exposed to the environment. In such case, concrete starts shrinking as soon as the curing is stopped and free shrinkage is defined as the shrinkage of specimen from the end of curing to the time considered. The mechanism of the subsequent shrinkage under restraint is illustrated in Figure 5-2.

As in Figure 5-2 if concrete shrinks without restraint, the shrinkage strain of concrete will be free shrinkage ($\varepsilon_{shr,free}$) and there is no stress inside. However, in the restrained condition, the restrained shrinkage strain includes elastic tensile strain ($\varepsilon_{t,e}$) which produces tensile stress of concrete and tensile creep strain ($\varepsilon_{tensile\ creep}$). Following Figure 5-2, the strain produces compressive stress of steel bar is ($\varepsilon_{shr,free}(t) - \varepsilon_{exp,net}(t_c) - \varepsilon_{c,e}(t_c) - \varepsilon_{t,e}(t) - \varepsilon_{tensile,creep}(t)$).

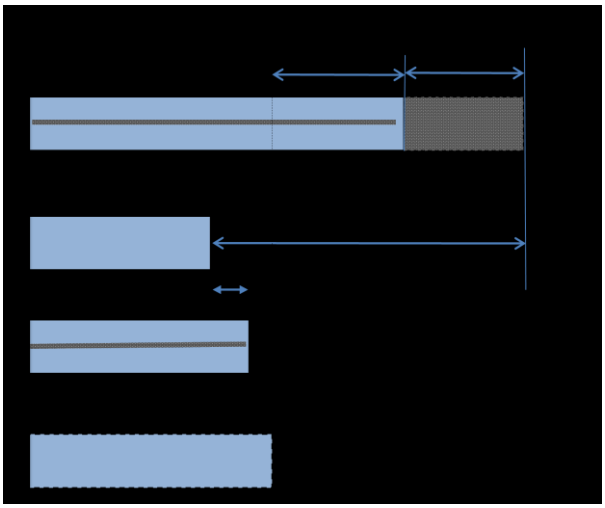

Figure 5-2 Shrinkage mechanisms of expansive concrete under restraint

t_c and t	: Length of curing period of concrete and age of concrete, (days)
$\varepsilon_{shr,free}$	: Free shrinkage strain of concrete after curing (μ)
ε_c	: The restrained shrinkage strain of concrete after curing (μ)
$\varepsilon_{t,e}$	: Elastic tensile strain portion of ε_c (μ)
$\varepsilon_{tensile\ \ creep}$	: Tensile creep during shrinkage period after curing (μ)

+ Stress strain relation (Hook's law) for reinforcing steel:

$$\sigma_s(t) = E_s(\varepsilon_{shr,free}(t) - \varepsilon_{exp,net}(t_c) - \varepsilon_{c,e}(t_c) - \varepsilon_{t,e}(t) - \varepsilon_{tensile\ \ creep}(t)) \quad (5\text{-}5)$$

+ Stress strain relation (Hook's law) for concrete:

$$\sigma_c(t) = E_c(t).\varepsilon_{t,e}(t) \quad (5\text{-}6)$$

+ Force equilibrium in case of shrinkage:

$$\sigma_s(t).A_s = \sigma_c(t).A_c \quad (5\text{-}7)$$

Substituting (5-4), (5-5) and (5-6) into the force equilibrium (5-7) to achieve the elastic tensile strain of concrete as equation (5-8)

$$\varepsilon_{t,e}(t) = \frac{\rho.n(t)}{1+\rho.n(t)}\left(\varepsilon_{shr,free}(t) - \left(1+\rho.n(t)\right).\varepsilon_{exp,net}(t_c) - \varepsilon_{tensile\ \ creep}(t)\right) \quad (5\text{-}8)$$

5.1.2 Shrinkage cracking of conventional concrete

In conventional concrete, tension in concrete is generated as soon as the concrete shrinks under restrained condition. The magnitude of the tensile force in concrete is governed by the balanced sectional forces and strain compatibility. Elastic tensile strain can be induced by restrained shrinkage concrete and can be expressed as shown in Equation (5-9).

$$\varepsilon_{t,e}(t) = \frac{\rho.n(t)}{1+\rho.n(t)}\left(\varepsilon_{shr,free}(t) - \varepsilon_{tensile\ \ creep}(t)\right) \quad for\ t > t_{curing} \tag{5-9}$$

In Equation (5-9), it is assumed that volume change during curing is not significant and thus neglected in the case of conventional concrete. At anytime t, if the elastic strain of concrete, $\varepsilon_{c,e}(t)$, exceeds the cracking strain, $\varepsilon_{c,cr}(t)$, cracking takes places. It should be noted that higher tensile creep strain reduces the induced tensile elastic strain of concrete under restrained shrinkage and is beneficial to the shrinkage cracking prevention.

5.1.3 Cracking age analysis and verification

In this research, the cracking age is defined as the time at which shrinkage cracking takes place. Based on the aforementioned derivation, Equation (5-8) and Equation (5-9) can be used to calculate the tensile elastic strain at any time and the cracking age can then be predicted as the time that the tensile elastic strain exceeds the cracking strain [33]. In order to verify the accuracy of the proposed equations, the predicted cracking ages ($t_{cr,predict}$) obtained by the equations are compared to the actual cracking ages ($t_{cr,actual}$) obtained experimentally.

For the cracking age prediction, the necessary parameters; i.e, free shrinkage strain ($\varepsilon_{shr,free}$), cracking strain ($\varepsilon_{c,cr}$), and net expansion ($\varepsilon_{exp,net}$) are obtained from separate tests for being substituted into the equations to obtain the predicted cracking age.

5.2 Measurement of parameters for prediction of cracking age

5.2.1 Free expansion/shrinkage measurement

Free expansions/shrinkages of almost all mixtures were measured by the length change as explained in 3.4.1. However, in the cases of w35, w55, w55FA30 and w55FA50, free shrinkages were calculated by applying the prediction model of Tongaroonsri [29]. Their total free shrinkages were computed from the summation of autogenuous shrinkage and drying shrinkage. Figure 5-3, Figure 5-4 and Figure 5-5 demonstrate the results of free expansion/shrinkage.

In Figure 5-3, w35, w50 and w55 are mixtures without fly ash and expansive additive. Their water to binder ratios were 0.35, 0.50 and 0.55, respectively. FA0EA30 is expansive concrete mixture with 30 kg/m^3 of EA but without fly ash.

In Figure 5-4, w50FA30 [21], w55FA30 and w55FA50 [29] represent mixtures with water to binder ratios of 0.50, 0.55 and 0.55, and with the amount of fly ash of 30%, 30% and 50%, respectively.

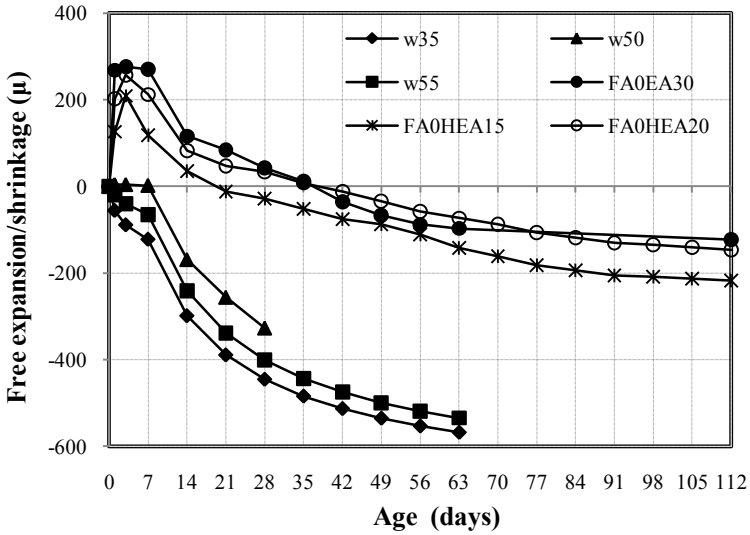

Figure 5-3 Free expansion/shrinkage of concrete without fly ash

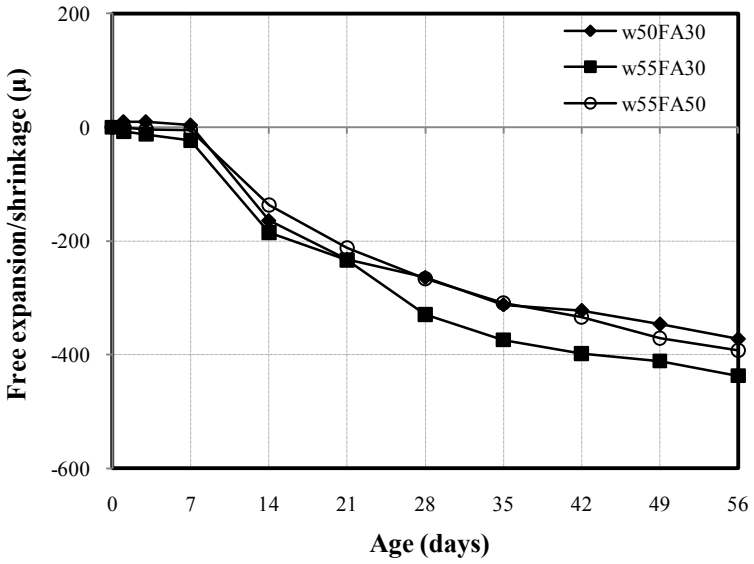

Figure 5-4 Free shrinkage of fly ash concrete

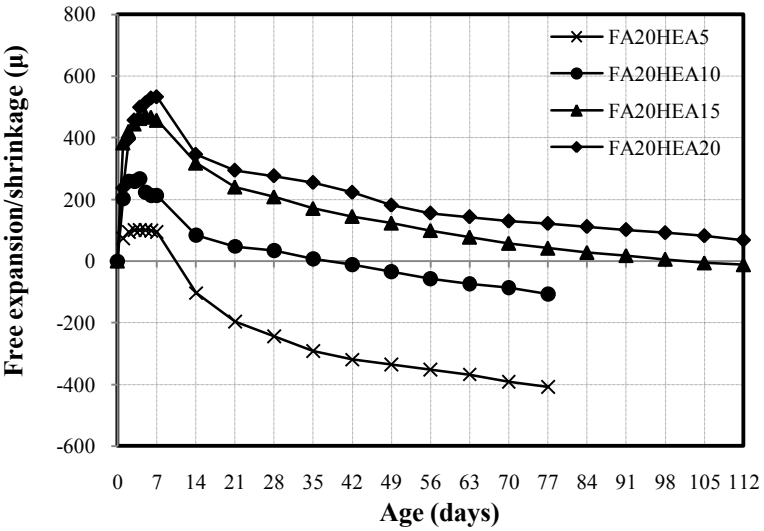

a) Free expansion and shrinkage of expansive concrete with 20% fly ash

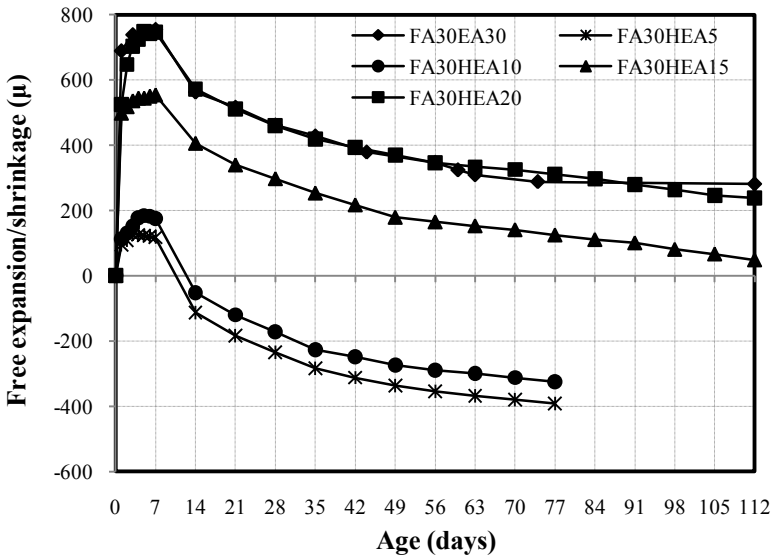

b) Free expansion and shrinkage of expansive concrete with 30% fly ash

Figure 5-5 Free expansion and shrinkage of expansive concrete using fly ash

5.2.2 Measurement of cracking strain

Bending tests on specimens were conducted to measure flexural cracking strain as explained in 3.4.3. They were converted to direct tensile cracking strain by multiplying with 0.7 as shown in Equation (5-10) [34]. The values of cracking strain at different ages are shown in Table 5-1. This measurement of cracking strain under free condition was assumed to be approximately equal to that of the restrained case.

$$\varepsilon_{cr,direct} = 0.7\varepsilon_{cr,flexural} \quad (5\text{-}10)$$

Where

$\varepsilon_{cr,direct}$: cracking strain under direct tension, μ

$\varepsilon_{cr,flexural}$: cracking strain obtained from flexure test, μ

Table 5-1 Cracking strain

No	Mix	Flexural cracking strain (μ)				Direct tensile cracking strain (μ)			
		3 days	7 days	28 days	56 days	3 days	7 days	28 days	56 days
1	w35	199	204	211	-	139	143	148	-
2	w50	223	233	239	-	156	163	167	-
3	w55	174	177	183	-	122	124	128	-
4	w55FA30	155	168	179	-	109	118	125	-
5	w55FA50	144	154	169	-	101	108	118	-
6	w50FA30	211	224	229	-	148	157	160	-
7	FA0EA30	207	229	237	-	145	160	166	-
8	FA30EA30	191	214	221	-	134	150	155	-
9	FA0HEA15	-	228	249	251	-	160	174	175
10	FA0HEA20	-	217	229	240	-	152	160	168
11	FA20HEA5	-	247	259	269	-	173	181	188
12	FA20HEA10	-	239	241	247	-	167	169	173
13	FA20HEA15	-	220	233	244	-	154	163	171
14	FA20HEA20	-	212	226	238	-	148	158	167
15	FA30HEA5	-	255	271	278	-	179	190	195
16	FA30HEA10	-	220	236	237	-	154	165	166
17	FA30HEA15	-	220	243	246	-	154	170	172
18	FA30HEA20	-	205	216	216	-	143	151	151

5.2.3 Measurement of modulus of elasticity

Modulus of elasticity is calculated from Equation (5-11) which conforms to ACI 318-05 [35]

$$E_c = 4700\sqrt{f_c'} \qquad \text{(for normal weight concrete)} \qquad (5\text{-}11)$$

Where

f_c' : compressive strength of concrete, MPa
E_c : modulus of elasticity of concrete, MPa

In case of normal concrete, compressive strength is measured following ASTM C 39/C 39M-99 [31]. For expansive concrete, compressive strength is measured under restraint condition as described in 3.4.2. The results of compressive strength and modulus of elasticity were shown in Table 5-2.

Table 5-2 Compressive strength and modulus of elasticity

		Compressive strength (MPa)				Modulus of elasticity (GPa)			
No	Mix	3 days	7 days	28 days	56 days	3 days	7 days	28 days	56 days
1	w35	32.62	40.35	54.71	-	26.84	29.86	34.76	-
2	w50	34.79	38.59	44.72	-	27.72	29.20	31.43	-
3	w55	17.93	23.05	32.57	-	19.90	22.56	26.82	-
4	w55FA30	9.00	14.03	23.36	-	14.10	17.60	22.72	-
5	w55FA50	3.73	9.16	19.24	-	9.08	14.22	20.62	-
6	w50FA30	25.97	34.33	42.35	-	23.95	27.54	30.59	-
7	FA0EA30	37.87	40.27	48.00	50.00	28.92	29.83	32.56	33.23
8	FA30EA30	26.53	33.78	45.39	48.00	24.21	27.32	31.66	32.56
9	FA0HEA15	33.51	35.65	41.52	43.65	27.21	28.06	30.28	31.05
10	FA0HEA20	31.33	33.08	38.02	41.85	26.31	27.03	28.98	30.40
11	FA20HEA5	22.97	32.32	37.73	38.45	22.53	26.72	28.87	29.14
12	FA20HEA10	23.8	33.11	37.16	37.89	22.93	27.04	28.65	28.93
13	FA20HEA15	23.38	30.48	35.75	37.7	22.73	25.95	28.10	29.04
14	FA20HEA20	25.17	30.97	33.36	35.14	23.58	26.16	27.15	28.04
15	FA30HEA5	21.3	24.49	29.22	35.78	21.69	23.26	25.41	28.11
16	FA30HEA10	21.08	25.66	32.04	34.77	21.58	23.81	26.60	27.71
17	FA30HEA15	21.14	22.42	27.07	28.50	21.61	22.25	24.45	25.09
18	FA30HEA20	19.99	21.9	24.86	26.60	21.01	21.99	23.43	24.24

5.3 Prediction of cracking age without tensile creep strain

In order to predict cracking age of concrete, the values of net expansion before shrinkage, free shrinkage, modulus of elasticity and restraining ratio are substituted into Equation (5-8) or Equation (5-9) in order to determine the elastic strain of concrete at any specified date. The calculated elastic strain was then compared with the cracking strain of the same concrete and the cracking age was estimated as the time that elastic strain is equal to cracking strain. The calculation is called 'cracking age analysis'. In this section, no tensile creep is considered in the analysis.

5.3.1 Prediction of cracking age of conventional concrete (non-expansive concrete)

Figure 5-6 shows the results of cracking age analysis of cement only concrete. The calculated cracking ages of w35, w55 and w50 are 10.8 days, 11.4 days and 19.8 days, respectively. These values are shorter than the actual cracking ages which are 11 days, 19 days and 21 days, respectively. Since, among cement-only concretes, w50 has the lowest paste content (γ), thus shrinkage was reduced (see Figure 5-3) and its cracking strain is the highest (see Table 5-1), its cracking age is then longer than w35 and w55.

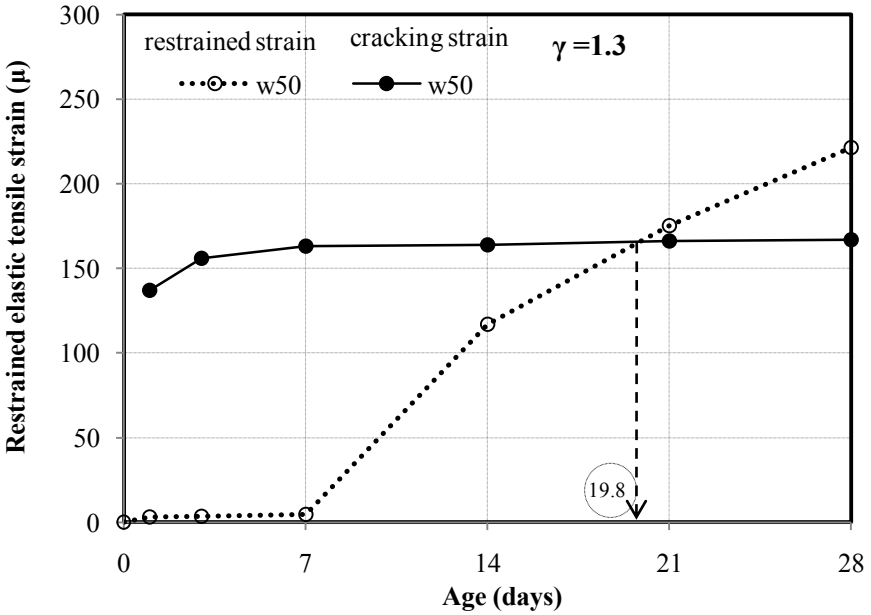

a) Normal concrete with γ = 1.3

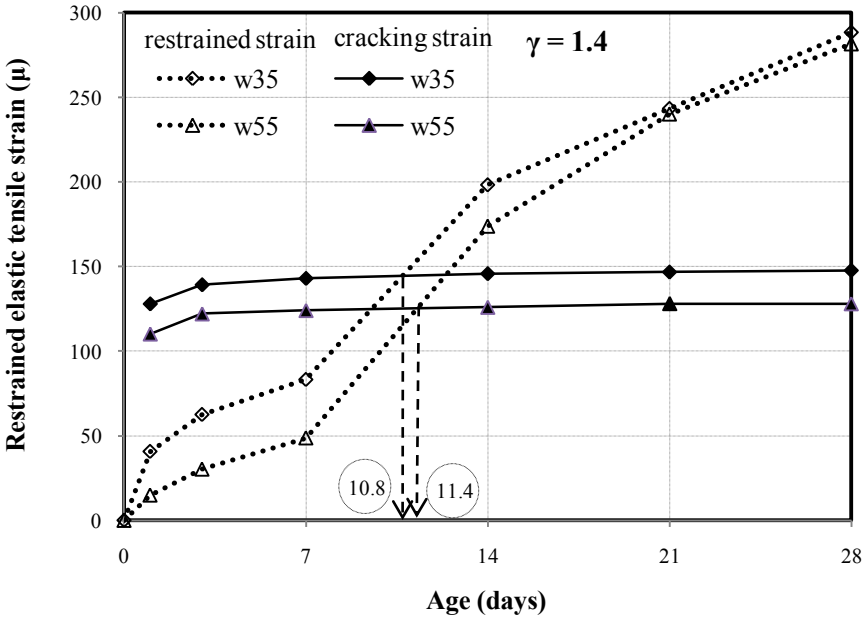

b) Normal concrete with γ = 1.4

Figure 5-6 Cracking analysis of cement-only concretes

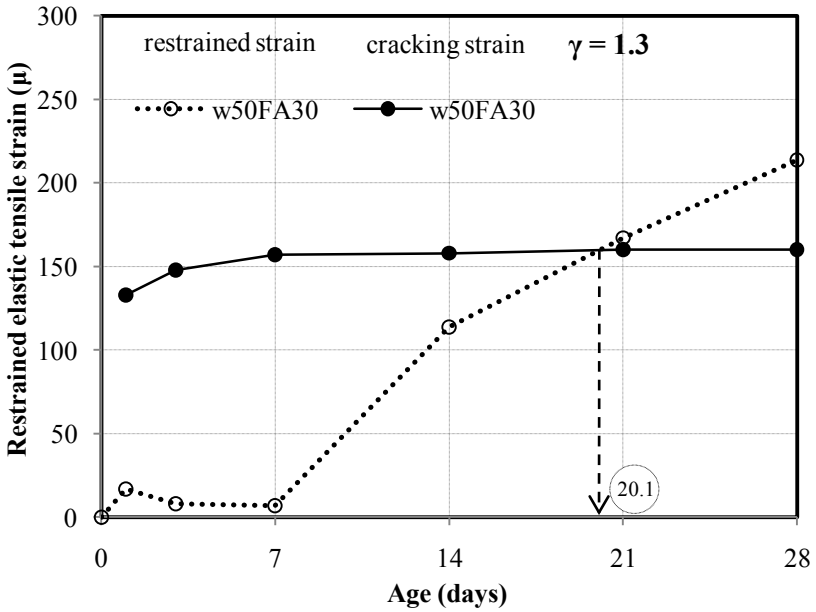

a) Fly ash concrete with γ = 1.3

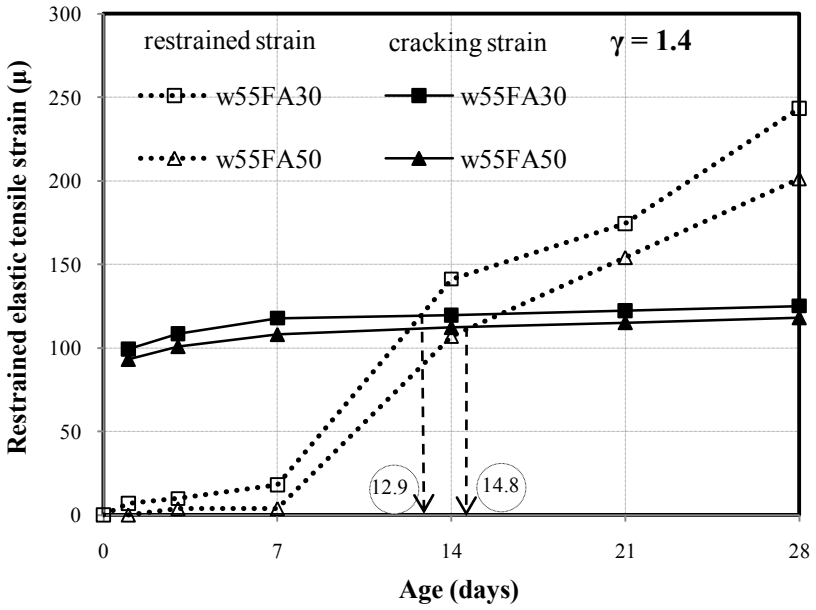

b) Fly ash concrete with $\gamma = 1.4$

Figure 5-7 Cracking analysis of non-expansive fly ash concretes

The similar results of cracking age analysis of the fly ash concretes are shown in Figure 5-7. Since w50FA30 has very low free shrinkage (Figure 5-3) and high cracking strain (Table 5-1), this mixture should have the longest cracking age. From the analysis, the calculated cracking ages of w55FA30, w55FA50, and w50FA30 are 12.9 days, 14.8 days and 20.1 days while the actual cracking ages were 20 days, 22 days and 23 days, respectively. From the comparison between calculated cracking ages and the actual ones, it was found that the actual cracking ages, in all cases, are longer. Creep is expected to be a major cause of the differences since the tensile creep can reduce the elastic restrained strain in concrete and thus delay the occurrence of cracking.

5.3.2 Prediction of cracking age of expansive concrete under 1D external restraint

Figure 5-8, Figure 5-9, Figure 5-10 and Figure 5-11 show the results of cracking age analysis of expansive concrete with expansive additives at 22.04% and 31.35% external restraining ratio. The major difference from those of non-expansive concretes is the induced compressive strain at the early age. The analytical results shown in Figure 5-8 indicate that the calculated cracking age of FA30EA30 (40.8 days) is shorter than that of FA0EA30 (70 days). In the experiment, cracking took place at 64.1 days in the case of FA30EA30 and there were no crack in the case of FA0EA30 until 112 days. Although FA30EA30 has higher early age expansion, it cracked earlier because of its larger subsequent shrinkage. This is a good example that the concrete which gives highest expansion may not be the best and all related parameters should be considered carefully for a successful application.

As shown in Figure 5-9 the calculated cracking ages of FA0HEA15 and FA0HEA20 were 50.0 and 54.4 days, respectively, while the actual cracking ages took place at 63.0 days and 80.0 days, respectively. Figure 5-10 shows the cracking ages analysis of expansive concrete with HEA and 30% fly ash. The calculated cracking ages of FA30HEA5, FA30HEA10, FA30HEA15 and FA30HEA20 were 23.2, 24.1, 40.6, and 38.9 days. Their actual cracking ages obtained experimentally were 27, 29, 47, and 50 days. The calculation

showed cracking ages of FA30HEA15 nearly 2 days longer than that of FA30HEA20 mainly because cracking strain of FA30HEA20 was lower than that of FA30HEA15. However, the test results showed that cracking age of FA30HEA20 was longer. It can be understood that expansive additive gives higher tensile creep (see 5.4 and Table 5-3) and tensile creep was ignored in the calculation, hence the calculation could give the different trend.

Similarly, Figure 5-11 shows the similar results of expansive concrete with HEA and containing 20% fly ash. The calculated cracking ages of FA20HEA5, FA20HEA10, FA20HEA15 and FA20HEA20 were 24.3, 24.5, 36.4 and 43.8 days while their actual cracking ages were 31, 33, 50 and 56 days, respectively. It can be found that fly ash shortens cracking age of expansive concrete.

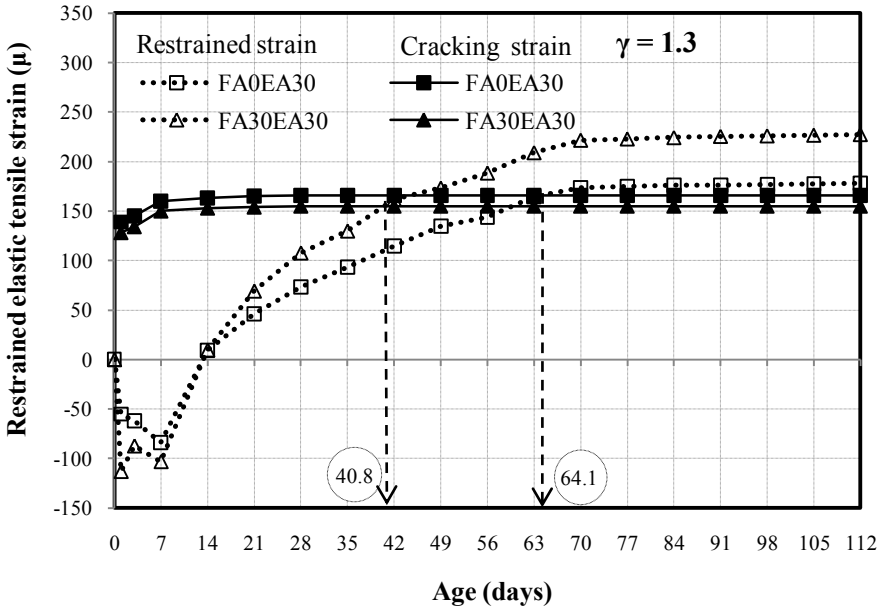

Figure 5-8 Cracking age analysis of expansive concrete with EA

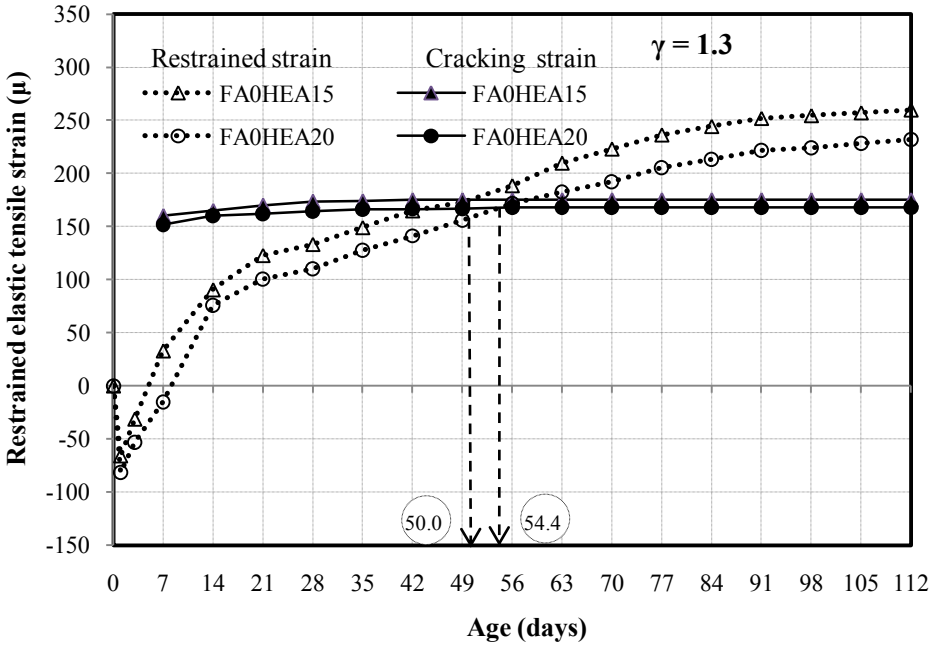

Figure 5-9 Cracking age analysis of expansive concrete with HEA and without fly ash

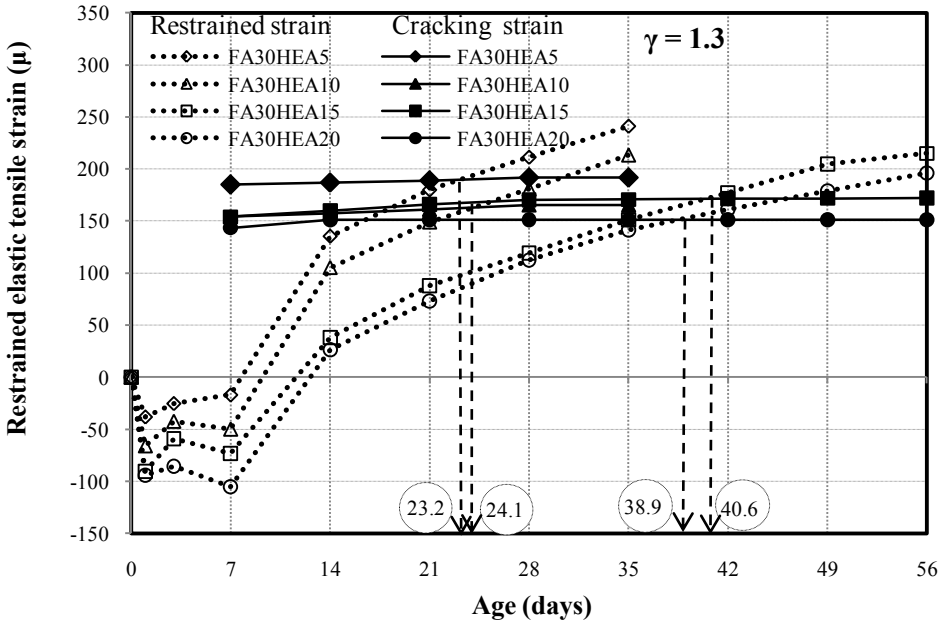

Figure 5-10 Cracking age analysis of expansive concrete with HEA and 30% fly ash

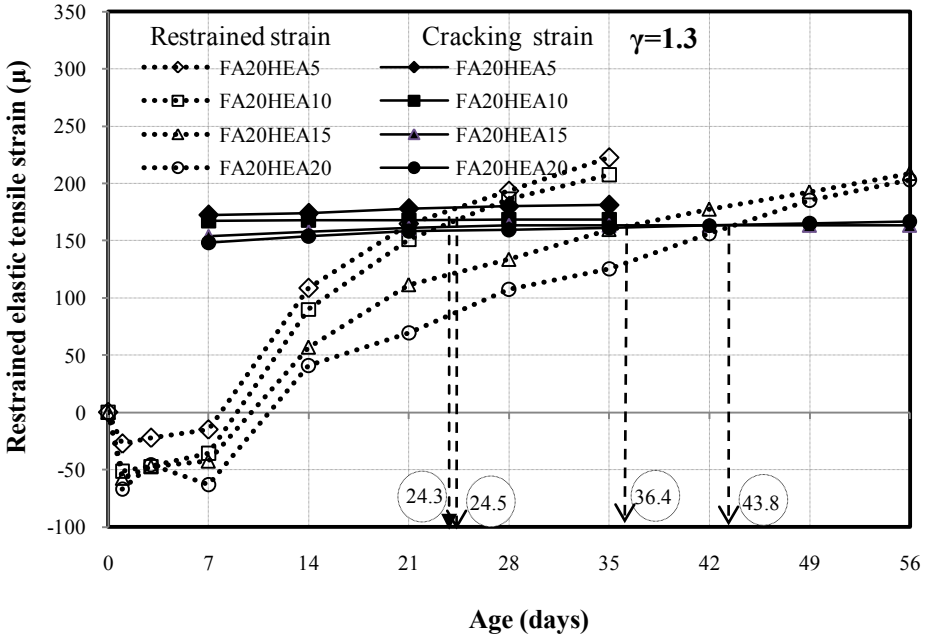

Figure 5-11 Cracking age analysis of expansive concrete with HEA and 20% fly ash

From the results, effect of fly ash seems to be different in the case of non-expansive concrete and expansive concrete. Cracking age of fly ash concrete is longer than concrete without fly ash in the case of non-expansive concrete. However, in the case of expansive concrete, more fly ash content shortens the cracking age. This observation can be partially explained by the fact that in the case of seal curing of 7 days, more fly ash induces larger subsequent shrinkage in expansive concrete while the cracking strains are similar. It can be understood that cracking of non-expansive concrete often takes place at early ages when autogenous shrinkage is dominant. Fly ash is able to reduce autogenous shrinkage of conventional concrete, hence, it can prolong cracking age of conventional concrete. However, in the case of expansive concrete, under seal curing of 7 days, cracking often

takes place at long age when drying shrinkage plays major role. Fly ash produces higher subsequent drying shrinkage, hence, it results in earlier cracking age of expansive concrete. This phenomenon can be seen in Figure 5-12, total free shrinkage of fly ash expansive concrete are lower than those of concrete without fly ash at early age day, however, it is higher afterwards.

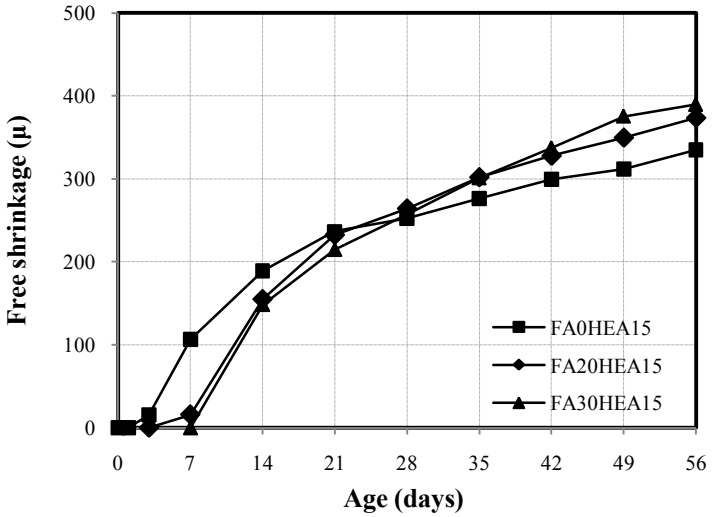

a) Free shrinkage of expansive concrete with 15kg HEA

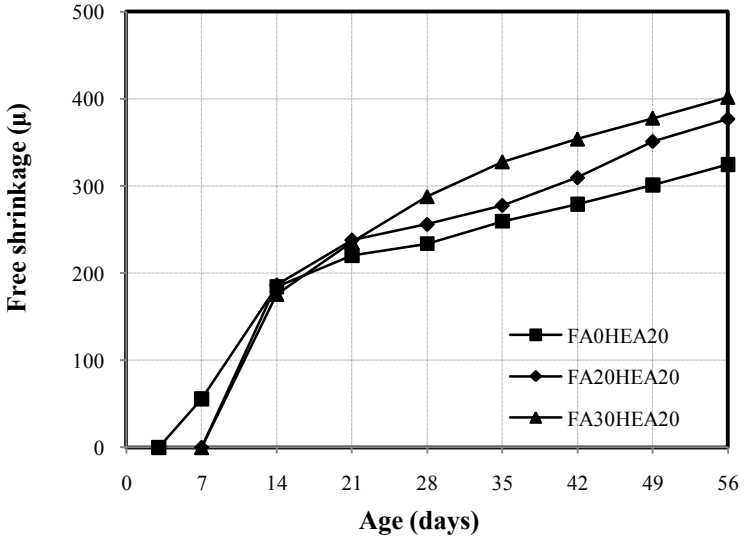

b) Free shrinkage of expansive concrete with 20kg HEA

Figure 5-12 Rate of free shrinkage of conventional and expansive concrete

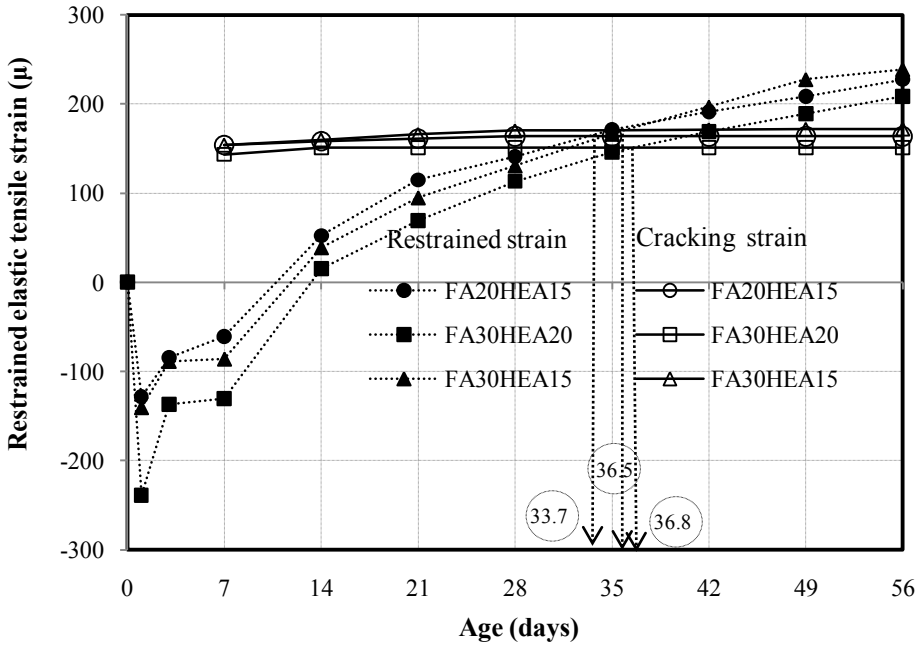

Figure 5-13 Cracking age analysis of HEA expansive concrete at 52.15% restraining ratio

Figure 5-13 shows the results of cracking age analysis of expansive concrete with HEA at 52.15% external restraining ratio. Both the analytical and actual results show that fly ash drives expansive concrete cracking sooner. The calculated results revealed that the cracking ages of FA30HEA15 and FA20HEA15 were 33.7 and 36.8 days, respectively, while the actual cracking ages were 38 and 42 days, respectively. The calculated and actual cracking ages of FA30HEA20 were 36.5 and 44 days, respectively.

It can be found that at higher restraining ratio, the prediction of cracking ages seems to be more precise. It can be explained that higher restraining ratio causes expansive concrete cracking sooner when tensile creep is small, hence, the ignorance of tensile creep has less effect on the calculated cracking age when compared to the case of low restraint.

5.3.3 Prediction of cracking age of expansive concrete under combined external and internal restraint

Figure 5-14 shows the results of cracking age analysis of HEA expansive concrete with 31.35% external and 2.79% internal restraining ratio. The analytical results indicate that the calculated cracking age of FA30HEA15 and FA30EA20 were 34.9 and 35.1 days, respectively. In the experiment, cracking took place at 90 days and 109 days, respectively.

Figure 5-15 indicates the analytical results of the cracking age of FA20HEA15 with 52.15% external and 2.79% internal restraining ratio. The calculated cracking age was 30.8 days, while the actual crack happened at 73 days.

It can be seen that although total restraining steel ratio is larger than the case of 1D external restraint, the shrinkage cracking under 1D combined external and internal restraint combination took place longer. It can be understood that, in the case of combined external and internal restraint, reinforcing bars, as internal restraining object, prevent localization of strain and lead to longer cracking age.

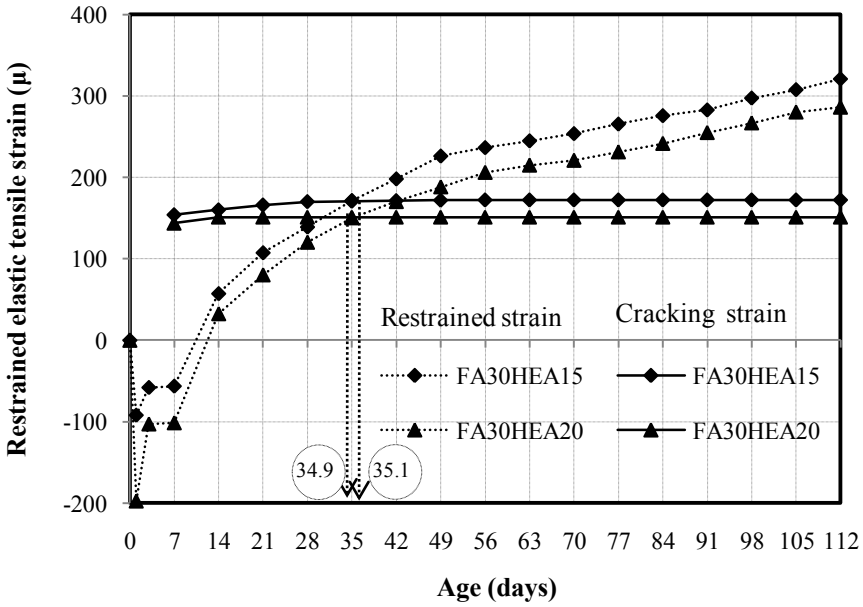

Figure 5-14 Cracking age analysis of expansive concrete with HEA under 31.35% external and 2.79% internal restraining ratio

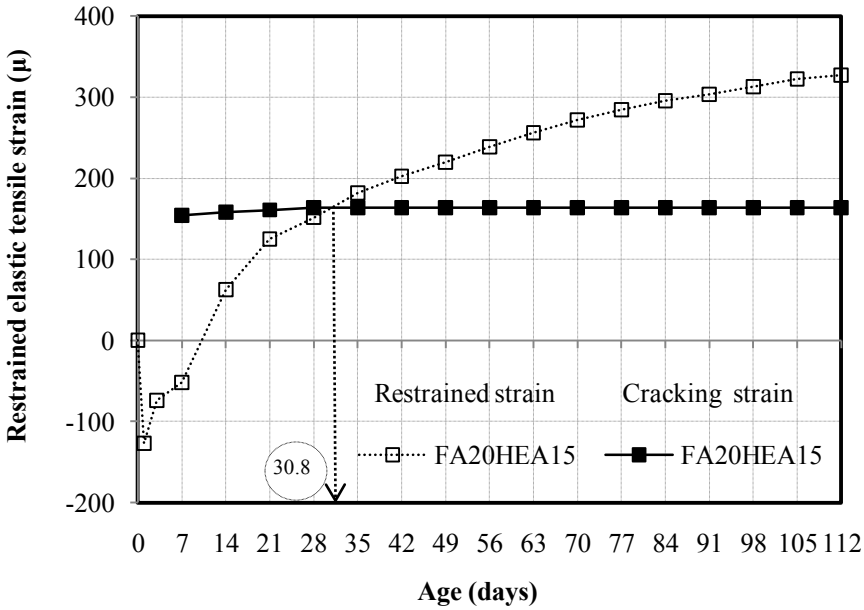

Figure 5-15 Cracking age analysis of expansive concrete with HEA under 52.15% external and 2.79% internal restraining ratio

5.4 Creep at actual cracking age

Creep is a time-dependent behaviour of concrete. Creep, under constant stress, gives a time-dependent deformation, while under enforced fixed deformation, induces stress relaxation. Under the actual condition where stress and deformation are not constant with time, the magnitude of creep can be described in term of 'creep strain' or 'stress relaxation'.

Tensile creep is beneficial to cracking problem of concrete structures as it allows stress relaxation to some extent and the cracking age is consequently delayed. The discrepancy between predicted cracking age ($t_{cr,predict}$) and the actual cracking age ($t_{cr,actual}$) in the

previous sections implies a significant effect of creep (stress relaxation) which has not been considered in the prediction of cracking age. Table 6 compares the predicted cracking age and actual cracking age of each specimen at 22.04% and 31.15% restraining ratio. The difference can be as high as 40 days as in the case of FA0EA30 or can be so low that the predicted cracking age and the actual one are almost equal as in the case of w35. It was also found that the difference between predicted cracking age and actual cracking age increased for the concrete with larger dosage of expansive additive.

In addition, due to its complicated mechanisms, cumulative creep of concrete is highly dependent on the stress-history and development of strength and microstructures of each specimen. The creep of the concretes with same mix proportion under the same stress at a specified age may be different if they experiences different level of stress in the past. For example, specimen with expansive concrete shall experience both compressive and tensile stress while specimens with conventional (non-expansive) concrete hardly experienced the compressive stress under tested condition. Therefore, comparing creep of different specimens must be done carefully.

In this study, the magnitude of creep is described in term of 'creep strain' and was calculated by substituting the measured variables into Equation (5-8). The final form of 'creep strain calculation is shown in Equation (5-12). The creep coefficient is consequently determined according to Equation (5-13). The creep strain at the actual cracking age and the tensile creep coefficient of each specimen is summarized in Table 5-3.

$$\varepsilon_{creep}\left(t_{cr,actual}\right) = \varepsilon_{shr,free}\left(t_{sh}\right) - \left[1+\rho.n\left(t_{cr,actual}\right)\varepsilon_{exp,Net}\left(t_c\right)\right] - \left[\frac{1+\rho.n\left(t_{cr,actual}\right)}{\rho.n\left(t_{cr,actual}\right)}\right]\varepsilon_{c,cr}\left(t_{cr,actual}\right) \quad (5\text{-}12)$$

$$C = \frac{\varepsilon_{creep}\left(t_{cr,actual}\right)}{\varepsilon_{c,e}\left(t_{cr,actual}\right)} \quad (5\text{-}13)$$

Where
$\varepsilon_{creep}(t_{cr,actual})$: creep strain at the actual cracking age (μ)
C : tensile creep coefficient

In the case of cement-only concrete, based on Equation (5-13), the tensile creep coefficients were 0.047, 0.109 and 0.300 for ratios of water to binder 0.35, 0.50 and 0.55, respectively. In the case of concrete using fly ash, based on Equation (5-13), the tensile creep coefficients were 0.186, 0.398 and 0.431 for specimens w50FA30, w55FA30 and w55FA50; respectively. The relationship between the tensile creep coefficients and water to binder ratio of conventional (non-expansive) concrete are shown in Figure 5-16. It is obvious that the creep coefficient is larger for higher water to binder ratio and slightly increases for concrete with higher fly ash content.

In the case of concrete with 30 kg/m^3 of normal expansive additive (EA), the creep coefficient of FA0EA30 was at least 0.154 (the specimen did not crack) and one of FA30EA30 was 0.455 (Figure 5-17a). The cracking ages of FA0EA30 (>112 days) and FA30EA30 (70 days) are much higher than those of w50 (21 days) and w50FA30 (23 days) hence EA expansive concrete under tensile tress longer than conventional concrete. It leads to tensile creep of EA expansive concrete larger than those of convention concrete. Therefore, the creep coefficients of expansive concrete with EA were thus higher than those of equivalent conventional (non-expansive) concrete, i.e., w50 and w50FA30.

Table 5-3 Calculated tensile creep coefficient at actual cracking ages

No	Mix	Predicted cracking age (days)	Actual cracking age (days)	Tensile creep strain (μ)	Tensile elastic strain without tensile creep (μ)	Tensile creep coefficient (C)
1	w35	10.8	11	7	148	0.047
2	w50	19.8	21	19	175	0.109
3	w55	11.4	19	66	220	0.300
4	w55FA30	12.9	21	70	174	0.398
5	w55FA50	14.8	22	69	160	0.431
6	w50FA30	20.1	23	30	179	0.186
7	FA0EA30	64.1	> 112	> 27	178	> 0.154
8	FA30EA30	40.8	70	100	221	0.455
9	FA0HEA15	50.0	63	52	210	0.248
10	FA0HEA20	54.4	84	67	213	0.315
11	FA20HEA5	24.3	31	42	206	0.202
12	FA20HEA10	24.5	33	45	202	0.224
13	FA20HEA15	36.4	50	45	195	0.231
14	FA20HEA20	43.8	56	52	203	0.257
15	FA30HEA5	23.2	27	24	206	0.116
16	FA30HEA10	24.1	29	32	189	0.167
17	FA30HEA15	40.6	47	38	196	0.191
18	FA30HEA20	38.9	50	42	181	0.230

Considering the case of concrete with 30 % of fly ash and 5 kg/m^3, 10 kg/m^3 of HEA, the cracking age was slightly delayed (23 days for w50FA30 and 27 days, 29 days for FA30HEA5, FA30HEA10, respectively. The tensile creep strains of w50FA30 and FA30HEA5, FA30HEA10 were found to be approximately same (30μ for w50FA30 but 24μ and 32μ for FA30HEA5, FA30HEA10, respectively). In this case of small dosage of HEA, the slight delay of shrinkage cracking (from 30 days of w50FA30 to 32 days of FA30HEA10) is apparently a result of early expansion but not the change of creep characteristic.

However, in the case of expansive concrete with higher amount of HEA, the tensile creep was significantly changed (see Table 5-3). Larger tensile creep strain developed in the case of concrete with 15 or 20 kg/m^3 of HEA (see Table 5-3 and Figure 5-17b). The concrete with higher HEA content was found to undergo higher tensile creep strain. In the case of mixtures without fly ash, the creep coefficients were found to be 0.248 and 0.315 for FA0HEA15 and FA0HEA20, respectively. Besides, in the case of using fly ash, tensile creep coefficients were 0.219 and 0.257 for FA20HEA15 and FA20HEA20, while they were 0.191 and 0.23 for FA30HEA15 and FA30HEA20, respectively.

It can be seen in HEA expansive concrete that the larger tensile creep strain seems to be corresponding to the period that each specimen was under tension. In the case of concrete

with HEA, a higher amount of expansive additive extended a period of being under tension (the period from the time that stress in concrete changed from compression to tension to the time that shrinkage cracking took place) due to early age expansion while more fly ash shortened a period of being under tension due to a faster rate of subsequent of shrinkage after expansion is stopped. The periods of being under tension were 19.5 days, 21 days, 37.5 days and 40 days for FA30HEA5, FA30HEA10, FA30HEA15 and FA30HEA20 (expansive concrete with HEA and 30% fly ash) and were 23 days, 24 days, 40 days and 45 days for FA20HEA5, FA20HEA10, FA20HEA15 and FA20HEA20 (expansive concrete with HEA and 20% fly ash), respectively. Besides, the periods of being under tension were 45 days and 46.4 days for FA0HEA15 and FA0HEA20. As the period under tension of expansive concrete with HEA and lower fly ash content was longer, the creep coefficient of expansive concrete was higher (Figure 5-17b).

While combination of fly ash and expansive additive has a potential to increase early age expansion and improve resistance to shrinkage cracking of concrete, the results show that special care on the content of fly ash and expansive additive must be taken. Under testing condition in this study, too much fly ash in expansive concrete may lead to higher rate of subsequent shrinkage and thus accelerates the occurrence of shrinkage cracking when compared with equivalent expansive concrete without fly ash. The higher rate of subsequent shrinkage found in the case of expansive concrete with HEA and 30% fly ash significantly shortened the period of being under tension. While effect of fly ash content slightly affect cracking strain of expansive concrete with HEA, the shorter period under tension limited the tensile creep strain develops in the case of expansive concrete with HEA and 30% fly ash when compared with the expansive concrete with HEA and 20% fly ash or HEA expansive concrete without fly ash.

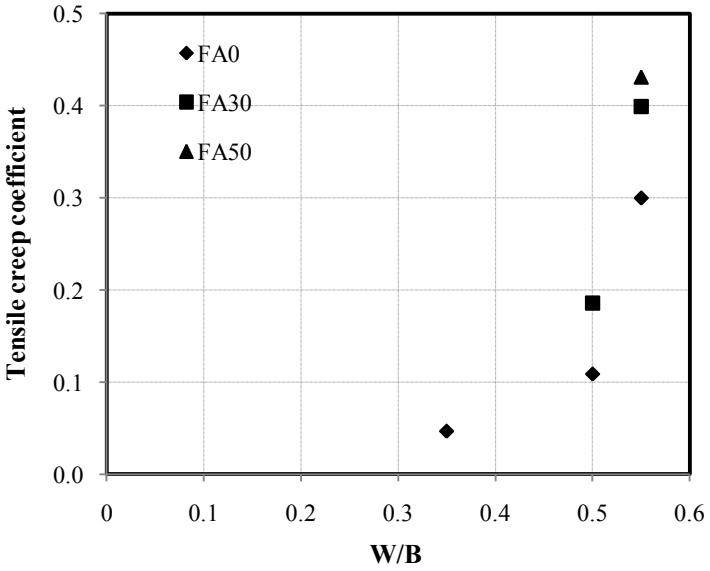

Figure 5-16 Relationship between tensile creep coefficient and ratio water to binder

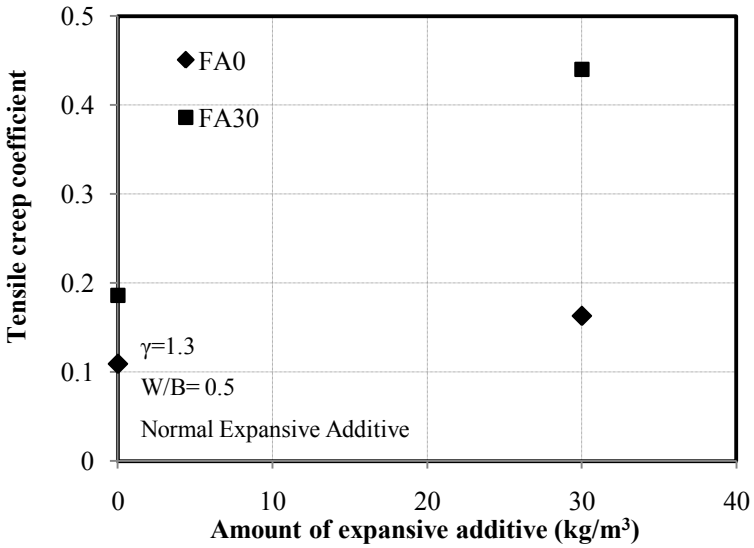

a) Concretes with normal expansive additive (EA)

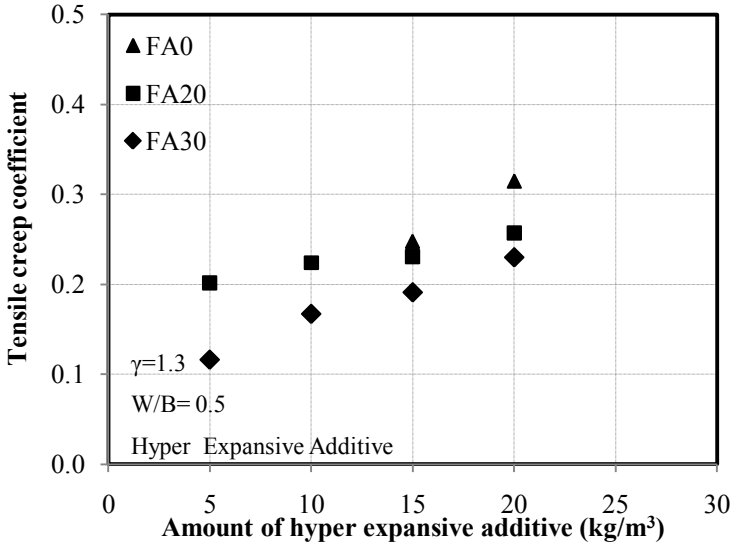

b) Concretes with hyper expansive additive (HEA)

Figure 5-17 Effect of fly ash replacement and amount of expansive additive on tensile creep coefficient

Chapter 6 Conclusion and Recommendations

6.1 Conclusion

1. The results indicate that the expansion (including both free and restrained conditions) increases, while strengths (tensile and compressive strengths under free and restrained condition) decrease with increasing the amount of expansive additive or fly ash.

2. Compressive strength of HEA expansive concrete under restraining condition is much larger than compressive strength under free condition, especially at high dosage of HEA.

3. Net expansion highly depends on restraining ratio and the amount of expansive additive. At high restraining ratio, the effect of HEA dosage to net expansion is much smaller than in the case of low restraining ratio.

4. In the case of multi-directional restraint, the net expansion along main direction is not affected by restraint in other direction.

5. In the case that seal curing for 7 days is provided after casting, although fly ash improves early age expansion of expansive concrete, it also increases the rate of subsequent shrinkage. Under the test condition in this study, it was found that expansive concrete with higher fly ash replacement cracked earlier. This matter should be carefully considered in the real application.

6. Creep has significant effect on the cracking age. It was found that the creep coefficient of non-expansive concrete increases for higher w/b ratio or higher fly ash replacement.

7. In the case of expansive concrete, it was found that expansive additive slightly increases the creep coefficient.

8. The results demonstrate that the proposed cracking age analysis can be conservatively applied in the design for shrinkage cracking resistance of concrete structure. There is also a possibility to incorporate the effect of creep in the analysis.

9. Combination of internal and external restraint prolongs cracking age because concrete is reinforced by internal steel bars.

6.2 Recommendations

1. The mechanism of tensile creep has not been clarified yet. Prediction of tensile creep behavior needs to be formulated with time dependent parameters such as tensile stress, strength, etc. in order to predict cracking age more precisely.

2. More studies on prediction of cracking age for internal and external restraint as well as 2D and 3D restraint are necessary for real application.

3. High strength concrete often involves high autogenous shrinkage, HEA can reduce that cracking risk due to that shrinkage. However, HEA causes reduction of strength. Therefore, the application of HEA should be investigated in case of high strength concrete under various restraining ratios.

4. Sometimes, it is not reasonable to totally prevent cracking but crack width should be limited. Therefore, crack width prediction after cracking should be investigated.

References

1. Konik, Z., Malolepszy, J., Roszczynialski, W., and Stok, A., 2007. Production of expansive additive to portland cement. *Journal of the European Ceramic Society*, 27, 2-3: 605-609.
2. Kr´ol, M., 1996. Use of expansive materiale in concrete repairs. *Cement-Wapno-Beton (in Polish)*. Volume 5: 177–179.
3. ASTM C 845-96, 1996. Standard specification for expansive hydraulic cement. *American society for testing and materials*, 04, 01.
4. Fu, Y., Xie, P., Gu, P., and Beaudoin, J. J., 1994. Characteristics of shrinkage compensating expansive cement containing a pre-hydrated high alumina cement-based expansive additive. *Cement and Concrete Research*, 24, 2: 267-276.
5. Yan, P. Y., Zheng, F., and Xu, Z. Q., 2003. *Hydration of shrinkage-compensating binders with different compositions and water-binder ratios. Journal of Thermal Analysis and Calorimetry*, 74, 1.
6. Cohen, M. D., 1983. Theories of expansion in sulfoaluminate - type expansive cements: Schools of thought. *Cement and Concrete Research*, 13, 6: 809-818.
7. Sun, W., Chen, H., Luo, X., and Qian, H., 2001. The effect of hybrid fibers and expansive agent on the shrinkage and permeability of high-performance concrete. *Cement and Concrete Research*, 31, 4: 595-601.
8. Lam, N. T., Sahamitmongkol, R., and Tangtermsirikul, S., 2008. *Expansion and Compressive Strength of Concrete with Expansive Additive. Research and Development Journal of the Engineering Institute of Thailand*, 19, 2: 40-49.
9. Tazawa, E.-i., Kawai, K., and Miyaguchi, K., 2000. Expansive concrete cured in pressurized water at high temperature. *Cement and Concrete Composites*, 22, 2: 121-126.
10. Shuguang, H. and Yue, L., 1999. Research on the hydration, hardening mechanism, and microstructure of high performance expansive concrete. *Cement and Concrete Research*, 29, 7: 1013-1017.
11. Lam, N. T., Sahamitmongkol, R., Samranwanich, T., Krammart, P., and Tangtermsirikul, S., 2008. *Durability Properties of Concrete with Expansive Additives. Research and Development Journal of the Engineering Institute of Thailand*.
12. Almusallam, A. A., Maslehuddin, M., Abdul-Waris, M., and Khan, M. M., 1998. Effect of mix proportions on plastic shrinkage cracking of concrete in hot environments. *Construction and Building Materials*, 12, 6-7: 353-358.
13. Benboudjema, F., Meftah, F., and Torrenti, J. M., 2005. Interaction between drying, shrinkage, creep and cracking phenomena in concrete. *Engineering Structures*, 27, 2: 239-250.
14. Bazant, Z. P. and Chern, J. C., 1985. Concrete creep at variable humidity: constitutive law and mechanism. *Materials and Structures*, 18, 1: 1-20.
15. Slowik, V., Hübner, T., Schmidt, M., and Villmann, B., 2009. Simulation of capillary shrinkage cracking in cement-like materials. *Cement and Concrete Composites*, 31, 7: 461-469.
16. Barr, B., Hoseinian, S. B., and Beygi, M. A., 2003. Shrinkage of concrete stored in natural environments. *Cement and Concrete Composites*, 25, 1: 19-29.
17. Gesoglu, M., Özturan, T., and Güneyisi, E., 2004. Shrinkage cracking of lightweight concrete made with cold-bonded fly ash aggregates. *Cement and Concrete Research*, 34, 7: 1121-1130.
18. Holt, E. and Leivo, M., 2004. Cracking risks associated with early age shrinkage. *Cement and Concrete Composites*, 26, 5: 521-530.

19. Passuello, A., Moriconi, G., and Shah, S. P., 2009. Cracking behavior of concrete with shrinkage reducing admixtures and PVA fibers. *Cement and Concrete Composites*, 31, 10: 699-704.
20. Yuan, Y. and Wan, Z. L., 2002. Prediction of cracking within early-age concrete due to thermal, drying and creep behavior. *Cement and Concrete Research*, 32, 7: 1053-1059.
21. *Lam, N. T.*, 2008. *Properties and cracking age analysis of concrete with expansive additive. MSc.dissertation*.
22. Vandewalle, L., 2000. Concrete creep and shrinkage at cyclic ambient conditions. *Cement and Concrete Composites*, 22, 3: 201-208.
23. Kim, J. K. and Lee, C. S., 1998. Prediction of differential drying shrinkage in concrete. *Cement and Concrete Research*, 28, 7: 985-994.
24. Garas, V. Y., Kahn, L. F., and Kurtis, K. E., 2009. Short-term tensile creep and shrinkage of ultra-high performance concrete. *Cement and Concrete Composites*, 31, 3: 147-152.
25. Lee, Y., Yi, S.-T., Kim, M.-S., and Kim, J.-K., 2006. Evaluation of a basic creep model with respect to autogenous shrinkage. *Cement and Concrete Research*, 36, 7: 1268-1278.
26. Tao, Z. and Weizu, Q., 2006. Tensile creep due to restraining stresses in high-strength concrete at early ages. *Cement and Concrete Research*, 36, 3: 584-591.
27. Nagataki, S. and Gomi, H., 1998. Expansive admixtures (mainly ettringite). *Cement and Concrete Composites*, 20, 2-3: 163-170.
28. ASTM C33-97, 1997. Standard Specification for Concrete Aggregates. *American society for testing and materials*, 04, 02.
29. Tongaroonsri, S., 2009. *Prediction of autogenous shrinkage, drying shrinkage and shrinkage cracking in concrete. PhD dissertation*.
30. ASTM C 157/C 157M-99, 1999. Standard test method for Length change of Hardened Hydraulic - Cement Mortar and Concrete. *American society for testing and materials*, 04, 02.
31. ASTM C 39/C 39M-99, 1999. . Standard test method for Compressive strength of Cylindrical Concrete Specimens. *American society for testing and materials*, 04, 02.
32. ASTM C 78-94, 1994. Standard Test Method for Flexural Strength of Concrete (Using Simple Beam with Third-Point Loading. *American society for testing and materials*, 04, 02.
33. Sahamitmongkol, R., Lam, N. T., Yodmalai, D., and Tangtermsirikul, S., 2008. *Cracking analysis for shrinkage-compensating concrete under high restraint. The 3rd ACF International Conference- ACF/VCA 2008*: 114-120.
34. Wee, T. H., Lu, H. R., and Swaddiwudhipong, S., 2000. Tensile strain capacity of concrete under various states of stress. *Magazine of Concrete Research*, 52, 3: 185 - 193.
35. ACI 318-05, 2005. *Building Code Requirement for Structural Concrete and Commentary American Concrete Institute*.

Appendix

Appendix A. Results of expansion/shrinkage of concrete

Table A 1 Free shrinkage of non-expansive concrete [21], [29]

Age (days)	Free shrinkage, μ					
	w35	w50	w55	w50FA30	w55FA30	w55FA50
0	0	0	0	0	0	0
1	56	4	19	0	8	0
3	89	2	40	0	12	4
7	122	4	66	0	23	5
14	299	169	241	155	186	136
21	372	256	338	235	233	212
28	445	327	400	307	330	266
90	608	-	576	-	450	410

Table A 2 Length change of specimens for measurement of free expansion/shrinkage of EA expansive concrete [21]

Age (days)	Free expansion/shrinkage, μ	
	FA0EA30	FA30EA30
0	0	0
1	268	689
3	276	739
7	271	755
14	116	563
21	84	516
28	43	461
35	12	428
44	-36	379
56	-67	347
60	-88	324
63	-97	309
74	-115	288
112	-123	281

Note:
+ means the length of specimen is longer than initial length
- means the length of specimen is shorter than initial length

Table A 3 Length changes of specimens for measurement of free expansion/shrinkage of HEA expansive concrete without fly ash

Age (days)	Free expansion/shrinkage, μ	
	FA0HEA15	FA0HEA20
0	0	0
1	126	202
2	225	260
3	209	258
4	201	268
5	185	224
6	118	212
7	118	212
14	36	83
21	-12	48
28	-28	34
35	-51	8
42	-75	-12
49	-87	-34
56	-110	-57
63	-142	-73
70	-162	-87
77	-181	-107
84	-193	-118
91	-205	-130
98	-209	-134
105	-213	-140
112	-216	-146

Note:
+ means the length of specimen is longer than initial length
- means the length of specimen is shorter than initial length

Table A 4 Length change of specimens for measurement of free expansion/shrinkage of HEA expansive concrete using 20% fly ash

Age (days)	Free expansion/shrinkage, μ			
	FA20HEA5	FA20HEA10	FA20HEA15	FA20HEA20
0	0	0	0	0
1	74	99	383	236
2	94	113	421	395
3	100	127	445	456
4	100	125	463	498
5	100	117	473	512
6	98	117	467	528
7	94	111	457	532
14	-104	-68	318	345
21	-196	-155	240	294
28	-244	-207	209	276
35	-292	-239	171	254
42	-320	-265	145	222
49	-336	-297	123	181
56	-352	-314	99	155
63	-368	-339	77	143
70	-392	-348	58	129
77	-408	-354	42	121
84	-	-	28	111
91	-	-	18	101
98	-	-	6	91
105	-	-	-6	81
112	-	-	-12	67

Note:
+ means the length of specimen is longer than initial length
- means the length of specimen is shorter than initial length

Table A 5 Length change of specimens for measurement of free expansion/shrinkage of HEA expansive concrete using 30% fly ash

Age (days)	Free expansion/shrinkage, μ			
	FA30HEA5	FA30HEA10	FA30HEA15	FA30HEA20
0	0	0	0	0
1	74	99	383	236
2	94	113	421	395
3	100	127	445	456
4	100	125	463	498
5	100	117	473	512
6	98	117	467	528
7	94	111	457	532
14	-104	-68	318	345
21	-196	-155	240	294
28	-244	-207	209	276
35	-292	-239	171	254
42	-320	-265	145	222
49	-336	-297	123	181
56	-352	-314	99	155
63	-368	-339	77	143
70	-392	-348	58	129
77	-408	-354	42	121
84	-	-	28	111
91	-	-	18	101
98	-	-	6	91
105	-	-	-6	81
112	-	-	-12	67

Note:
+ means the length of specimen is longer than initial length
- means the length of specimen is shorter than initial length

Table A 6 Net expansion of HEA expansive concrete using 20% fly ash

Age, days	Net expansion, μ											
	FA20HEA5				FA20HEA15				FA20HEA20			
	Restraining ratio,%				Restraining ratio,%				Restraining ratio,%			
	0.79	1.57	3.14	8.04	0.79	1.57	3.14	8.04	0.79	1.57	3.14	8.04
0.0	0	0	0	0	0	0	0	0	0	0	0	0
0.5	33	25	16	15	103	87	67	33	147	108	79	47
1.0	43	36	22	18	117	93	75	47	169	127	95	57
1.5	46	37	23	18	119	101	84	53	178	137	104	65
2.0	47	39	25	17	120	102	88	55	183	142	107	66
2.5	50	40	26	20	123	103	87	58	189	147	112	71
3.0	50	39	25	20	125	104	88	61	190	148	113	72
3.5	51	40	26	20	124	106	91	62	192	149	114	74
4.0	50	40	25	21	126	107	91	63	192	149	114	72
4.5	51	39	26	22	129	107	92	63	194	149	115	73
5.0	50	41	28	22	126	108	88	63	194	150	116	73
5.5	51	40	27	24	128	109	93	63	194	154	115	74
6.0	50	38	27	22	128	108	94	64	196	154	116	73
6.5	47	39	27	21	127	109	99	65	197	156	119	76
7.0	49	39	25	22	130	109	97	65	198	158	120	77

Table A 7.a Net expansion of HEA expansive concrete using 30% fly ash

Age, days	Net expansion, μ							
	FA30EA5				FA30EA10			
	Restraining ratio,%				Restraining ratio,%			
	0.79	1.57	3.14	8.04	0.79	1.57	3.14	8.04
0.0	0	0	0	0	0	0	0	0
0.5	46	21	19	14	54	44	34	22
1.0	50	42	25	20	79	60	47	32
1.5	52	44	32	20	91	68	55	36
2.0	54	46	32	21	92	74	54	35
2.5	54	47	34	21	98	76	60	37
3.0	54	45	32	21	98	73	59	37
3.5	55	45	32	22	100	75	63	39
4.0	55	45	33	20	98	73	60	38
4.5	55	46	33	21	100	76	63	38
5.0	54	45	34	22	99	74	59	37
5.5	56	46	33	23	100	77	63	39
6.0	57	45	33	21	100	72	59	38
6.5	56	44	32	22	100	73	58	36
7.0	56	43	32	21	100	74	58	36

Table A-7b Net expansion of HEA expansive concrete using 30% fly ash

Restrained expansion, μ								
	FA30EA15				FA30EA20			
Age,	Restraining ratio,%				Restraining ratio,%			
days	0.79	1.57	3.14	8.04	0.79	1.57	3.14	8.04
0.0	0	0	0	0	0	0	0	0
0.5	0	99	89	54	171	126	101	72
1.0	0	115	103	68	196	148	113	77
1.5	0	124	111	68	206	156	123	78
2.0	0	131	117	74	209	159	125	78
2.5	0	132	119	75	213	162	128	79
3.0	0	134	121	76	212	161	126	75
3.5	0	135	117	74	215	164	128	76
4.0	0	136	118	76	214	163	127	75
4.5	0	136	118	76	216	165	127	76
5.0	0	136	118	75	217	165	126	76
5.5	0	136	118	75	219	167	127	81
6.0	0	136	118	75	219	167	125	79
6.5	0	136	118	75	219	167	130	83
7.0	0	137	118	75	219	167	127	83

Appendix B. Results of compressive strength of hyper expansive concrete

Table B 1 Compressive strength of HEA expansive concrete using 20% fly ash, under free expansion

Age, (days)	Compressive strength, Mpa			
	FA20EA5	FA20EA10	FA20EA15	FA20EA20
3	18.49	18.77	16.72	16.34
7	29.35	27.92	24.66	21.52
28	30.62	29.38	27.53	27.02
56	31.35	30.11	29.06	28.68

Table B 2 Compressive strength of HEA expansive concrete using 30% fly ash, under free expansion

Age, (days)	Compressive strength, Mpa			
	FA30EA5	FA30EA10	FA30EA15	FA30EA20
3	17.06	15.39	13.26	12.18
7	19.75	18.64	18.60	18.65
28	27.35	26.67	23.23	22.55
56	28.75	27.27	25.09	23.15

Table B 3 Compressive strength of HEA expansive concrete without fly ash, under restraint

Age, (days)	Compressive strength, Mpa	
	FA0EA15	FA0EA20
3	33.51	31.33
7	35.65	33.08
28	41.52	38.02
56	43.65	41.85

Table B 4 Compressive strength of HEA expansive concrete using 20% fly ash, under restraint

Age, (days)	Compressive strength, Mpa			
	FA20EA5	FA20EA10	FA20EA15	FA20EA20
3	22.97	23.80	23.38	25.17
7	32.32	33.11	30.48	30.97
28	37.73	37.16	35.75	33.36
56	38.45	37.89	37.71	35.14

Table B 5 Compressive strength of HEA expansive concrete using 30% fly ash, under restraint

Age, (days)	Compressive strength, Mpa			
	FA30EA5	FA30EA10	FA30EA15	FA30EA20
3	21.31	21.08	21.14	19.99
7	24.50	25.66	22.42	21.90
28	29.22	32.04	27.07	24.86
56	35.78	34.77	28.51	26.63

Appendix C. Results of tensile strength and cracking strain of hyper expansive concrete

Table C 1 Tensile strength of HEA expansive concrete without fly ash

Age (days)	Tensile strength, Mpa	
	FA0HEA15	FA0HEA20
7	5.2	4.7
28	5.7	5.2
56	5.8	5.4

Table C 2 Tensile strength of HEA expansive concrete using 20% fly ash

Age (days)	Tensile strength, Mpa			
	FA20HEA5	FA20HEA10	FA20HEA15	FA20HEA20
7	5.0	4.8	4.5	4.2
28	5.7	5.6	5.2	4.9
56	6.1	5.9	5.5	5.3

Table C 3 Tensile strength of HEA expansive concrete using 30% fly ash

Age (days)	Tensile strength, Mpa			
	FA30EA5	FA30EA10	FA30EA15	FA30EA20
7	4.4	4.2	3.3	3.1
28	5.4	5.1	4.6	4.3
56	5.9	5.7	5.4	5.1

Table C 4 Cracking strain of HEA expansive concrete without fly ash

Age (days)	Cracking strain, μ	
	FA20HEA5	FA20HEA10
7	229	217
28	248	235
56	250	240

Table C 5 Cracking strain of HEA expansive concrete using 20% fly ash

Age (days)	Cracking strain, μ			
	FA20HEA5	FA20HEA10	FA20HEA15	FA20HEA20
7	247	239	220	213
28	257	241	234	226
56	262	247	244	239

Table C 6 Cracking strain of HEA expansive concrete using 30% fly ash

Age (days)	Cracking strain, μ			
	FA30HEA5	FA30HEA10	FA30HEA15	FA30HEA20
7	265	220	220	205
28	274	238	243	216
56	278	236	246	216

Appendix D. Results of net expansion/shrinkage of UHSFRM

Table D 1 Net expansion/shrinkage of UHSFRM with 6 mm long steel fiber

Age, (days)	Net expansion/shrinkage, μ		
	SF(6mm)EA0%	SF(6mm)EA10%	SF(6mm)EA15%
0	0	0	0
1	-392	340	1070
2	-540	220	976
3	-578	200	966
4	-592	222	964
5	-614	178	964
6	-632	170	968
7	-648	166	978
14	-734	144	-

Note:
+ means the length of specimen is longer than initial length
- means the length of specimen is shorter than initial length

Table D 2 Net expansion/shrinkage of UHSFRM with 13 mm long steel fiber

Age,	Net expansion/shrinkage, μ		
(days)	SF(13mm)EA0%	SF(13mm)EA10%	SF(13mm)EA15%
0	0	0	0
1	-160	294	628
2	-172	266	618
3	-246	242	548
4	-264	212	506
5	-296	184	486
8	-304	148	500
14	-382	90	431
21	-442	14	421
28	-436	50	496

Note:
+ means the length of specimen is longer than initial length
- means the length of specimen is shorter than initial length